



U.S. Department of  
Transportation

**Federal Railroad  
Administration**

## **Heat Release Rate Requirements for Rail Car Interior Finish**

---

Office of Research,  
Development  
and Technology  
Washington, DC 20590



#### NOTICE

This document is disseminated under the sponsorship of the Department of Transportation in the interest of information exchange. The United States Government assumes no liability for its contents or use thereof. Any opinions, findings and conclusions, or recommendations expressed in this material do not necessarily reflect the views or policies of the United States Government, nor does mention of trade names, commercial products, or organizations imply endorsement by the United States Government. The United States Government assumes no liability for the content or use of the material contained in this document.

#### NOTICE

The United States Government does not endorse products or manufacturers. Trade or manufacturers' names appear herein solely because they are considered essential to the objective of this report.

<b>REPORT DOCUMENTATION PAGE</b>			<i>Form Approved</i> <b>OMB No. 0704-0188</b>	
Public reporting burden for this collection of information is estimated to average 1 hour per response, including the time for reviewing instructions, searching existing data sources, gathering and maintaining the data needed, and completing and reviewing the collection of information. Send comments regarding this burden estimate or any other aspect of this collection of information, including suggestions for reducing this burden, to Washington Headquarters Services, Directorate for Information Operations and Reports, 1215 Jefferson Davis Highway, Suite 1204, Arlington, VA 22202-4302, and to the Office of Management and Budget, Paperwork Reduction Project (0704-0188), Washington, DC 20503.				
1. AGENCY USE ONLY (Leave blank)		2. REPORT DATE December 2019		3. REPORT TYPE AND DATES COVERED Technical Report May 2017–September 2018
4. TITLE AND SUBTITLE Heat Release Rate Requirements for Railcar Interior Finish			5. FUNDING NUMBERS DTRT57-12-D-30011, Order 0035 DTRF53-15-X-00019	
6. AUTHOR(S) Charles Luo, Stefan Kraft, Matthew DiDomizio, Mark McKinnon, Jonathan Hodges, Soroush Yazdani, and Brian Lattimer				
7. PERFORMING ORGANIZATION NAME(S) AND ADDRESS(ES) Jensen Hughes 3610 Commerce Drive, Suite 817 Baltimore, MD 21227			8. PERFORMING ORGANIZATION REPORT NUMBER	
9. SPONSORING/MONITORING AGENCY NAME(S) AND ADDRESS(ES) U.S. Department of Transportation Federal Railroad Administration Office of Railroad Policy and Development Office of Research, Development and Technology Washington, DC 20590			10. SPONSORING/MONITORING AGENCY REPORT NUMBER  DOT/FRA/ORD-19/39	
11. SUPPLEMENTARY NOTES COR: Melissa Shurland				
12a. DISTRIBUTION/AVAILABILITY STATEMENT This document is available to the public through the FRA <a href="#">website</a> .			12b. DISTRIBUTION CODE	
13. ABSTRACT (Maximum 200 words) The focus of this research was to establish heat release rate (HRR) based performance requirements for intercity and commuter passenger railcar interior finish materials. A database of HRR results from passenger railcar components was compiled for developing new HRR requirements. Initiating fire exposures within a passenger railcar were quantified and compared with different initiating fires in room-corner test standards. The initiating fire of National Fire Protection Association (NFPA) 286, Standard Methods of Fire Tests for Evaluating Contribution of Wall and Ceiling Interior Finish to Room Fire Growth, was determined to be a representative exposure fire for the interior of a passenger railcar. A flammability parameter empirical model was developed to predict the occurrence of flashover due to the lining material in NFPA 286 room-corner tests. Fire Dynamics Simulator (FDS) computational fluid dynamics (CFD) model was also demonstrated to predict detailed fire growth in the NFPA 286 room and a railcar. Both small and large-scale tests were performed on seven railcar interior finish materials. The testing results along with the HRR database provided data to validate both models for use in development of HRR requirements. HRR-based flammability requirements were developed for railcar interior materials listed in "Other vehicle components" in NFPA 130, Standard for Fixed Guideway Transit and Passenger Rail Systems. Materials used in seating areas within a railcar can be evaluated using a flammability requirement of maximum average rate of heat emission (MARHE) less than 90 kW/m <sup>2</sup> .				
14. SUBJECT TERMS Rail car, interior finish, heat release rate, HRR, flammability performance requirement, fire safety			15. NUMBER OF PAGES 142	
			16. PRICE CODE	
17. SECURITY CLASSIFICATION OF REPORT Unclassified	18. SECURITY CLASSIFICATION OF THIS PAGE Unclassified	19. SECURITY CLASSIFICATION OF ABSTRACT Unclassified	20. LIMITATION OF ABSTRACT	

## METRIC/ENGLISH CONVERSION FACTORS

### ENGLISH TO METRIC

#### LENGTH (APPROXIMATE)

1 inch (in)	=	2.5 centimeters (cm)
1 foot (ft)	=	30 centimeters (cm)
1 yard (yd)	=	0.9 meter (m)
1 mile (mi)	=	1.6 kilometers (km)

#### AREA (APPROXIMATE)

1 square inch (sq in, in <sup>2</sup> )	=	6.5 square centimeters (cm <sup>2</sup> )
1 square foot (sq ft, ft <sup>2</sup> )	=	0.09 square meter (m <sup>2</sup> )
1 square yard (sq yd, yd <sup>2</sup> )	=	0.8 square meter (m <sup>2</sup> )
1 square mile (sq mi, mi <sup>2</sup> )	=	2.6 square kilometers (km <sup>2</sup> )
1 acre = 0.4 hectare (he)	=	4,000 square meters (m <sup>2</sup> )

#### MASS - WEIGHT (APPROXIMATE)

1 ounce (oz)	=	28 grams (gm)
1 pound (lb)	=	0.45 kilogram (kg)
1 short ton = 2,000 pounds (lb)	=	0.9 tonne (t)

#### VOLUME (APPROXIMATE)

1 teaspoon (tsp)	=	5 milliliters (ml)
1 tablespoon (tbsp)	=	15 milliliters (ml)
1 fluid ounce (fl oz)	=	30 milliliters (ml)
1 cup (c)	=	0.24 liter (l)
1 pint (pt)	=	0.47 liter (l)
1 quart (qt)	=	0.96 liter (l)
1 gallon (gal)	=	3.8 liters (l)
1 cubic foot (cu ft, ft <sup>3</sup> )	=	0.03 cubic meter (m <sup>3</sup> )
1 cubic yard (cu yd, yd <sup>3</sup> )	=	0.76 cubic meter (m <sup>3</sup> )

#### TEMPERATURE (EXACT)

$$[(x-32)(5/9)]^{\circ}\text{F} = y^{\circ}\text{C}$$

### METRIC TO ENGLISH

#### LENGTH (APPROXIMATE)

1 millimeter (mm)	=	0.04 inch (in)
1 centimeter (cm)	=	0.4 inch (in)
1 meter (m)	=	3.3 feet (ft)
1 meter (m)	=	1.1 yards (yd)
1 kilometer (km)	=	0.6 mile (mi)

#### AREA (APPROXIMATE)

1 square centimeter (cm <sup>2</sup> )	=	0.16 square inch (sq in, in <sup>2</sup> )
1 square meter (m <sup>2</sup> )	=	1.2 square yards (sq yd, yd <sup>2</sup> )
1 square kilometer (km <sup>2</sup> )	=	0.4 square mile (sq mi, mi <sup>2</sup> )
10,000 square meters (m <sup>2</sup> )	=	1 hectare (ha) = 2.5 acres

#### MASS - WEIGHT (APPROXIMATE)

1 gram (gm)	=	0.036 ounce (oz)
1 kilogram (kg)	=	2.2 pounds (lb)
1 tonne (t)	=	1,000 kilograms (kg)
	=	1.1 short tons

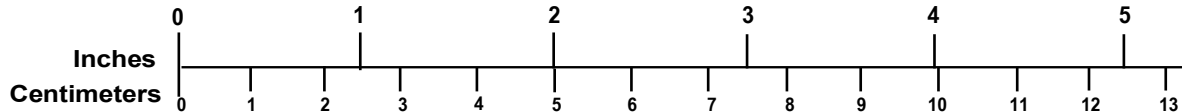
#### VOLUME (APPROXIMATE)

1 milliliter (ml)	=	0.03 fluid ounce (fl oz)
1 liter (l)	=	2.1 pints (pt)
1 liter (l)	=	1.06 quarts (qt)
1 liter (l)	=	0.26 gallon (gal)
1 cubic meter (m <sup>3</sup> )	=	36 cubic feet (cu ft, ft <sup>3</sup> )
1 cubic meter (m <sup>3</sup> )	=	1.3 cubic yards (cu yd, yd <sup>3</sup> )

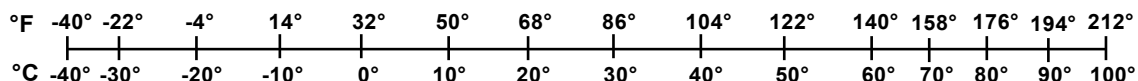
#### TEMPERATURE (EXACT)

$$[(9/5) y + 32]^{\circ}\text{C} = x^{\circ}\text{F}$$

### QUICK INCH - CENTIMETER LENGTH CONVERSION



### QUICK FAHRENHEIT - CELSIUS TEMPERATURE CONVERSION



For more exact and or other conversion factors, see NIST Miscellaneous Publication 286, Units of Weights and Measures. Price \$2.50 SD Catalog No. C13 10286

Updated 6/17/98

## **Acknowledgements**

---

This work is supported by the U.S. Department of Transportation Volpe Transportation Systems Center (Volpe Center). The authors appreciate the input and discussions with Volpe Center's Mark Gentile, Suzanne Horton and Bernard Kennedy IV, and the Federal Railroad Administration (FRA) sponsored Melissa Shurland, Jeffrey Gordon and David Mao, and industry representative Mr. Steve Roman from LTK Engineering. The authors also appreciate all the rail operators that allowed our researchers access to their facilities and staff that escorted us so that we could obtain measurements and geometry information to support input into the modeling efforts. This included Amtrak (i.e., New York City, NY, Los Angeles, CA, and Seattle, WA), New Jersey Transit, Long Island Railroad in New York City, NY, Metrolink in Los Angeles, CA. The researchers would also like to thank the FRA Regional Motive Power & Equipment Inspectors who facilitated visits to the California and Washington maintenance facilities, Roman Chavez and Matthew Thomas, respectively.

## Contents

---

Executive Summary .....	1
1. Introduction.....	2
1.1 Background.....	2
1.2 Objectives .....	3
1.3 Overall Approach .....	4
1.4 Scope.....	5
1.5 Organization of the Report.....	5
2. HRR Database for Rail Car Lining Materials .....	7
2.1 Summary of Acquired HRR Data .....	7
2.2 Characteristics of Collected Data.....	8
2.3 Section Summary .....	8
3. Quantifying Plausible Fire Exposure for Rail Car Fires.....	10
3.1 Review of Realistic Initiating Fires .....	10
3.2 Room Fire Testing Standards and Their Application to Rail Car Fires.....	12
3.3 Application of Room Fire Exposures in Literature .....	15
3.4 Comparison of Fire Exposures .....	16
3.5 Section Summary .....	23
4. Empirical Model for Predicting Flashover in NFPA 286 Room-corner Test .....	25
4.1 Flammability Model to Predict Room-Corner Test .....	25
4.2 NFPA 286 Room-Corner Test.....	25
4.3 Theoretical Basis .....	26
4.4 Model Performance .....	28
4.5 Model Predictions .....	30
4.6 Section Summary .....	32
5. Fire Growth Modeling of Room-corner Tests with Rail Car Geometry .....	34
5.1 Literature Review .....	34
5.2 Fire Growth Modeling.....	36
5.3 Fire Growth Modeling using FDS .....	40
5.4 Validation of FDS Models .....	47
5.5 Section Summary .....	49
6. Cone Calorimeter Testing of Rail Car Interior Materials .....	51

6.1	Methodology .....	51
6.2	Materials Selection and Test Matrix .....	56
6.3	Results and Discussion .....	58
6.4	Section Summary .....	65
7.	NFPA 286 Room-corner Testing of Rail Car Interior Materials .....	67
7.1	Experimental Approach .....	67
7.2	Results .....	72
7.3	Section Summary .....	79
8.	Validation of FDS and Empirical Model in Predicting Rail Car Lining Fire Growth Contribution .....	80
8.1	Empirical Flammability Model .....	80
8.2	Evaluation of Empirical Model Predictions .....	81
8.3	FDS Modeling of Room-corner Tests .....	85
8.4	Section Summary .....	90
9.	Development of HRR Requirements for Rail Car Interior Materials .....	92
9.1	Flammability Parameter Based HRR Requirements .....	93
9.2	Evaluation Using EN-45545-2 HRR Requirements .....	100
9.3	Database Evaluation of Potential Requirements .....	105
9.4	Section Summary .....	106
10.	Calorimeter Tests on Seating Assemblies for Model Validation .....	107
10.1	Experimental Approach .....	107
10.2	Experiment Description .....	110
10.3	Results .....	111
10.4	Discussion .....	117
10.5	Section Summary .....	118
11.	Conclusion .....	119
11.1	Recommendations .....	120
12.	References .....	122
	Appendix .....	127
	Abbreviations and Acronyms .....	128

## Illustrations

---

Figure 3-1. Representative interior environments of rail cars .....	11
Figure 3-2. HRR curves of initiating fires in rail cars from literature .....	12
Figure 3-3. Initiating fires from standard room corner fire tests .....	17
Figure 3-4. Standard fire exposures compared with HRR curves of different realistic fires, (a) high peak HRR and short duration and (b) low peak HRR and long duration .	18
Figure 3-5. Standard fire exposures compared with average HRRs of different fires, (a) high peak HRR and short duration and (b) low peak HRR and long duration .....	19
Figure 3-6. Comparison of real initiating fires with fire test standards .....	23
Figure 4-1. NFPA 286 room configuration with hood and instrumentation (image source NFPA 286) [11]. HRR is determined using the temperature and gas measurements ...	26
Figure 4-2. Flashover time vs. flammability parameter. Orange line at $F = 0.6$ indicates proposed critical value which will cause flashover. Data from [45]–[49] .....	29
Figure 4-3. Full scale HRR in NFPA room-corner test vs. flammability parameter. Line at $F = 0.6$ is proposed critical value. Data from [45] [46] .....	30
Figure 4-4. Histogram of flammability parameters for materials in the passenger rail car material database. Black line at $F = 0.6$ indicates critical flammability parameter which will cause flashover in NFPA 286 room.....	31
Figure 4-5. Comparison of ASTM E162 flame spread and flammability parameter.....	32
Figure 5-1. Example mass fraction and reaction rate of a burning material .....	38
Figure 5-2. HRR of 6 mm plywood in cone calorimeter test .....	40
Figure 5-3. Mass loss rate of 6 mm plywood in cone calorimeter test.....	40
Figure 5-4. NFPA 286 standard room corner test .....	41
Figure 5-5. Full scale rail car geometry with corner fire .....	42
Figure 5-6. Time history of temperature at ceiling center .....	43
Figure 5-7. Flow velocity of the center section of NFPA 286 rooms at 360 s (left) with door and (right) without door .....	45
Figure 5-8. Temperature of the center section of NFPA 286 rooms at 360 s (left) with door and (right) without door .....	45
Figure 5-9. NFPA 286 room wall temperature at 360 s (left) with door and (right) without door. View from floor looking up to the ceiling.....	45
Figure 5-10. Temperature of rail car center section at 360 seconds .....	46
Figure 5-11. Rail car interior wall temperature at (a) 360 s and (b) 600 seconds.....	47
Figure 5-12. Time history of center ceiling gas temperature in the NFPA 286 room and rail car geometries.....	48



Figure 5-13. Time history of HRR in the NFPA 286 room and rail car geometries .....	49
Figure 6-1. ASTM E1354 cone calorimeter test apparatus (image reproduced from the SFPE Handbook of Fire Protection Engineering [8]) .....	52
Figure 6-2. Specimen prepared in accordance with ASTM E1354 using the retainer frame .....	53
Figure 6-3. ASTM E162 radiant panel test apparatus (image reproduced from test standard ASTM E162 [65]) .....	56
Figure 6-4. Specimen prepared with retainer frame and wire grid .....	59
Figure 6-5. Preliminary test of Sample 1 with the retainer frame and the wire grid .....	60
Figure 6-6. Preliminary test Sample 1 with the retainer frame and without the wire grid .....	60
Figure 6-7. Preliminary test of Sample 1 without the retainer frame or the wire grid .....	61
Figure 6-8. HRRPUA of Sample 1 at 50 kW/m <sup>2</sup> in various configurations .....	61
Figure 6-9. HRRs for the materials tested in the study (refer to Table 6-1 for descriptions of each sample) .....	63
Figure 6-10. HRRs for the materials tested in the study, truncated (refer to Table 6-1 for descriptions of each sample) .....	64
Figure 7-1. NFPA 286 room configuration with hood and instrumentation (image source NFPA 286) [11] with HRR measured using the hood calorimeter (side view) .....	68
Figure 7-2. Thermoplastic three wall panels screwed to 5/8-inch drywall sandwich with steel studs .....	71
Figure 7-3. Sample 6 setup. Spreader poles held the wall panels in place, with flanges screwed to the material .....	71
Figure 7-4. NFPA 286 test HRR vs. time for Sample 1 .....	73
Figure 7-5. NFPA 286 test HRR vs. time for Sample 2 .....	74
Figure 7-6. NFPA 286 test HRR vs. time for Sample 3 .....	75
Figure 7-7. NFPA 286 test HRR vs. time for Sample 4 .....	76
Figure 7-8. NFPA 286 test HRR vs. time for Sample 5 .....	76
Figure 7-9. NFPA 286 test HRR vs. time for Sample 6 .....	77
Figure 7-10. NFPA 286 test HRR vs. time for Sample 7 .....	78
Figure 8-1. Comparison of time to flashover and flammability parameter for newly tested materials .....	83
Figure 8-2. Time to flashover in the NFPA 286 room-corner test versus flammability parameter for all available materials [27], [45]–[48], [68] .....	84
Figure 8-3. Flammability parameter versus ASTM E162 flame spread index of database rail car materials .....	85

Figure 8-4. Effect of material falling on flashover prediction for sample 1: (left) HRR and (right) ceiling center temperature .....	86
Figure 8-5. Simulation of Sample 1 materials falling at time of 900 second .....	86
Figure 8-6. Effect of facesheet failing on flashover prediction for Sample 2 (left) HRR and (right) ceiling center temperature.....	87
Figure 8-7. Time history of HRR (left) and center ceiling temperature (right) of Sample 3 tested in NFPA 286 room .....	88
Figure 8-8. Time history of HRR (left) and center ceiling temperature (right) of Sample 4 tested in NFPA 286 room .....	88
Figure 8-9. Time history of HRR (left) and center ceiling temperature (right) of Sample 5 tested in NFPA 286 room .....	89
Figure 8-10. Time history of HRR (left) and center ceiling temperature (right) of Sample 6 tested in NFPA 286 room .....	89
Figure 8-11. Time history of HRR (left) and center ceiling temperature (right) of Sample 7 tested in NFPA 286 room .....	90
Figure 9-1. Predicting flashover with the empirical flammability model. The critical flammability parameter of $F=0.6$ delineates materials which are likely to cause flashover from those that will not .....	94
Figure 9-2. Comparison of passenger rail car materials with flammability parameters of 0.6 and 0.9 with initial requirements.....	96
Figure 9-3. Flammability parameter and average HRR for passenger rail car materials. $Q''_{avg} < 90 \text{ kW/m}^2$ accepts all materials with $F < 0.6$ .....	96
Figure 9-4. K-means clustering on database of passenger rail car materials.....	97
Figure 9-5. Evaluating material database with requirements for average and peak HRR .....	98
Figure 9-6. FDS simulation result for rail car ceiling lining material with flammability parameter of 0.69 .....	99
Figure 9-7. FDS simulation result for rail car toilet room lining material with flammability parameter of 0.89 .....	99
Figure 9-8. Comparison of MARHE and average HRR for Sample 3 cone calorimeter test .....	102
Figure 9-9. Comparison of MARHE and average HRR for Sample 2.....	102
Figure 9-10. MARHE and flammability parameter comparison. Requirement $MARHE < 90 \text{ kW/m}^2$ accepts all materials with $F \leq 0.75$ .....	104
Figure 9-11. Comparison of initial requirements with those specified in EN 45545-2..	104
Figure 10-1. Test room configuration with hood and instrumentation with HRR measured using the hood calorimeter .....	108

Figure 10-2. Setup of the samples in the room before testing.....	110
Figure 10-3. HRR vs. time for seating assembly Sample 1 .....	113
Figure 10-4. HRR vs. time for seating assembly Sample 2 .....	115
Figure 10-5. HRR vs. time for seating assembly Sample 3 .....	117

## Tables

---

Table 1-1. Materials focused on in the study of this report .....	5
Table 3-1. EN 45545-1 Ignition models [12] .....	13
Table 3-2. Total HRR of initiating fires.....	20
Table 3-3. Fuel diameter and flame height of standard fires and realistic initiating fires	22
Table 4-1. Variation of flammability parameters with cone calorimeter test results .....	28
Table 5-1. Material properties of 6 mm plywood .....	39
Table 5-2. Time to flashover for the NFPA 286 room-corner test of plywood .....	49
Table 6-1. Description and end-use of tested samples .....	56
Table 6-2: Test matrix for the primary cone calorimeter test series.....	57
Table 6-3. Summary of cone calorimeter test results for each sample .....	63
Table 6-4. Summary of radiant panel test results for each sample .....	65
Table 7-1. Samples selected for testing .....	69
Table 7-2. Sample NFPA 286 test results .....	72
Table 7-3. Test log for Sample 1 .....	73
Table 7-4. Test log for Sample 2 .....	74
Table 7-5. Test log for Sample 3 .....	75
Table 7-6. Test log for Sample 4 .....	76
Table 7-7. Test log for Sample 5 .....	77
Table 7-8. Test log for Sample 6 .....	78
Table 7-9. Test log for Sample 7 .....	78
Table 8-1. Material samples selected for testing .....	81
Table 8-2. Small and large-scale fire tests results for materials with flammability parameter calculated from ASTM E1354 data at 50 kW/m <sup>2</sup> .....	82
Table 9-1. NFPA 130 [3] material fire performance criteria table .....	93
Table 9-2. FDS results for materials in NFPA 286 and rail car geometries .....	98
Table 9-3. Operation category definitions from EN 45545-2 .....	100
Table 9-4. Hazard level matrix for qualifying materials in train vehicles .....	101
Table 9-5. Requirements for material sets according to hazard levels. All testing done in ISO 5660-1 at 50 kW/m <sup>2</sup> .....	103
Table 9-6. Requirements for material sets according to hazard levels. All testing done in ISO 5660-1 at 25 kW/m <sup>2</sup> .....	103
Table 9-7. Fraction of materials which pass selected HRR requirements .....	105

Table 10-1. Samples selected for testing .....	109
Table 10-2. Sample full seating assembly calorimeter test results .....	111
Table 10-3. Test log for seating assembly Sample 1.....	112
Table 10-4. Test log for seating assembly Sample 2.....	114
Table 10-5. Test log for seating assembly Sample 3.....	116

## Executive Summary

---

The Federal Railroad Administration (FRA) funded research through the Volpe National Transportation Systems Center to investigate fire safety of passenger rail interior finishes. This research effort began on May 1, 2017, and ended on August 31, 2018. The research was conducted by Jensen Hughes. The research was conducted in Blacksburg, VA, and Baltimore, MD. The focus of this effort was to establish heat release rate (HRR) based flammability performance requirements for passenger rail car interior finish materials.

Based on the evaluation in this research, materials used in seating areas within a rail car can be evaluated using the American Society of Testing Materials (ASTM) E1354 cone calorimeter test [1] at 50 kW/m<sup>2</sup> with a flammability requirement of maximum average rate of heat emission (MARHE) less than 90 kW/m<sup>2</sup>. No flashover is expected in large rail car spaces (seating area) for these materials. This is also currently used in European Norms (EN) 45545-2 for many materials in hazard level HL1 and HL2 applications [2]. EN operation and design categories are different than those in the U.S. This flammability requirement as stated above would align U.S. and EN standards allowing manufacturers to maintain supply chains. A more restrictive requirement may be needed for smaller spaces such as bathrooms and sleeping areas. The range of MARHE between 60 kW/m<sup>2</sup> and 90 kW/m<sup>2</sup> might be appropriate for smaller spaces, but more data and analysis are needed to refine the requirement value. Additional research is also required for HRR-based flammability requirements of other materials listed in the National Fire Protection Association (NFPA) 130 (Standard for Fixed Guideway Transit and Passenger Rail Systems) categories including “Cushioning,” “Fabrics,” “Other Vehicle Components” that are transparent or adhesive/sealants, and “Elastomers” [3].

The purpose of this work was to re-evaluate the current flammability standards governing the use of interior finish materials in passenger rail cars and provide a basis for establishing HRR-based performance requirements to evaluate the flammability of interior finish materials to be used in a passenger rail car. Currently, NFPA 130 [3] and the Title 49 Code of Federal Regulations (CFR) § 283.103 [4] generally use two different standard test methodologies for rail car interior finish material flammability and smoke emission acceptance. These are the ASTM E662 Standard Test Method for Specific Optical Density of Smoke Generated by Solid Materials [5], and the ASTM E162 Standard Test Method for Surface Flammability of Materials Using a Radiant Heat Energy Source [6]. During the last rulemaking process, there was an interest in whether the HRR-based tests provide a more practical and valuable alternative option to the current standards for determining the fire safety performance of interior materials used in passenger rail cars. The HRR-based performance requirements would allow designers, engineers, scientists, testing and acceptance personnel a better understanding of the fire hazard threat, flashover HRR and contribution of individual materials to a fire inside a rail car. This would provide for improvements in the fire hazard analysis, emergency egress analysis and threats analysis of an enclosed space of a station or tunnel for heat and smoke control, and a better understanding of the performance of various construction materials.

# 1. Introduction

---

In recent years, rail technology has improved infrastructure and travel speed such that this industry is competitive with other forms of transportation throughout the world. As the global population increases and the world moves increasingly toward environmental consciousness, energy-efficient methods of mass transit, including rail, will need to continue to develop to meet the increased demand. To ensure the safety of passengers and personnel in passenger rail cars in the United States, the Federal Railroad Administration (FRA) published fire safety requirements in 1999 and 2002 that were intended to provide a requisite level of safety for passenger rail cars ordered on or after September 8, 2000, or placed in service September 9, 2002, or later; rail cars refurbished or overhauled on November 9, 1999, or later in which new materials introduced in the rail car were required to meet the standards. An area of interest is the adequacy of the fire performance requirements for combustible materials to minimize the impact of burning materials on passengers during a fire. FRA provided funding for the research in collaboration with the Volpe National Transportation Systems Center (Volpe). Jensen Hughes conducted the research between May 1, 2017, and August 31, 2018. The work performed for this report is an initial effort to provide a basis for establishing heat release rate (HRR) based performance requirements for passenger rail car interior finish materials.

## 1.1 Background

FRA has long recognized the importance of maintaining and improving the level of passenger train fire safety and emergency preparedness. In 1999, as part of the passenger rail equipment safety standards rulemaking process required by Congress, FRA issued regulations in Title 49 Code of Federal Regulations (CFR) § 238.103 that include fire safety requirements for new and existing passenger rail cars and locomotives. An update to the FRA fire safety requirements was issued in 2002 [4], which included clarification of certain fire performance requirements, as well as responses to comments to the 1999 final rule.

Following the release of the rule in 2002, several technical issues related to the fire performance of certain component materials were identified by FRA, Volpe, National Institute of Standards and Technology (NIST), and industry as warranting further study. One of these issues is material acceptance considering HRR performance criteria. In 49 CFR § 238.103, materials approvals are based on not exceeding the limits prescribed in both the American Society of Testing Materials (ASTM) E662 Standard Test Method for Specific Optical Density of Smoke Generated by Solid Materials [5], and the ASTM E162 Standard Test Method for Surface Flammability of Materials Using a Radiant Heat Energy Source [6]. During the last rulemaking process, there was an interest in whether the HRR of materials was a more practical and valuable performance test to evaluate the fire safety of materials to be used in a passenger rail car design. The HRR-based performance requirements would allow designers, engineers, scientists, testing and acceptance personnel a better understanding of the fire hazard threat, flashover HRR and time-temperature curve resulting from burning materials. This understanding would allow for improvements in the fire hazard analysis, emergency egress analysis and

threats analysis of an enclosed space of a station or tunnel for heat and smoke control, and a better understanding of the performance of various construction materials.

## 1.2 Objectives

The overall objective of this research effort was to develop HRR-based flammability requirements for materials used on the interior of rail cars. HRR requirements are based on small-scale fire test data, therefore, it is necessary to demonstrate the connection between small-scale performance and large-scale/end-use behavior to ensure the desired level of safety. Data from literature survey as well as new data needed to be collected and consolidated to achieve this. In addition, models capable of predicting the contribution of combustible linings on fire growth required validation to demonstrate material performance inside of rail car geometries. HRR-based flammability requirements from small-scale test data were then developed and demonstrated using these data and models. With the objective to establish HRR-based flammability performance requirements for passenger rail car interior finish materials, the following work was performed in this research:

- A database of HRR results from passenger rail car components was compiled from the literature survey and provide data for construction of a criterion for material qualification. The database was used in the formulation of an empirical flammability model and in the development of the HRR-based performance requirements.
- Initiating fire exposures within a rail car from published data and previous fire testing research [7]–[9] were quantified and compared with different initiating fires in room-corner fire test standards. The NFPA 286 initiating fire of 40 kW for 5 minutes followed by 160 kW for 10 minutes was determined to be the most suitable standard initiating fire when compared with realistic initiating fires that are plausible inside of a rail car. The NFPA 286 initiating fire is recommended as a representative exposure fire for the interior of a rail car.
- An empirical model based on the flammability parameter was developed to predict flashover in NFPA 286 room-corner tests. The flammability parameter is calculated from the cone calorimeter data from tests conducted with a heat flux of  $50 \text{ kW/m}^2$ , which is similar to the average exposure from a standard ignition source near the base of the flame to a surface. The use of this model on rail car materials provided a basis for the determination of an appropriate HRR requirement for interior finish materials on rail cars.
- Fire growth modeling using the Fire Dynamics Simulator (FDS) [13] was validated by comparing it with the NFPA 286 standard room-corner fire test data. The simulation results for gas temperature, HRR, wall temperature, and time-to-flashover demonstrated that NFPA 286 standard room-corner fire test is reasonably conservative and well represents the fire behaviors that develop in a rail car with one door open. These modeling results suggest that the NFPA 286 standard room corner test is representative of conditions that would develop inside of a rail car.



- Seven rail car interior material samples were tested in the small-scale cone calorimeter per ASTM E1354 [1] and the flame spread apparatus per ASTM E162 [6], as well as in the large-scale NFPA 286 room-corner test [11]. The combined data from small and large-scale testing were used to validate the flammability parameter empirical model that predicts the occurrence of flashover as well as the FDS fire growth model that predicts more detailed fire growth within a rail car. Both the flammability parameter empirical model and FDS fire growth model were demonstrated to be capable of generally predicting the performance of materials in large scale.
- Analyses were conducted to establish HRR requirements for rail car interior lining materials used in seating areas within a rail car. The evaluation suggested that these materials should be evaluated using the ASTM E1354 cone calorimeter test at 50 kW/m<sup>2</sup> using a flammability requirement of maximum average rate of heat emission (MARHE) less than 90 kW/m<sup>2</sup>. No flashover is expected in large rail car spaces (seating areas) for these materials. A more restrictive requirement may be needed for smaller spaces such as bathrooms and sleeping areas.
- Large-scale calorimeter tests were performed for three types of passenger rail car seating assemblies inside an NFPA 286 standard room with inert wall and ceiling linings. The results of these tests including gas temperature rise, combustion product generation, and overall HRR provide validation data and input for the models that can be used to predict fire growth inside of rail cars. These models will be used to demonstrate the fire performance of materials meeting the proposed HRR-based performance requirements in their end-use environment.

### 1.3 Overall Approach

The overall approach in this study was to utilize existing data, and conduct modeling, simulation, testing, and analysis to provide a basis and establish HRR-based performance requirements for rail car interior materials. The existing HRR data from literature and unpublished test reports were reviewed and consolidated to generate a rail car lining materials flammability database. An appropriate large-scale fire test as well as initiating fire exposure to evaluate the material flammability performance was determined so that interior finish materials could be assessed on a consistent basis. Models were developed to predict material performance in the large-scale tests as well as performance in the rail car end-use geometry configuration. Models included a basic model that could be used to quickly evaluate many different materials as well as a detailed computational fluid dynamics (CFD) model developed with Fire Dynamics Simulator (FDS) that could be used to assess performance inside actual rail car geometries and provide more detailed predictions. These modeling results were used to demonstrate that large-scale room-corner fire tests could be used to represent the performance of materials in their end-use rail car geometry. Additional fire test data were developed to further bridge the gap between small-scale fire performance and large-scale fire growth behavior as well as validate models. These data were used to validate models to predict large-scale/end-use application performance based on small-scale data input. The models and small-scale test data were used along with other

existing international standards requirements to develop the proposed HRR-based requirements.

## 1.4 Scope

In NFPA 130 [3], 49 CFR § 238.103, and Appendix B [4], the interior finish is broken down into different categories by material function on the rail car. As seen in the table and further described in the notes for each material function (not shown), there may be special requirements and testing needs for particular materials based on their function. The focus of the work reported here is on the materials that are listed in “Other Vehicle Components” in [Table 1-1](#) from NFPA 130 [3]. This study only considered a HRR-based requirement to replace the existing the ASTM E162 flammability requirement. The smoke requirements established through testing in ASTM E662 were outside the scope of this research.

**Table 1-1. Materials focused on in the study of this report**

Other vehicle components	Seat and mattress frames, wall and ceiling lining and panels, seat and toilet shrouds, toilet seats, trays and other tables, partitions, shelves, opaque windscreens, combustible signage, end caps, roof housings, articulation bellows, exterior shells, nonmetallic skirts, battery case material, and component boxes and covers	ASTM E162	$I_s \leq 35$
		ASTM E662	$D_s(1.5) \leq 100$ $D_s(4.0) \leq 200$
	Thermal and acoustical insulation	ASTM E162	$I_s \leq 25$
		ASTM E662	$D_s(4.0) \leq 100$
	HVAC ducting	ASTM E162	$I_s \leq 25$
		ASTM E662	$D_s(4.0) \leq 100$

Besides the seating and the floor coverings, these materials in [Table 1-1](#) represent a large portion of surface materials inside the rail car that could burn. Seating assemblies and floor coverings already have appropriate, modern fire tests and requirements. NFPA 130 requires a complete seat assembly (including cushions, fabric layers, and upholstery) be tested according to ASTM E1537 using the pass/fail criteria of California Technical Bulletin 133 [3]. The other interior finish materials not considered in this work were cushioning, fabrics, windows, elastomers, and sealants/adhesives. These are special classes of materials where the fire safety behavior, physical performance, and end-use configuration all need to be considered, but were outside the scope of this effort. Electric cabling and wiring were considered in a separate effort with the current minimum fire safety testing requirements determined to be adequate.

## 1.5 Organization of the Report

This report is divided into several sections based on different aspects of the research. [Section 2](#) summarizes the review of literature test reports and the development of a HRR database. [Section 3](#) provides an overview of plausible fire exposures for rail car interior fires and a comparison of the realistic fire exposures to identify the most appropriate standard initiating fire exposure used in large-scale fire growth testing of lining materials. [Section 4](#) contains the development of an empirical model for predicting flashover in standard large-scale room-corner fire tests through input of small-scale

cone calorimeter test data. [Section 5](#) includes fire growth modeling of large-scale room-corner fire growth tests and rail car geometries using FDS to demonstrate that the NFPA 286 room-corner fire test can be used to assess material performance in the rail car geometry. [Section 6](#) and [Section 7](#) summarize test data and findings of the small-scale ASTM E1354 cone calorimeter tests and large-scale NFPA 286 room-corner tests, respectively, on rail car interior lining materials. [Section 8](#) contains the validation of the developed empirical model using the data from the tests and database. [Section 9](#) focuses on development of HRR performance requirements based on the empirical model, FDS model, and rail car HRR data from the database developed in [Section 2](#). [Section 10](#) presents the testing data and findings of the calorimeter tests on full seating assemblies in passenger rail cars for future fire growth model validation. [Section 11](#) summarizes the key findings and conclusions from the current work as well as provides the recommendations for future research.

## 2. HRR Database for Rail Car Lining Materials

---

A database of HRR results from passenger rail car components was compiled from the literature as well as unpublished sources to determine a baseline equivalency for existing standards and provide data for creating a material HRR requirement.

The database discussed in this section is primarily composed of small-scale HRR test results from the ASTM E1354 cone calorimeter of passenger rail car lining materials. Also included were test results for the existing FRA standard qualification using the ASTM E162 flame spread test. This flame spread test data, which are currently used for material qualification, are also included for many of the materials for which cone calorimeter heat release data are available. This will enable a quantification of how proposed HRR-requirements will compare with existing requirements. Both foreign and domestic sources were included.

The database will be used for several tasks in this project series. One of the first uses will be in the formulation of an empirical flammability model in [Section 4](#). This model will predict flashover in a large-scale room-corner test using small-scale material data from the cone calorimeter. All available data were collected, although only some parameters were used in the model. The database will also be used to validate a fire growth model using FDS for more detailed predictions of fire growth in a large-scale room-corner test. The validated model will be used to assess and compare the NFPA 286 room-corner test conditions with those developed in a rail car during a fire. Therefore, both ASTM E1354 test data and NFPA 286 room-corner test results are required. While the database contains a limited number of NFPA 286 material test results, more are needed to develop the empirical model. The model will be developed with non-rail car specific data, and validation will use experimental data which will be collected as part of this program. Lastly, this database of materials was used in this research to support the development of new HRR-base requirements and comparing them with existing requirements.

### 2.1 Summary of Acquired HRR Data

Data from a variety of sources, both published [14]–[21] and unpublished [22]–[26], were gathered and compiled in the appendices of this report. The ongoing literature survey for the project provided sources for published data. Unpublished data were acquired from internal projects and external industry contacts. Most of the small-scale data from the cone calorimeter were obtained from unpublished sources.

The data is contained in a spreadsheet located in the appendices, and the configuration allows for easy sorting and filtering of the data by each of the test parameters. This will allow convenient usage of the data in models and reports. The data will enable an evaluation of the current level of safety provided by the standards in place. The database will also be a resource for the testing phase of this work, to provide information for material selection and comparison of experimental data.

## 2.2 Characteristics of Collected Data

The database in the appendices contains a total of 759 items. Most of these data (662 total) are cone calorimeter test results. The database also contains 325 ASTM E162 flame spread tests. There were only four materials for which NFPA 286 data were available, which are reported in [Appendix A.1](#) with accompanying E162 flame spread and E1354 data. Most materials are used directly in the manufacture of rail car components. The only relevant NFPA 286 data found for rail car materials were in a report [27] done by the National Association of State Fire Marshals (NASFM), which included results performed by Underwriter's Laboratory (UL) [14]. Testing was performed on rail car specific materials, but also on plywood material for benchmark reference. These data are included in [Appendix A.1](#) for the same reason. Although the cone calorimeter testing on the materials was performed at three heat fluxes, only one each of NFPA 286 and ASTM E162 tests were performed, hence in the table only one line of the three has a test result.

All the ASTM E1354 and E162 data are tabulated in [Appendix A.2](#). The HRR results included in the database are from both ASTM E1354 and ISO 5660-1 cone calorimeter tests, and common output parameters were listed for each sample. Reported data usually contained, at a minimum, time to ignition (s), peak HRR ( $\text{kW/m}^2$ ), and time to peak HRR (s). Additional parameters often included the sample thickness (mm), initial mass (g), percentage burned, flame duration (s), total heat released ( $\text{MJ/m}^2$ ), average effective heat of combustion ( $\text{MJ/kg}$ ), average heat released at 300 seconds ( $\text{kW/m}^2$ ), and average heat release for the entire test ( $\text{kW/m}^2$ ). Smoke specific extinction area (SEA) ( $\text{m}^2/\text{kg}$ ) was also reported for some tests. A 'Sample ID' field was created to describe the configuration or sample material detail.

ASTM E162 flame spread rating data were also included for many of the same materials for which cone calorimeter data were available. Since the goal of this study is to determine a material qualification standard which uses HRR parameters, no flame spread rating results were included which were not accompanied by cone calorimeter data.

Room corner test data per NFPA 286 standard were sparse, and only four tests on materials used in passenger rail cars were found. In lieu of more full or real scale test data for the materials, [Appendix A.3](#) contains mockup and furniture calorimeter data from multiple sources. Many of the items tested in the furniture calorimeter tests were seats, and mockups often included both seats, wall materials, and windows. Since these data come from a variety of literature, each test configuration was unique, and for full details the original source must be consulted. These data, while not relevant in the empirical model development, will provide a convenient reference for input and validation data for the computational modeling efforts.

## 2.3 Section Summary

The database includes over 700 items in total, and over 650 of these include HRR data from cone calorimeter tests. These data will aid in the development of an empirical model to qualify passenger rail car materials for fire safety. The substantial lack of NFPA 286 room-corner test data for the materials used in rail cars indicates the need

for additional experimental testing to relate large scale (room-corner test) behavior to small-scale (cone calorimeter) test data.

### 3. Quantifying Plausible Fire Exposure for Rail Car Fires

---

The focus of this section is to quantify plausible initiating fire exposures on the interior of rail cars and identify which standard initiating fire best represents these exposures.

Initiating fires are objects that burn inside of a rail car that serve to ignite the interior finish (walls, linings, seating, etc.) of the rail car. There are a variety of objects that could be considered as initiating fires inside of rail cars including passenger carry-on items (computers, baggage), trash, and flammable liquid arson-related fires. Some data exist in the literature describing the burning of these items. To adequately evaluate the performance of interior finish materials, the exposure fire in standard testing should be representative of the initiating fires that could occur in the end-use application.

One way of evaluating the flammability fire performance of interior finish materials is to conduct a large-scale test in a room lined with the material. The room-corner fire test has evolved as the fire industry standard for evaluating wall and ceiling lining materials. In this test, a specified initiating fire is placed in a corner lined with the interior finish to assess its flammability performance. The initiating fire HRR profile as a function of time controls the severity of the room-corner test. To evaluate which standard fire exposure would be most appropriate for rail car applications, the plausible initiating fires for the rail car interior need to be compared with the standard initiating fire exposures.

This section provides a review of realistic initiating fires that may occur inside rail cars from accident reports and international scientific literature. In addition, initiating fires from different room-corner fire test standards used to evaluate combustible interior finish were reviewed and compared with realistic initiating fires. Based on the review and comparison of these data, a standard fire for rail car applications in a room-corner fire test was recommended.

#### 3.1 Review of Realistic Initiating Fires

A review was conducted on identifying the different types of initiating fires that have been considered for exposure of rail car interior finish materials. [Section 2](#) presented an extensive analysis of HRR measurements available for rail car interior finish components. Items other than these interior finish materials may serve as initiating fires including trash, luggage, pillows, etc. as shown in [Figure 3-1](#).



**Figure 3-1. Representative interior environments of rail cars**

The scientific literature was reviewed to identify measurements of the HRR of items as a function of time to compare with standard initiating fire exposures. Peak HRR is often reported as the critical result for full-scale and real-scale calorimetry tests. However, peak HRR alone does not provide a full picture of realistic initiating fires and their growth. As a result, this report focuses on time-resolved HRR data.

HRR curves as a function of time for items that may be brought onto a rail car are shown in [Figure 3-2](#) [7]–[9]. Some fires, such as shirts and trash bags, reached their peak HRR within 1–2 minutes (60–120 s) and typically lasted less than 10 minutes (600 s). In other cases, it took longer, 5–20 minutes (300–1,200 s), for fires to reach peak HRRs but the fires could last 10–50 minutes (600–3,000 s). The peak HRR varied significantly, from 25 kW to more than 400 kW, for different fires; however, the majority of the fires had a duration of 15 minutes (900 s) or less.



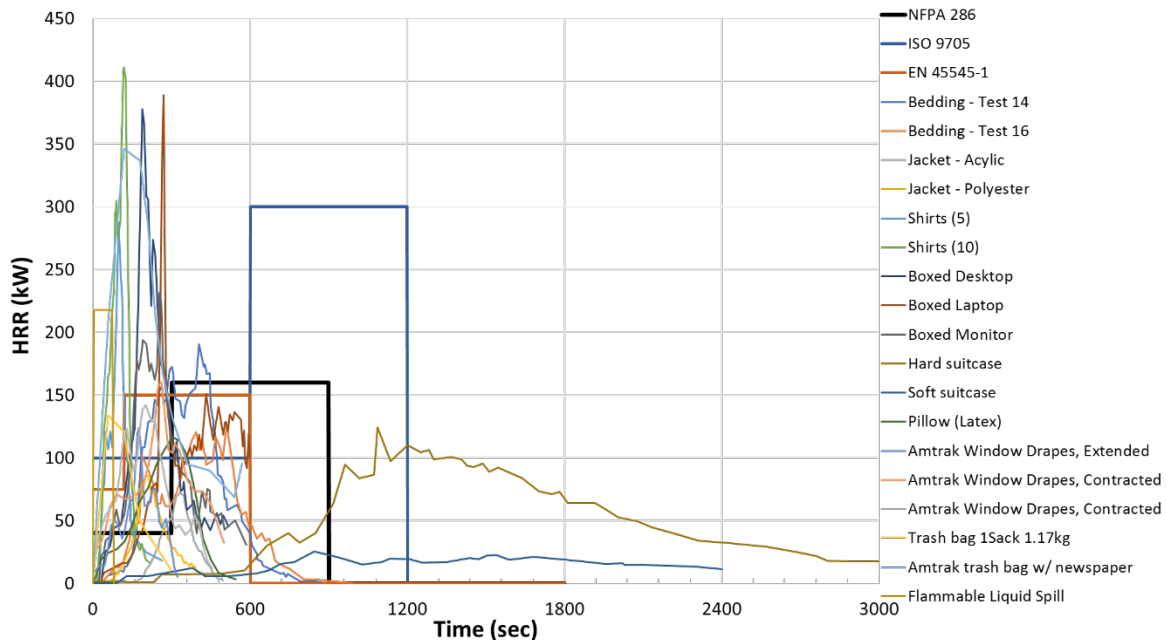


**Figure 3-2. HRR curves of initiating fires in rail cars from literature**

### 3.2 Room Fire Testing Standards and Their Application to Rail Car Fires

A room-corner fire test is often used to evaluate the flammability of interior finish materials since fire growth is fastest in a corner [28]. There are two primary standards for room-corner fire tests used to evaluate interior finish materials: ISO 9705 [10] and NFPA 286 [11]. These standards contain the details of the tests including recommended exposure fire burners and HRRs. Other rail car standards and guides (including EN 45545-1 [12] and ASTM E2061[29]) provide guidance on rail car specific exposure fires. Details of each standard are summarized in the following subsections.

#### 3.2.1 ISO 9705

The International Organization for Standardization (ISO) published the *Fire Tests -- Full-Scale Room Test for Surface Products* in 1993 (revised 1996) in ISO 9705 [10]. The test is conducted in a room with dimensions of 12 ft. (3.66 m) deep, 8 ft. (2.44 m) wide, and 8 ft. (2.44 m) high with a doorway having dimensions of 2.6 ft. x 6.6 ft. (0.79 m x 2.0 m). The back wall, two side walls and ceiling are lined with the combustible interior finish material to be evaluated. The initiating fire in the room consists of a propane sand burner placed flush against the test specimen in one of the back corners of the room. Two options are given for sand burner dimensions and HRR output levels. The standard initiating fire is a 0.6 ft. x 0.6 ft. (0.17 m x 0.17 m), 0.5 ft. (0.15 m) high burner with a HRR of 100 kW for 10 minutes followed by a HRR of 300 kW for 10 minutes with a total test duration of 20 minutes. The alternative initiating fire is a 1 ft. x 1 ft. (0.30 m x 0.30 m), 1 ft. (0.30 m) high burner with a HRR of 40 kW for 5 minutes and 160 kW for 10 minutes with a total test duration of 15 minutes.

### 3.2.2 NFPA 286

The NFPA published *The Standard Methods of Fire Tests for Evaluating Contribution of Wall and Ceiling Interior Finish to Room Fire Growth* in 2015 in NFPA 286 [11]. The test is conducted in a room with the dimensions 12 ft. (3.66 m) deep, 8 ft. (2.44 m) wide, and 8 ft. (2.44 m) high with a doorway having dimensions of 2.6 ft. x 6.6 ft. (0.79 m x 2.0 m). The back wall, side walls, and ceiling are lined with the combustible interior finish sample to be evaluated. The initiating fire in the room consists of a propane sand burner placed flush against both walls in one of the back corners of the room. The initiating fire is a 1 ft. x 1 ft. (0.30 m x 0.30 m), 0.5 ft. (0.15 m) high burner with the top surface of the burner is 1 ft. (0.30 m) above the floor. The burner HRR regiment is 40 kW for 5 minutes followed by 160 kW for 10 minutes for a total test duration of 15 minutes. Flashover is defined to have occurred when two of the following are true: HRR exceeds 1 MW, heat flux at the floor exceeds 20 kW/m<sup>2</sup>, average upper layer temperature exceeds 600 °C, flames exit doorway, or a paper target on the floor auto ignites.

### 3.2.3 EN 45545

The European Union published the *Railway applications – Fire protection on railway vehicles – Part 1: General* in 2013 in EN 45545-1 [12] and *Railway applications – Fire protection on railway vehicles – Part 2: Requirements for fire behavior of materials and components* in 2016 in EN 45545-2 [2]. Five ignition models are described in EN 45545-1 which can be used to describe different ignition scenarios inside of a rail car. These are summarized in [Table 3-1](#). In test series conducted by researchers [7] [30] [31], full-scale compartment testing has used Ignition Model 5 (Arson) to represent an initiating fire. This standard emphasizes full-scale testing of seats as well as components in rail cars.

**Table 3-1. EN 45545-1 Ignition models [12]**

Ignition Model	Represents	Source Profile
Model 1	Arson or vandalism (such as newspapers or rubbish)	Flaming source 7 kW for 3 min generating a flux of 25–30 kW/m <sup>2</sup>
Model 2	Early developing fire on surfaces near to the fire (for example horizontal seats and floors)	Radiant flux of nominal value 25 kW/m <sup>2</sup> applied to an area of 1.08 ft <sup>2</sup> (0.1m <sup>2</sup> )
Model 3	Developed fire or the effect of a developing fire on surfaces above or alongside the fire (for example wall and ceiling surfaces)	Radiant flux of nominal value 50 kW/m <sup>2</sup> applied to an area of 1.08 ft <sup>2</sup> (0.1m <sup>2</sup> )
Model 4	Arcing resulting from normal operation of high power electrical equipment and low power electronic equipment faults	Flaming source 1 kW for 0.5 min

Ignition Model	Represents	Source Profile
Model 5	Luggage fires and arson	Flaming source 75 kW for 2 min followed by 150 kW for 8 min

### 3.2.4 EN 13823 - Single Burning Item (SBI)

Test method EN 13823—Single Burning Item (SBI) test was developed for the European Commission to provide the key test method for assessing the fire performance of construction products [32]. The SBI test is an intermediate-scale open corner method for measuring lateral flame spread, rate of heat release, propensity to produce flaming drops and rate of smoke production. The test specimens comprise two vertically orientated walls, arranged to form a 90-degree corner. It provides data suitable for comparing the performance of materials, composites, or assemblies that are used primarily as the exposed surfaces of walls. The test procedure sets out to simulate the performance of these products fixed to the walls and ceiling of a small room under end-use conditions where the ignition fire is a nominal 30 kW SBI such as a wastebasket in a corner of the room. The testing period is 20 minutes.

### 3.2.5 ASTM E2061

The ASTM published the *E2061-15 Standard Guide for Fire Hazard Assessment of Rail Transportation Vehicles* in 2015, intended for use by those undertaking the development of fire hazard assessments for rail transportation vehicles and products contained within rail transportation vehicles [29]. It provides information on an approach to develop a fire hazard assessment, but fixed procedures are not established. It has been written to assist professionals, including fire safety engineers, who wish to assess the fire safety of rail transportation vehicles, during or after their design. In the E2061-15 standard guide, a list of fires that originate within the rail car are recommended for consideration in such assessments:

- a. An incendiary ignition involving the use of accelerants and prior damage exposing the fillings of the two upholstered seats nearest the point of ignition
- b. Trash fire that begins under a passenger seat assembly and spreads to that seat assembly
- c. Cooking fire originating at the cooking equipment and involving initial ignition of cooking fuel or oil, if cooking is permitted on any passenger vehicle
- d. Small open-flame ignition of bedding in an unoccupied bed in a vehicle with other beds occupied by sleeping people, if there are one or more vehicles provided for overnight sleeping
- e. Small open-flame ignition of a combustible, for example trash, in a fully filled cargo vehicle, if there are one or more vehicles provided for cargo, or cargo storage space is provided within a passenger vehicle

The initiating fires in [Figure 3-2](#) provide fires that represent Options a, b, d, and e. Option c would be in a kitchen area where combustible wall linings would not be present; therefore, this initiating fire is not relevant for the current report.

### **3.3 Application of Room Fire Exposures in Literature**

A literature review was conducted to identify studies that used initiating fires to evaluate the flammability or fire growth behavior inside of rail cars. This includes research on full-scale and real-scale testing of rail car materials and assemblies using standard room-corner fire tests and large-scale mock-up fire growth testing.

#### **3.3.1 Standard Fire Exposure Testing**

Large-scale rail car mock-up tests were performed by several research groups to quantify the initial fire growth and HRR of rail car interiors. A series of experiments were conducted to investigate the contribution of rail car interior finish wall materials on fire growth in rail cars as part of the FIRESTARR [7]. The initiating fire was Ignition Model 5 in EN 45545-1, with a HRR of 75 kW for 2 minutes followed by a HRR of 150 kW for 8 minutes. A series of reduced-scale experiments were also conducted to investigate the contribution of rail car interior finish wall materials on fire growth in rail cars as part of the FIRESTARR program [7] [15]. Tests were performed in the SBI standard corner test [32] with a 75 kW fire for 10 minutes in a corner lined with the combustible sample.

A series of tests in an open corner beneath a calorimetry hood were conducted to measure the HRR contribution of seating and wall linings for model validation by Lee and Park et al. [30] [33]. The tests were conducted within ISO 9705 room corner test equipment. A 0.6 ft. x 0.6 ft. (0.17 m x 0.17 m) sand burner with a HRR consistent with the EN 45545-1 Ignition Model 5 was used as the initiating fire. Park and Lee et al. [34] also performed a series of tests on a mock-up rail car section, which was a rectangular parallel-piped test room 11.8 ft. (3.6 m) long, 7.9 ft. (2.4 m) wide, and 7.9 ft. (2.4 m) high. The initiating fire was placed between the seats, a sand burner of ISO 9705 standard burner size starting with the EN 45545-1 Ignition Model 5 for the first 10 minutes, followed by an increase in HRR of 50 kW each additional 2 minutes [33]. This was done to determine the initiating fire HRR that would cause the interior finish materials to contribute sufficiently to result in flashover.

The NASFM with Underwriters Laboratory (UL) conducted an experimental study in 2008 to evaluate the use of cost-effective, more modern tests to improve material fire safety on rail cars [35]. Their study included ASTM E1354 cone calorimeter tests conducted on rail car materials as well as NFPA 286 [11] standard room corner fire tests on these materials. Four samples were included in this study: two rail car lining materials, a fiber reinforced plastic (FRP) used in a different application, and ordinary plywood. The rail car materials and the FRP met the ASTM E162 requirements, but the plywood did not [15]. All materials except the FRP caused flashover in the room-corner fire test.

### 3.3.2 Other Fire Exposure Testing

A series of tests were conducted within an Amtrak passenger rail coach car [36] [37]. The testing indicated that an initiating fire size between 25 kW and 200 kW is necessary to promote significant flame spread. In a follow-on study, a large-scale test inside a portion of an actual rail car was performed by Capote et al. [15] using a backpack as an initiating fire (35 to 45 kW fire) with its location modified from case to case. In the four tests, the ignition source was placed under the seat in the eighth row adjacent to the aisle, on the seat in the eighth row adjacent to the aisle, on the seat in the fifth row adjacent to the aisle and on the seat in the first row adjacent to the aisle, respectively. The contribution of combustibles was not sufficient to cause the rail car interior finish materials to reach flashover.

A series of mock-up rail car tests were conducted by Claesson et al. using an enclosure 20 ft. long, 8 ft. high and 10 ft. wide (6 m long, 2.44 m high and 3 m wide) with a side door and open end beneath a hood calorimeter [38]. In their tests, the initiating fire consisted of wood cribs and 1 liter of petrol in a milk container, respectively. The estimated HRR was 150 kW per wood crib. The peak HRR of the petrol used for ignition was found to be 440 kW. It was found that an ignited pool of petrol releases a high amount of heat during a short period. For the fire to spread, fuel in the vicinity of the pool must ignite from this heat, but since the heat from the petrol will start to decay quickly the ignited fuel must be able to maintain a sufficient heat release for the fire to keep spreading.

A series of ignition experiments were conducted by White and Dowling [35] in a full-scale rail car to evaluate what types of fires could cause flashover. The initiating fire occurred with a 0.13 gallon (0.5 liter) kerosene fuel spill on the seat and wall, 1.32 lb. (0.6 kg) of crumpled paper on the seat by a wall, and 0.66-1 lb. (0.3–0.45 kg) of paper behind the seat [39]. The fire resulted in the rail car interior finish materials reaching flashover conditions.

### 3.4 Comparison of Fire Exposures

The standard exposures described above were compared with plausible, real fires to determine which standard exposure best represents a real fire inside a rail car. The HRR, total heat release, flame height and peak heat flux from the fire to the wall were considered in the comparison.

The HRR curves of the standard fire exposures are shown in [Figure 3-3](#) [10]–[12]. ISO 9705 has the longest duration of 20 minutes as well as the highest HRRs, 100 kW for 10 minutes followed by 300 kW for another 10 minutes. The EN 45545-1 Model 5 has the shortest duration of 10 minutes and lowest HRRs, 75 kW for 2 minutes and then 150 kW for 8 minutes. NFPA 286 starts with a HRR of 40 kW for 5 minutes followed by 160 kW for 10 minutes, which is between ISO 9705 and EN 45545-1 in terms of both HRR and duration. The EN 13823 is not shown in [Figure 3-3](#), because this is a reduced scale test.

The red dashed line in [Figure 3-3](#) is not a standard fire exposure, but it is a variation on the EN 45545-1 Ignition Model 5 used by Park et al. [34] in a study to evaluate the flashover potential of mock-up rail car sections. The EN 45545-1 Ignition Model 5 was

used for the first 10 minutes and then followed by an increase in HRR of 50 kW each additional 2 minutes. In this case, the fire developed rapidly and flame spread had involved sufficient combustible materials by 11–12 minutes (660–720 s) resulting in flashover conditions.

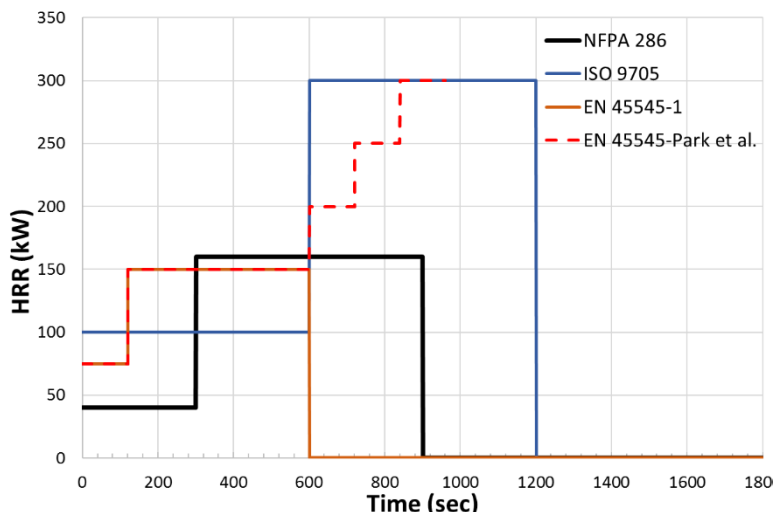
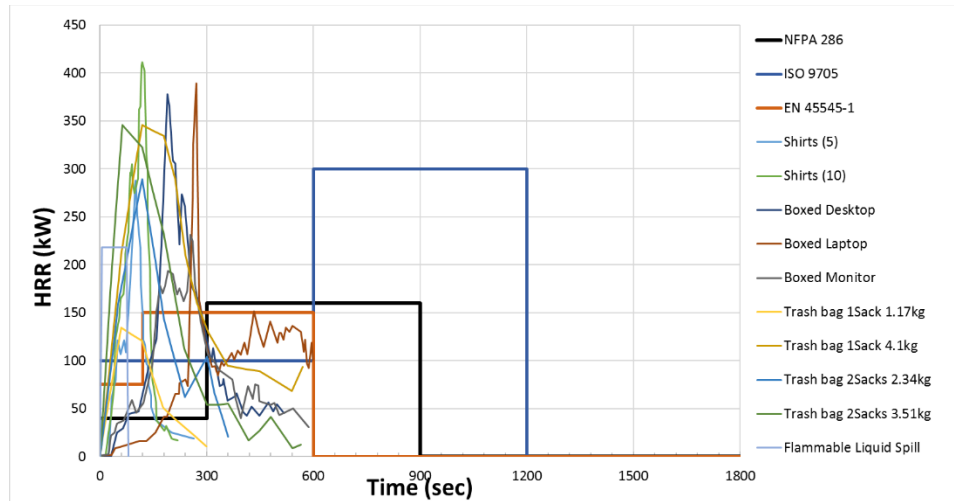


**Figure 3-3. Initiating fires from standard room corner fire tests**

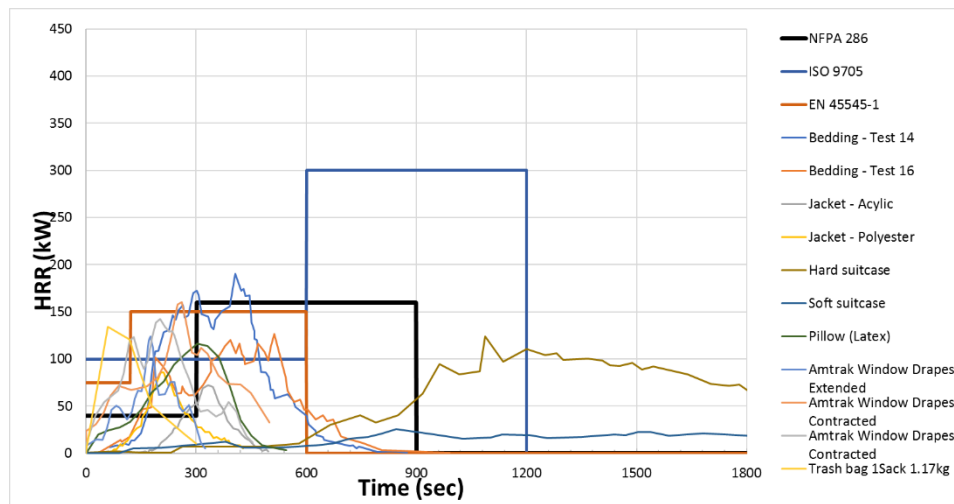
### 3.4.1 HRR and Duration

Standard initiating fire HRR and durations were compared with different realistic fires that are plausible inside of rail cars. As presented in [Figure 3-2](#), some of the real fires had high peak HRRs and short durations while others had low peak HRRs and long durations. As a result, the realistic fires were divided as two groups, a) high peak HRR and short duration and b) low peak HRR and long duration. These groups were compared with standard fire exposures in [Figure 3-4](#).

As shown [Figure 3-4](#), the ISO 9705 standard has a HRR of 300 kW, which is comparable to real fires with high peak HRRs. However, these higher HRRs only last for up to 5 minutes while the ISO 9705 exposure at 300 kW lasts for 10 minutes. The HRRs of EN 45545-1 Ignition Model 5 and NFPA 286 standards are more comparable to the low peak HRR/long duration real fires, though the duration of most real fires is less than 10 minutes compared to the 15-minute duration for the NFPA 286. The exception to this are the hard and soft suitcase fires, which have a lower HRR but longer than 30-minute burning duration.



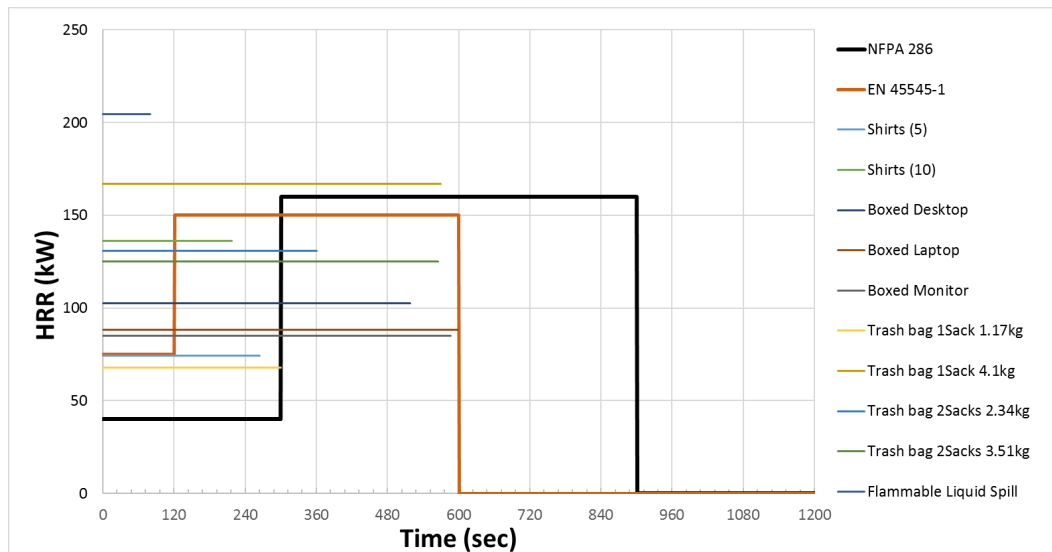
(a)



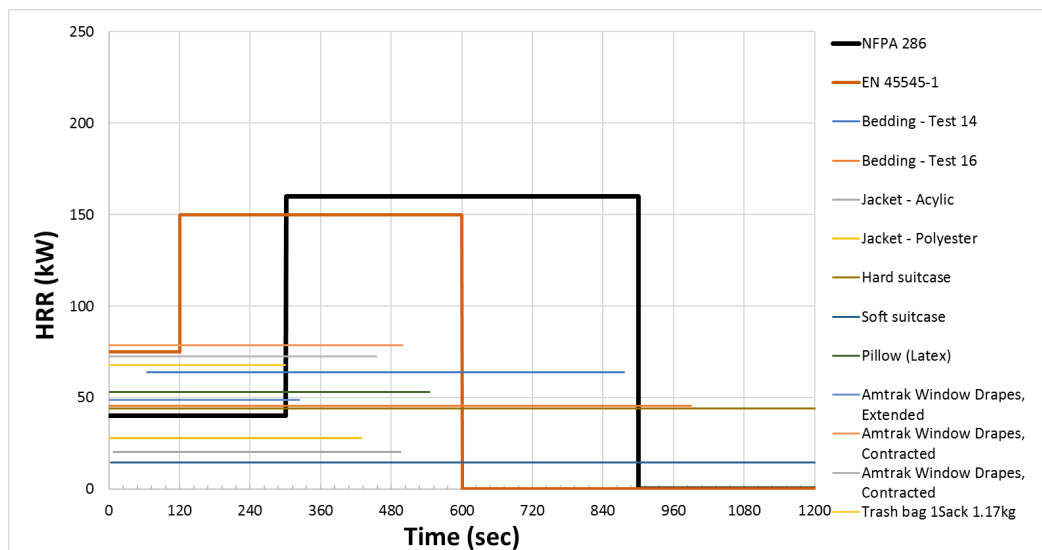
(b)

**Figure 3-4. Standard fire exposures compared with HRR curves of different realistic fires, (a) high peak HRR and short duration and (b) low peak HRR and long duration**

The realistic fire HRRs vary with time and only remain at peak levels for a short (less than 5 minute) period. Therefore, it is worthwhile to compare the average HRRs of these real fires to the standard fire exposures as in [Figure 3-5](#). The average HRRs for nearly all fires were lower or within 5 percent of the 160 kW HRR of the NFPA 286 exposure. In addition, most fires lasted less than approximately 10 minutes, which is the duration of the 160 kW HRR level in the NFPA 286 test. The flammable liquid spill fire has a 205 kW HRR, but the duration was only 85 seconds in total. The longer duration fires seen in [Figure 3-5\(b\)](#) had lower HRR levels.



(a)



(b)

**Figure 3-5. Standard fire exposures compared with average HRRs of different fires, (a) high peak HRR and short duration and (b) low peak HRR and long duration**

Another metric to consider when comparing the different fires is the total heat release, which is related to both average HRR and duration. A comparison of the total heat release from the realistic and standard fires is provided in [Table 3-2](#). It can also be seen from [Table 3-2](#) that the total heat release using the NFPA 286 standard is greater than or equal to that of nearly all realistic exposure fires for rail cars. The only exception is the hard suitcase filled with 22.8 lb. (10.34 kg) of clothes, which has an average HRR of 44 kW and 50 minute duration. Due to the lower HRR of the exposure, the hard suitcase is not considered to be a more severe exposure compared with NFPA 286.



**Table 3-2. Total HRR of initiating fires**

Standard Fires	Average HRR(kW)	Duration (sec)	Total Heat Release (kJ)
NFPA 286 (Step 2, 160 kW HRR for 10 min.)	160	600	96000
ISO 9705 (Step 2, 300 kW HRR for 10 min.)	300	600	180000
EN 45545-1 Model 5 (Step 2, 150 kW for 8 min.)	150	480	72000
Initiating Fires	Average HRR(kW)	Duration (sec)	Total Heat Release (kJ)
Bedding - Test 14	64	875	55816
Bedding - Test 16	46	990	45209
Jacket - Acrylic	20	498	10148
Jacket - Polyester	28	428	11945
5 Shirt	74	263	19563
10 Shirt	136	217	29590
Boxed Desktop	103	518	53138
Boxed Laptop	88	598	52756
Boxed Monitor	85	588	49862
Hard suitcase	44	3244	143408
Soft suitcase	14	2402	34683
Pillow (Latex)	53	545	29025
Amtrak Window Drapes, Extended	49	324	15793
Amtrak Window Drapes, Contracted	79	500	39407
Amtrak Window Drapes, Contracted	72	455	32954
Trash bag 1Sack 1.17kg	68	300	20371
Trash bag 1Sack 4.1kg	167	570	95113
Trash bag 2Sacks 2.34kg	131	360	47069
Trash bag 2Sacks 3.51kg	125	568	70780
Amtrak trash bag w/ newspaper	167	570	95423
Spill fire with 1mm depth	204	85	17340

The above comparison of average HRR, total heat released, and fire duration for the different fires demonstrates that the NFPA 286 fire is the most representative of the realistic initiating fires. It has a duration that bounds most realistic initiating fires and a HRR during the second step that is greater than the average HRR for nearly all realistic fires. In addition, its total HRR bounds all the realistic fires.

### **3.4.2 Flame Height and Peak Heat Flux**

The severity of the fire exposure can also be assessed by comparing the height of the flame as well as the heat transfer from the fire to an adjacent wall as a heat flux. Fires in a corner of a room have been shown to cause more rapid flame spread and growth to flashover compared to cases with fires in other locations within the room [40]. As a result, empirical correlations exist to predict the flame height and peak heat flux to the corner. These were used to compare the exposures for both standard and realistic fires.

Flame height was calculated using a correlation that is based on both the HRR of the fire and fuel diameter [40],

$$L_{f,tip} = 5.9D \left( \frac{Q}{\rho_{\infty} C_p T_{\infty} \sqrt{g} D^{5/2}} \right)^{1/2} \quad (3-1)$$

where  $L_{f,tip}$  is height of the flame tip (m),  $Q$  is the fire HRR (kW),  $D$  is the fuel diameter (m),  $\rho_{\infty}$  is the density of ambient air (kg/m<sup>3</sup>),  $C_p$  is the specific heat of ambient air (kJ/kg),  $T_{\infty}$  is the temperature of ambient air (K), and  $g$  is the gravitational acceleration constant (m/s<sup>2</sup>). Given the fuel diameter and HRR of an initiating fire, the flame tip height can be obtained using Equation (3-1). In the realistic fire tests where the fuel diameter was not provided, it was estimated as,

$$D = \left( \frac{Q}{Q''} \right)^{1/2} \quad (3-2)$$

where  $Q''$  is heat release rate per unit floor area (HRRPUA) that the fire occupies. From the same experimental study, empirical correlations were developed to predict the heat flux from the fire to the walls and ceiling of a corner [40]. The peak heat flux from the fire to the corner walls was determined using the following correlation,

$$\dot{q}_{peak}'' = 120[1 - e^{-4.0D}] \quad (3-3)$$

where  $D$  is fuel diameter (m).

The fuel diameter, flame height, and peak heat flux of the initiating fires were calculated from Equations (3-1)–(3-3) and are given in Table 3-3. For realistic fires other than the flammable liquid, the diameter was determined using a HRRPUA 400 kW/m<sup>2</sup> [40], which is generally representative of the HRRPUA for Class A fuel packages (ordinary combustibles such as wood, paper, trash or anything else that leaves an ash). For the standard fire tests, only the HRR of the second step was used for results in Table 3-3.

The diameter of different realistic initiating fires varies from 0.8–2.3 ft. (0.23–0.71 m) and are generally greater than the diameters of standard fire burners. The flame height of ISO 9705 fire is 15.8 ft. (4.8 m), which is 6.6–12.5 ft. (2.0–3.8 m) higher than the highest flame among the initiating fires. Flame heights of EN45545-1 and NFPA 286 initiating fires are approximately 9.8 ft. (3.0 m), which is 0.6–3.3 ft. (0.2–1.0 m) higher than the flame heights of all initiating fires. Even though the HRR of some realistic initiating fires are similar to the NFPA 286 and EN45545-1 standards, their flame heights are lower due to their larger diameters.

The peak heat flux of the ISO 9705 fire is 59 kW/m<sup>2</sup>, which is lower than the peak heat flux of all the realistic initiating fires. EN45545-1 Model 5 and NFPA 286 have a similar peak heat flux of approximately 85 kW/m<sup>2</sup>. This is lower than some realistic initiating fires, but is more representative of peak heat fluxes from realistic initiating fires compared with the ISO 9705 fire. Based on flame height and peak heat flux, the NFPA 286 and EN45545-1 Model 5 fires are most representative of the realistic initiating fires.

**Table 3-3. Fuel diameter and flame height of standard fires and realistic initiating fires**

<b>Standard Fires</b>	<b>Average HRR(kW)</b>	<b>Diameter (m)</b>	<b>Flame Height (m)</b>	<b>Peak Heat Flux (kW/m<sup>2</sup>)</b>
NFPA 286 (Step 2, 160 kW HRR for 10 min.)	160	0.31	3.03	85
ISO 9705 (Step 2, 300 kW HRR for 10 min.)	300	0.17	4.80	59
EN 45545-1 Model 5 (Step 2, 150 kW for 8 min.)	150	0.30	2.94	84
<b>Initiating Fires</b>	<b>Average HRR(kW)</b>	<b>Diameter (m)</b>	<b>Flame Height (m)</b>	<b>Peak Heat Flux (kW/m<sup>2</sup>)</b>
Bedding - Test 14	64	0.36	1.84	91
Bedding - Test 16	4	0.34	1.58	89
Jacket - Acrylic	20	0.23	1.17	71
Jacket - Polyester	2	0.26	1.31	78
5 Shirt	74	0.43	1.89	99
10 Shirt	13	0.58	2.38	108
Boxed Desktop	103	0.51	2.14	104
Boxed Laptop	8	0.47	2.02	102
Boxed Monitor	85	0.46	1.99	101
Hard Suitcase	4	0.33	1.56	88
Soft Suitcase	14	0.19	1.02	64
Pillow (Latex)	5	0.36	1.67	92
Amtrak Window Drapes, Extended	49	0.35	1.62	90
Amtrak Window Drapes, Contracted	7	0.44	1.93	100
Amtrak Window Drapes, Contracted	72	0.43	1.87	98
Trash bag 1Sack 1.17 kg	6	0.41	1.83	97
Trash bag 1Sack 4.1 kg	167	0.65	2.56	111
Trash bag 2Sacks 2.34 kg	13	0.57	2.34	108
Trash bag 2Sacks 3.51 kg	125	0.56	2.30	107
Amtrak trash bag w/ newspaper	16	0.65	2.57	111
Spill fire with 1 mm depth	204	0.71	2.76	113

Figure 3-6 presents a comparison of the realistic initiating fire exposures with different initiating fires in room-corner fire test standards. Average HRR, duration, total heat release, flame height and peak heat flux of all fires were normalized by the NFPA 286 standard (step 2) initiating fire. Only the HRR of the second step was used for the standard fire tests in the comparison. For the ISO 9705 standard fire duration, the total heat release and flame height over-estimated the realistic fires. The duration and total heat release of the EN 45545-1 Ignition Model 5 standard fire under-estimated the realistic fires as shown in Figure 3-6. The NFPA 286 standard initiating fire is consistent

with nearly all the realistic fires in terms of HRR, duration, total heat release and flame height.

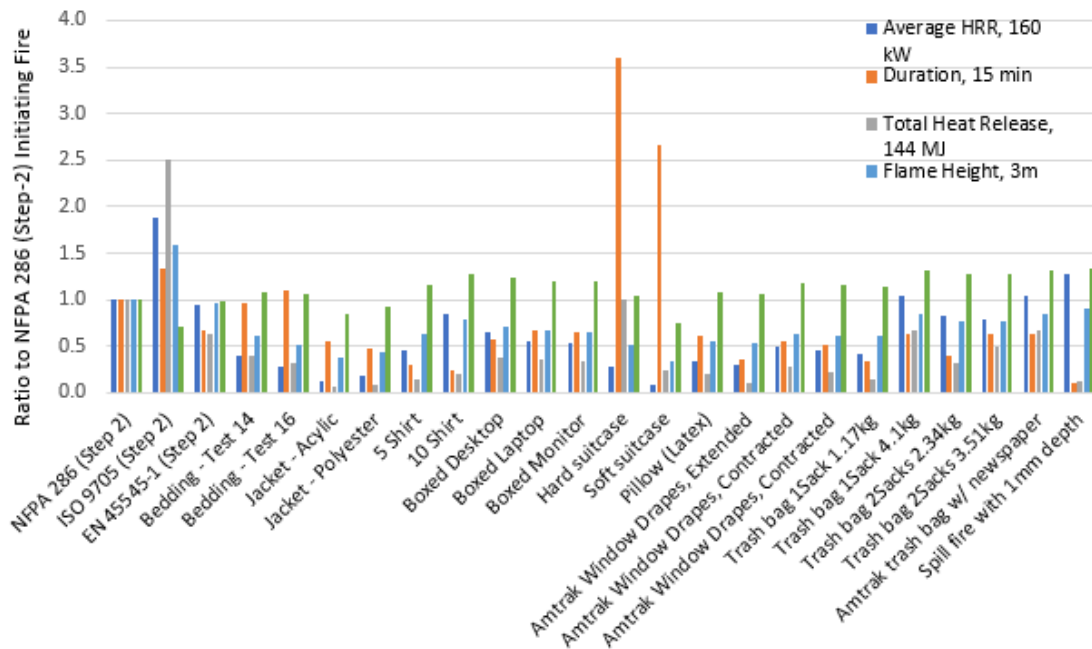


**Figure 3-6. Comparison of real initiating fires with fire test standards**

### 3.5 Section Summary

Initiating fire exposures within a rail car were quantified and compared to different initiating fires in room-corner fire test standards. The standard initiating fires were from the ISO 9705 room-corner fire test standard, NFPA 286 room-corner fire test standard, and EN45545-1 Ignition Model 5 European rail car fire standard. The parameters considered to evaluate the standard initiating fires with respect to the realistic fires included peak HRR, average HRR, duration, total heat release, flame height and peak heat flux of various fires.

The analysis in this section demonstrated that the initiating fire in the ISO 9705 standard of 100 kW for 10 minutes followed by 300 kW for 10 minutes has a HRR that bounds realistic fires. However, the ISO 9705 standard initiating fire duration, total heat release, flame height, and heat flux were not consistent with realistic fires. Therefore, the ISO 9705 initiating fire is not recommended for rail applications. The EN 45545-1 Ignition Model 5 standard recommended initiating fire of 75 kW for 2 minutes and 150 kW for 8 minutes had a HRR that was comparable to realistic fires. However, the duration was too short, and the total heat release were low compared with realistic fires. As a result, it is not recommended for evaluating performance of rail applications.

The NFPA 286 initiating fire of 40 kW for 5 minutes followed by 160 kW for 10 minutes was determined to be the most suitable standard initiating fire when compared with realistic initiating fires that are plausible inside of a rail car. This standard initiating fire was found to have a duration that bounds most realistic initiating fires and a HRR during the second step that is greater than the average HRR for nearly all realistic fires. The

NFPA 286 initiating fire has a total HRR and flame height that bound all of the realistic fires, and the peak heat flux is similar to that of realistic fires. As a result, the NFPA 286 initiating fire is recommended for rail car applications.

## **4. Empirical Model for Predicting Flashover in NFPA 286 Room-corner Test**

---

This section introduces an empirical flammability model which was developed to predict whether a material will contribute significantly to the growth of a fire inside a rail car and cause flashover. This model will be used to support the development of the HRR requirements for rail car interior finish materials.

It is common to evaluate the potential for flame spread over an interior finish through a large-scale room-corner fire test. One such test is NFPA 286 room-corner test [11], which is a standard large scale test used to measure the contribution of interior finish materials on fire growth. In [Section 3](#), the NFPA 286 initiating fire was determined to be the most suitable standard initiating fire and is recommended for rail car applications. In this section, an empirical model based on the flammability parameter was developed to predict the occurrence of flashover in a NFPA 286 test using cone calorimeter data as input. The model was validated with existing data which was mostly composed of tests on building material products. The latter phases of this work will further validate this model by conducting cone calorimeter and NFPA 286 tests on rail car interior lining materials, in [Sections 6](#) and [7](#), respectively. The validated model will be sufficiently simple to use allowing for numerous predictions on various material parameters, which will be used as the basis to develop HRR requirements for rail car interior finish.

### **4.1 Flammability Model to Predict Room-Corner Test**

An overview of the room-corner fire test is provided as well as the measurements used in the test to evaluate materials. In order to predict the behavior of interior finish materials in the room-corner test, a flammability parameter was developed based on flame spread theory as used as the basis for an empirical model. Using cone calorimeter data as input, the model was validated with experimental data. The data were selected from two main studies which investigated flashover potential of wood products in the NFPA 286 room. Although the data used to calibrate the flammability model are not from materials which are typically used in rail cars, the non-dimensional formulation allows results from various different materials to be compared. The flammability model uses both burning and ignitability characteristics of the material to determine a flashover potential.

### **4.2 NFPA 286 Room-Corner Test**

There are several different types of standard room-corner fire tests used to evaluate interior finish materials. In the U.S., the NFPA 286 room-corner test is the common standard large scale test used to measure the contribution of interior finish materials on fire growth and regulate the use of interior finish in certain building occupancies [11]. The room is 2.4 m wide by 3.6 m long by 2.4 m high (8 ft. x 12 ft. x 8 ft.), and has a doorway 2 m (79.5 in) in height and 0.78 m (37.5 in) in width. The lining materials are installed on ceiling and walls. A propane gas burner measuring 0.3 m x 0.3 m (12 in x 12 in) is placed in one of the back corners, in contact with the walls. The HRR for the burner is 40 kW for 5 minutes, and then 160 kW for 10 minutes.

The overall HRR from the burner and the interior finish are measured using a hood calorimeter system as shown in Figure 4-1. Gas temperatures are measured near the ceiling and at the top of the door, and heat flux to the floor is also measured. The occurrence of flashover during the test is evaluated through several parameters, including gas temperatures exceeding 600 °C, flame extension outside of the door, overall HRR greater than 1 MW, heat flux to the room floor exceeding 20 kW/m<sup>2</sup>, and ignition of crumpled paper. HRR and smoke production rate requirements are also sometimes used to evaluate the performance of interior finish.

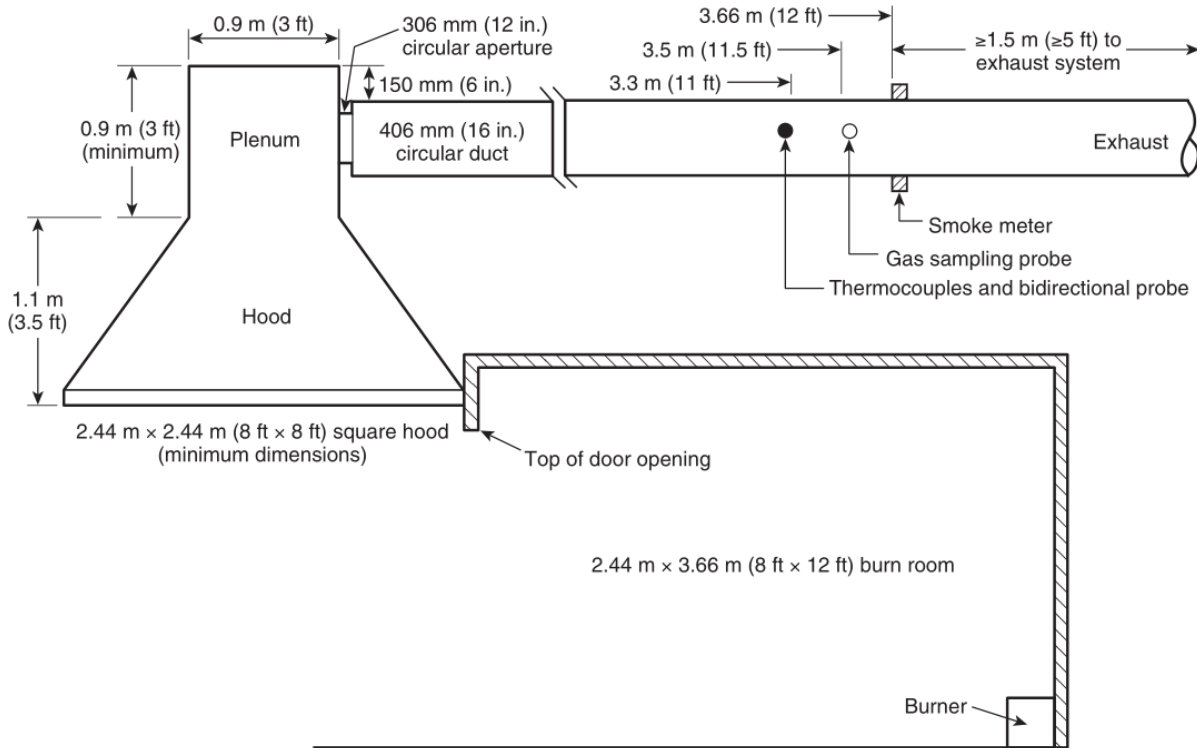


**Figure 4-1. NFPA 286 room configuration with hood and instrumentation (image source NFPA 286) [11]. HRR is determined using the temperature and gas measurements**

### 4.3 Theoretical Basis

The flammability parameter was developed based on flame spread theory based on work by Quintiere, Harkleroad, and Hasemi [41], Mowrer and Williamson [42], and Beyler et al. [43]. A full derivation and explanation of the theoretical approach is contained in Beyler's work [43]. A brief explanation of the governing equations is shown here to demonstrate the physics incorporated in the model.

Equation (4-1) contains the result from the derivation of the flame spread across a material. The flame spread extent is the same as the spread in the pyrolysis zone ( $x_p$ ). The equation provides a mathematical solution to the size of the pyrolysis zone ( $x_p - x_b$ ) after material has begun to burn out ( $t > t_b$ ). The growth or decay of the pyrolysis zone

is dependent on the term in the exponential. The sign of the term in the exponential is dependent on the first group in parentheses, and this factor constitutes the flammability parameter as shown in Equation (4-2).

$$(x_p - x_b) = (x_{p1} - x_{po}) \exp \left[ \left( k_f \dot{Q}'' - \frac{t_{ig}}{t_{bo}} - 1 \right) \left( \frac{t - t_b}{t_{ig}} \right) \right] \quad (4-1)$$

$$= k_f \dot{Q}'' - \frac{t_{ig}}{t_{bo}} \quad (4-2)$$

The flammability parameter is dimensionless and is calculated based on data from cone calorimeter tests.  $\dot{Q}''$  is the material HRR,  $t_{ig}$  is the time to ignition, and  $t_{bo}$  is the burning duration.

There has been much discussion in literature regarding appropriate data to use from the cone calorimeter. In this study, data at 50 kW/m<sup>2</sup> was used with  $\dot{Q}''$  being the test average HRR. This is an average heat flux which would correspond to a flux level from a standard burner to a wall at the base of the burner. The value of 50 kW/m<sup>2</sup> has been used in previous studies with good results [43]. The remaining parameter,  $k_f$ , is the flame height correlating factor. The value of 0.01 m<sup>2</sup>/kW is used, as it has been used in previous studies on this topic [42] [43].

Per Equation (4-1), it is expected that at  $F > 1$ , the flame spread will accelerate and propagate along its surface, eventually causing the room to experience flashover. At  $F < 1$ , the flames are predicted not to propagate along the surface. However, this is the theoretical result and assumes the material exposure conditions are the same as those in the cone calorimeter test where the data are resulting from. This result also does not account for preheating of the material from the hot gas layer. The critical  $F$  value will vary based on the initiating fire level and configuration of the compartment. A flammability parameter of around 0.5 has been found to delineate materials which cause flashover in an ISO 9705 room from those that do not [43] [44], but this critical value may not be valid for the NFPA 286 room-corner test since the ignition source is different. ISO 9705 tests are typically conducted using a 0.17 m square burner with 100 kW HRR for 10 minutes, and then a 300 kW HRR for another 10 minutes. NFPA 286 tests use a 0.3 m burner with 40 kW HRR for 5 minutes, then a 140 kW HRR for 10 minutes. The initiating fire is significantly more severe in ISO 9705. Table 4-1 contains a matrix of how the flammability parameter varies with the cone calorimeter testing data with a physical explanation. Larger average HRR values cause faster flame propagation due to more energy being available to pyrolyze unburned fuel. Longer ignition times slow flame spread, as the material is harder to ignite. Longer time to burn-out results in faster flame spread, as the contribution to the HRR of the fire is prolonged. The converse of these situations is also true. One benefit of this model is it provides a good measure of regulating thickness of a material in the small-scale test, as generally thicker materials will burn longer.



**Table 4-1. Variation of flammability parameters with cone calorimeter test results**

$\dot{Q}''_{avg}$	$t_{ig}$	$t_{bo}$	$F$	Explanation
↑	-	-	↑	Larger small-scale HRR, larger large-scale HRR
↓	-	-	↓	Smaller small-scale HRR, smaller large-scale HRR
-	↑	-	↓	Longer time to ignition, reduced risk of flashover test due to slower spread
-	↓	-	↑	Shorter time to ignition, larger risk of flashover due to faster spread
-	-	↑	↑	Longer burning duration, more capacity of the material to release heat
-	-	↓	↓	Shorter burning duration, less capacity of the material to release heat

#### 4.4 Model Performance

The flammability model was tested with data from varied sources where both cone calorimeter and NFPA 286 tests were performed. NFPA 286 data for materials with accompanying cone calorimeter test results is limited for most modern materials. Despite this, the current modeling scheme was previously used with good results for ISO 9705 room-corner test data as well as other room-corner tests for polymer, textile, and wood wall-coverings and Navy composite ship materials [43] [44]. In these studies, flashover in the compartment was predicted for materials with  $F > 0.5$ , and conversely  $F < 0$  indicated no flashover. This scheme was accurate for about 92 percent of the materials. The ISO 9705 data used by references had much more varied material selection than were available for the NFPA 286 test [43] [44]. Most of the materials for available NFPA 286 test data were wood products.

The results in [Figure 4-2](#) are from NFPA 286 room corner tests on wood and polymer materials. Some polymer foam materials were also included. Flammability parameters were evaluated from cone calorimeter results which used 50 kW/m<sup>2</sup> as the incident heat flux. The materials that did not ignite in the cone calorimeter test were assigned an  $F$  of -1. From the data in the plot, materials with a  $F < 0.6$  did not cause the room to reach flashover, while materials which had  $F > 0.6$  caused flashover. Therefore, a critical  $F$  value of 0.6 is proposed as regulating material selection for those that are acceptable to use as linings of passenger rail cars. For materials that reached flashover, flashover typically occurred after the exposure burner HRR was increased from 40 kW to 160 kW at 300 seconds. For these data, the range for time to flashover was about 230 to 430 seconds.

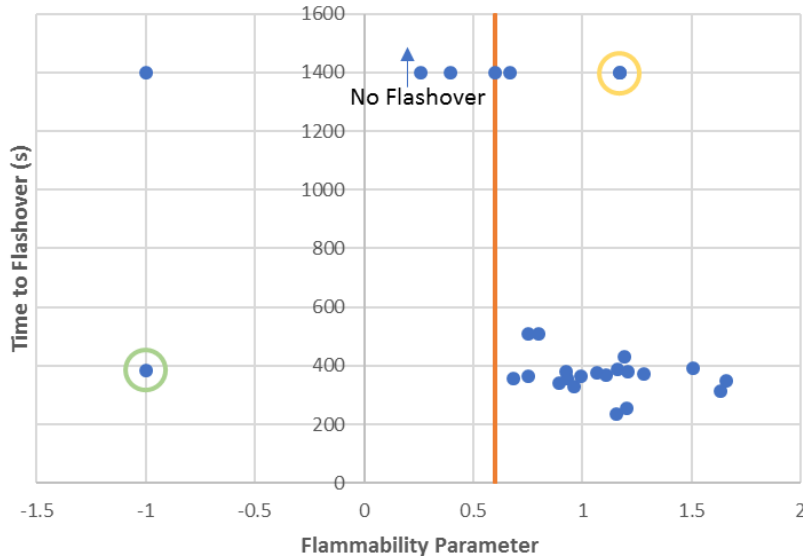


**Figure 4-2. Flashover time vs. flammability parameter. Orange line at  $F = 0.6$  indicates proposed critical value which will cause flashover. Data from [45]–[49]**

There are two materials which did not correlate well with the empirical model, but the complexity of the behavior of these materials makes them difficult to predict using this and other fire growth models. These data points are circled in Figure 4-2 and Figure 4-3. The green-circled data point was polyurethane foam, which caused flashover within 400 s in the NFPA 286 test. However, in the cone calorimeter test, the sample “swelled downward” and did not heat enough to be ignited [45]. This result is not expected for materials that would generally be used in passenger rail car linings.

The yellow circle indicates a test of polystyrene foam, which interestingly did not cause flashover in NFPA 286 tests, yet in the cone calorimeter test at 50 kW/m<sup>2</sup> had a high average HRR [45]. The material burned locally, close to the burner, but flame did not spread to other parts of the room [46]. This behavior is similar to the result for the cone calorimeter test at 25 kW/m<sup>2</sup>, where the sample shrunk and did not ignite. Although the polystyrene did burn in the room corner test, a lot of it melted before burning, which reduced the available material for flame spread.

Both the polystyrene and the polyurethane samples had rather low density, and when exposed to different heat flux levels had varying responses. The empirical flammability model developed here is expected to provide accurate results with the materials typically used as rail car linings, as these materials are generally of higher density and are expected to remain in place and not melt away.

A comparison of peak HRR for the NFPA 286 test and the flammability parameter is shown in Figure 4-3. The data points for polyurethane foam and the polystyrene are circled, and when these are removed a general correlation between these variables is apparent. An increase in flammability parameter usually causes an increase in HRR for the full-scale test.

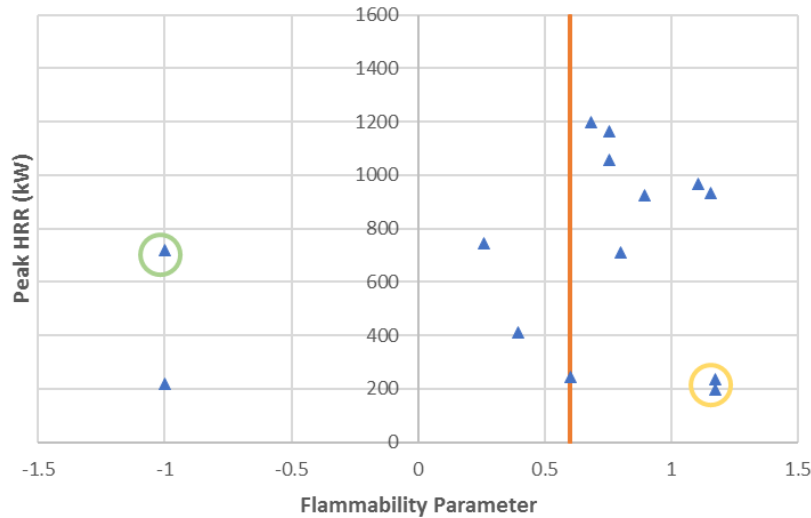


**Figure 4-3. Full scale HRR in NFPA room-corner test vs. flammability parameter. Line at  $F = 0.6$  is proposed critical value. Data from [45] [46]**

#### 4.5 Model Predictions

The empirical model based on the flammability parameter developed in the previous section was then used to predict the behavior of materials in the NFPA 286 test. A histogram of the flammability parameters computed for the approximately 200 rail car materials in the fire behavior database is shown in [Figure 4-4](#). The black line at  $F = 0.6$  indicates the critical value for materials that will or will not cause flashover in NFPA 286. Almost 50 percent of the materials had flammability parameters of less than 0.6, indicating half of the materials would not cause flashover in NFPA 286. No NFPA 286 room-corner test data were available for these materials; therefore, the model could not be validated with rail car materials.

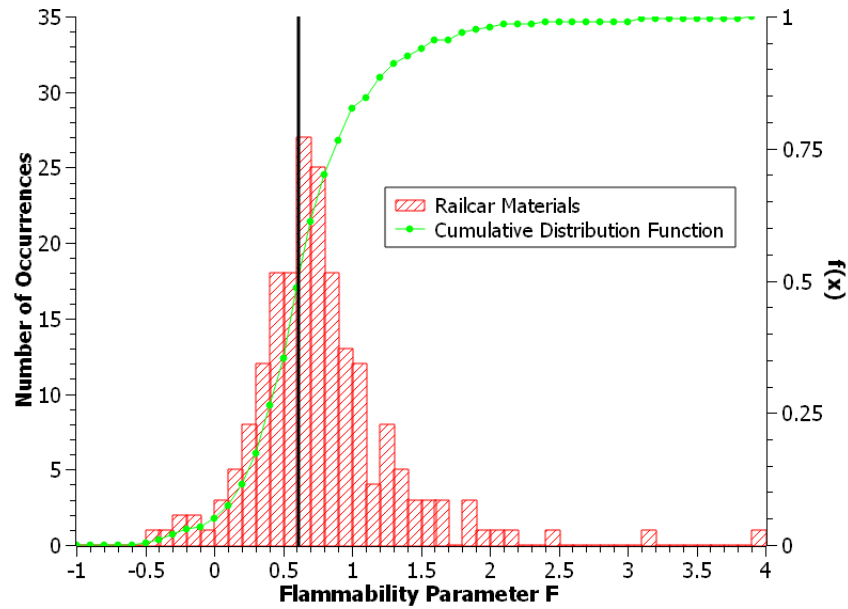


**Figure 4-4. Histogram of flammability parameters for materials in the passenger rail car material database. Black line at  $F = 0.6$  indicates critical flammability parameter which will cause flashover in NFPA 286 room**

Figure 4-5 contains a comparison between the flammability parameter and the flame spread rating. The ASTM E162 standard flame spread rating,  $I_s$ , is the current qualifying test [49]. For most rail car linings  $I_s$  must be less than 35, but some materials have a required flame spread rating of less than 25. In Figure 4-4, materials with  $F > 0.6$  had flame spread ratings from 0-65 and all are predicted using the flammability parameter to cause flashover in NFPA 286.

The orange shaded region in Figure 4-5 denotes materials which currently pass the ASTM E162 test with  $I_s < 25$  but have  $F > 0.6$ , indicating they are predicted to cause flashover in an NFPA 286 room-corner test. Conversely, materials that had  $F < 0.6$  had  $I_s < 25$ , with the exception of a few materials that have an  $F$  close to 0.6. These borderline materials will always be difficult to predict. Based on the results in Figure 4-4, clearly the ASTM E162 test may not adequately screen materials that will perform poorly in the full-scale. This partly due to the fact that the exposure in ASTM E162 is low relative to real fires and the test is a downward flame spread test instead of upward flame spread which is the more hazardous condition. Downward flame spread is opposed to the buoyancy driven airflow, and the hot gases from the fire do not preheat the unignited material. As a result, only radiation from the nearby flame preheats the unignited material. For upward flame spread, the hot gases from the flame preheat the unignited material through both radiation and convection and the preheated region is much larger, resulting in both faster ignition and more ignited material compared with the downward flame spread case.

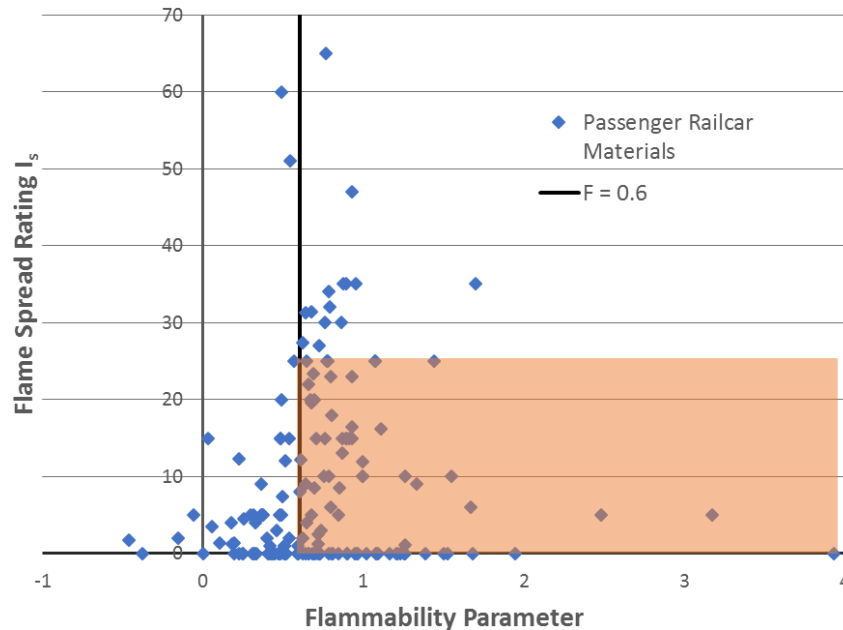


**Figure 4-5. Comparison of ASTM E162 flame spread and flammability parameter**

The orange shaded box represents materials that pass the current specification for ASTM E162, yet are predicted to cause flashover in an NFPA 286 room-corner test

#### 4.6 Section Summary

An empirical model based on the flammability parameter has been developed to predict flashover in NFPA 286 room-corner tests. The model uses cone calorimeter data from tests conducted with a heat flux of 50 kW/m<sup>2</sup>, which is similar to the exposure from a standard ignition source near the base of the flame to a surface. A flammability parameter is calculated from the cone calorimeter test data. A critical value of the flammability parameter to denote when a material may cause flashover in the NFPA 286 test was determined using wood and polymer lining materials that had undergone both cone calorimeter and NFPA 286 room-corner fire testing. Through this analysis, materials with a flammability parameter less than 0.6 are not expected to cause flashover in NFPA 286 while those with a flammability parameter greater than 0.6 are expected to cause flashover. Due to the simplicity of the flammability parameter, many predictions can be conducted to determine the performance for a range of material fire properties. The use of this model on rail car materials will provide a basis for the determination of an appropriate HRR requirement for interior finish materials on rail cars.

An initial assessment was performed on rail car materials where only cone calorimeter data and ASTM E162 flame spread index data were available. Based on the empirical model, nearly 50 percent of the materials were predicted to cause flashover in a NFPA 286 test. In addition, materials with a flame spread index of less than 25 in ASTM E162 were also predicted to cause flashover in NFPA 286. This is in part due to the fact that the exposure in ASTM E162 is low relative to real fires and the test is a downward flame spread test instead of upward flame spread, which is the more hazardous condition.

Both small-scale and large-scale tests on rail car materials will be conducted in latter phases of this work to further validate the empirical model for rail car interior materials so that it can be used to develop performance criteria based on cone calorimeter data.

## 5. Fire Growth Modeling of Room-corner Tests with Rail Car Geometry

---

One way of evaluating the flammability fire performance of interior finish materials is to conduct a large-scale test in a room lined with the material. The NFPA 286 standard room-corner fire test has evolved as the fire industry standard for evaluating wall and ceiling lining materials [11]. In this test, a specified initiating fire is placed in a corner lined with the interior finish to assess the flammability performance. As introduced in [Section 4.2](#), the standard room is 3.66 m (12 ft.) deep, 2.44 m (8 ft.) wide, and 2.44 m (8 ft.) high with a single standard door opening. This room is smaller than a rail car and the door opening is different as well. Some researchers have removed the wall with the door in the NFPA 286 standard room with the intention of creating conditions similar to that in a longer rail car. No studies have performed a comparison of conditions that develop in the NFPA 286 test with a door, the NFPA 286 without the wall with a door, and an actual rail car to see which test would best represent conditions that develop inside of a rail car.

The focus of this section is to determine the difference in the conditions that develop in the NFPA 286 standard room-corner test, the modified NFPA 286 test without the wall with the door, and a rail car geometry using the FDS [13]. In this fire growth modeling, the standard NFPA 286 burner and HRR regimen is used for all three geometries. The solid burning model and fire growth modeling using FDS are validated using cone calorimeter data and NFPA 286 data available in the literature [45] [46]. For the different geometries, a comparison was performed on the gas temperatures, HRR and layer height within the spaces.

### 5.1 Literature Review

A literature review was conducted to identify research that was performed on the influence of combustible materials on rail car fire safety. This included research on fire growth testing and modeling. For both areas, the review assessed the correlations and models that have been used to evaluate the effect of material behavior on fire conditions.

#### 5.1.1 Fire Growth Testing

The existing flammability requirements for materials used on rail cars are based on the small-scale flame spread test ASTM E162 [6]. This is a downward flame spread test with the peak heat flux onto the sample of 25 kW/m<sup>2</sup> and decreasing to 5 kW/m<sup>2</sup> at the end of the sample [28]. Though this test can identify poor performing materials, the materials that meet the standard requirements in NFPA 130 and 49 CFR § 238.103 may be sufficiently combustible to result in significant flame spread when exposed to a moderate to large incipient fire.

Tests that are dominated by upward flame spread (or wind-aided flame spread) are generally used to assess the flammability performance of materials. In addition, the heat flux from the incipient fires in standard tests and real fire exposures will typically range between 50–120 kW/m<sup>2</sup> [28]. It is now widely accepted that large-scale room-corner fire

tests or calorimetry tests on actual scale assemblies be used to quantify the contribution of room linings or assemblies to fire growth. These tests have requirements based on HRR and smoke production rate. In rail research, large-scale fire tests have been performed on mock-up rail car sections as well as entire rail cars to quantify the fire performance of a rail car. Due to the expense of conducting large-scale tests, several research efforts have developed correlations and models to predict large-scale fire behavior with some success.

#### **5.1.1.1 Standard Room-Corner Fire Testing**

Despite their widely-accepted use in the building and ship industries, a limited number of studies used standard room-corner fire tests to assist in evaluating and approving materials for the rail car industry. An overview of the results of these studies is provided in this section.

A series of experiments was conducted to investigate the contribution of rail car interior finish wall materials on fire growth in rail cars as part of the FIRESTARR program [31]. Tests were performed using the SBI standard corner test [32] procedure with a 75 kW fire for 10 minutes in a corner lined with the combustible sample. The linings covered half the wall height and the ceiling. The HRR contribution was measured for four different rail car linings as well as plywood as a reference material. Cone calorimeter tests at 50 kW/m<sup>2</sup> were performed on each lining and used as input for FDS CFD model predictions of the testing.

The NASFM with UL conducted an experimental study in 2008 to evaluate the use of cost-effective, more modern tests to improve material fire safety on rail cars [28]. Their study included ASTM E1354 cone calorimeter tests conducted on rail car materials as well as NFPA 286 standard room corner fire tests on these materials. Four samples were included in this study: two rail car lining materials, a FRP used in a different application, and ordinary plywood. The rail car materials and the FRP met the ASTM E162 requirements, but the plywood did not. All materials except the FRP caused the room to reach flashover. It was found that ASTM E162 test does not accurately reflect fire performance in a larger-scale room-corner fire test.

#### **5.1.1.2 Large-Scale Mock-Up Fire Growth Testing**

Several research groups have conducted large-scale rail car mock-up tests to quantify the initial fire growth and HRR of rail car interiors [15], [19], [30], [31], [33], [36], [38], [39], [50], [51], [34], [52], [53]. These tests were generally the size of a standard fire test room, 12 ft. long by 8 ft. wide by 8 ft. high. (3.66 m x 2.44 m x 2.44 m), that is used to quantify the contribution of room linings to fire growth and were positioned beneath a calorimetry hood to measure the HRR and smoke production rate. These mock-up tests commonly included wall linings, seats, windows, and personal items (i.e., luggage, back packs, etc.). Tests were performed to determine the influence of different incipient fires on fire growth, quantify the fire growth for materials and assemblies used in a specific rail car, assess fire growth when materials with improved fire performance were used, evaluate the impact of including personal items on fire growth, and provide model validation data.



## 5.2 Fire Growth Modeling

Both empirically-based models and computer models were used to predict the HRR and smoke contribution of materials during pre-flashover fire growth. Empirical models have been developed with flame spread theory and cone calorimeter test data to predict the occurrence of flashover in room-corner tests. Computer models have also been used to predict material behavior in room-corner tests as well as the contribution of materials in more complex geometries such as inside a rail car.

### 5.2.1 Empirical Models

An empirical model based on the flammability parameter has been developed to predict flashover in NFPA 286 room-corner tests in [Section 4](#) of this report. The model uses cone calorimeter data from tests conducted with a heat flux of 50 kW/m<sup>2</sup>, which is similar to the exposure from a standard ignition source near the base of the flame to a surface. A flammability parameter was calculated from the cone calorimeter test data. A critical value of the flammability parameter to denote when a material may cause flashover in the NFPA 286 test was determined using wood and polymer lining materials that had undergone both cone calorimeter and NFPA 286 room-corner fire testing. Through this analysis, materials with a flammability parameter less than 0.6 are not expected to cause flashover in NFPA 286 while those with  $F > 0.6$  are expected to cause flashover. The use of this model on rail car materials will provide a basis for the determination of an appropriate fire safety standard. The critical value for the flammability parameter will guide the selection of appropriate levels of HRR and other criteria for the new guidelines.

An initial assessment was performed on rail car materials where only cone calorimeter data and ASTM E162 flame spread index data were available. Based on the empirical model, nearly 50 percent of the materials were predicted to cause flashover in a NFPA 286 test. In addition, materials with a flame spread index of less than 25 in ASTM E162 were also predicted to cause flashover in NFPA 286. This is in part due to the fact that the exposure in ASTM E162 is low relative to real fires and the test is a downward flame spread test instead of upward flame spread, which is the more hazardous condition. Large scale test data on rail car materials are needed to further validate the empirical model for rail car materials so that it can be used to develop performance criteria based on cone calorimeter data.

### 5.2.2 Fire Growth Models

A fire growth model was developed by Lattimer et al. [54]–[56] to predict the contribution of combustible linings (walls, ceilings, seating) on the fire development. This model used a one-dimensional heat transfer model to predict surface temperature rise and ignition with thermal properties determined using cone calorimeter ignition data. HRR curves at a range of heat fluxes in the cone calorimeter were input into the model to predict material burning. The pre-heating effects of the gas layer were predicted using a two-layer compartment fire model. This was validated by conducting a series of room-corner fire model. This was validated by conducting a series of room-corner fire tests lined with FRP materials as well as wood building products. The model was used in

several projects to predict the development of fires onboard rail cars [9] [57] [58]. In these studies, select ignition scenarios from ASTM E2061 [29] with varying levels of severity were input as initiating fires to determine the fires that could cause flashover. Typically, larger, realistic fires between seats or in the corner of the rail car were required to cause the rail cars to reach flashover was performed by Guillaume et al. [51] as part of the Transport fire safety engineering in the European Union (TRANSFEU) project to predict the fire growth inside of a rail car using FDS Version 5.3.3 including the pyrolysis model in FDS. Decomposition parameters for the pyrolysis model were developed using thermogravimetric analysis (TGA) in inert and air environments with a genetic algorithm to obtain properties. Pyrolysis model predictions were validated with cone calorimeter data resulting in a good comparison. FDS model results compared well with tests containing a seat in a noncombustible corner with an adjacent incipient fire and tests in a combustible wall panel lined corner with the initiating fire in the corner. Simulations of a full-scale rail car using FDS compared well in terms of gas temperatures, but combustion products were not as well predicted.

### **5.2.3 Solid Burning Models in FDS**

FDS has several approaches for describing the burning of solids [13]. The approach to take depends largely on the availability of materials properties and the appropriateness of the underlying pyrolysis model. Real objects, like furnishings, rail car interior finishes, and so on, are often difficult to describe. A HRRPUA material burning model pyrolysis model are commonly used for simulating burning solids. Both models are introduced in this section.

### **5.2.4 HRRPUA Material Burning Model**

Sometimes the only information about a given material are its bulk thermal properties, ignition temperature and subsequent burning rate as a function of time from ignition. This model starts a surface burning at a prescribed HRR profile when it reaches the ignition temperature. The surface loses energy at a rate defined by the heat of vaporization of the fuel. There are three input parameters required by FDS [13] for this model, HRRPUA, ignition temperature, and heat of vaporization.

The ignition temperature is the temperature at which the material starts to burn. It can be measured during the ASTM E-1354 (Cone Calorimeter) test with a pyrometer, infrared camera, or thermocouple [60]. If testing data are not available, ignition temperature can also be estimated using relationships such as those identified by Quintiere [61]. HRRPUA defines the rate of burning and how much heat is released after material reaches the specified ignition temperature. Heat of vaporization accounts for the energy loss due to the vaporization of the solid fuel. The parameters HRRPUA, ignition temperature, and heat of vaporization control the burning rate to simulate the heating up and ignition of the solid material.

### **5.2.5 Pyrolysis Model**

There is another approach to model the reactions that occur within solid materials when they are burning. It calculates the reaction rate of each surface and uses the heat of

combustion of the materials to determine the instantaneous HRRPUA [13]. The general evolution equation for a material undergoing one or more reactions is

$$\frac{dY_{s,i}}{dt} = -\sum_{j=1}^{N_{r,j}} r_{ij} + \sum_{i'=1}^{N_m} \sum_{j=1}^{N_{r,i'}} v_{s,i'j} r_{i'j} \quad (i' \neq i) \quad (5-1)$$

$$r_{ij} = A_{ij} Y_{s,i}^{n_{s,ij}} \exp\left(-\frac{E_{ij}}{RT_s}\right) X_{O_2}^{n_{O_2,ij}}; \quad Y_{s,i} = \left(\frac{\rho_{s,i}}{\rho_s(0)}\right) \quad (5-2)$$

where  $Y_{s,i}$  is the mass fraction of material  $i$  (g/g),  $t$  is time (s),  $j$  represents a reaction,  $N_{r,j}$  is the number of reactions for a material,  $r_{ij}$  is the reaction rate of material  $i$  during reaction  $j$  (1/s),  $i'$  is another reaction but not reaction  $i$ ,  $N_m$  is the number of all reactions,  $N_{r,i'}$  is number of reactions in other materials,  $v_{s,i'j}$  are material yield from other reactions,  $r_{i'j}$  is the reaction rate of a material from other reactions (1/s),  $A_{ij}$  is the pre-exponential factor of material  $i$  during reaction  $j$  (1/s),  $n_{s,ij}$  is the reaction power for material  $i$  during reaction  $j$ ,  $R$  is the universal gas constant (8.314 J/mol-K),  $E_{ij}$  is the activation energy of material  $i$  during reaction  $j$  (J/mol),  $T_s$  is the material temperature,  $X_{O_2}$  is the oxygen concentration at the material surface,  $n_{O_2,ij}$  is the reaction power for material oxidation type reactions,  $\rho_{s,i}$  is the density of material  $i$ ,  $\rho_s(0)$  is the initial density of material  $i$ . The reaction is the rate of change of the mass fraction of material  $i$  as a function of time ( $dY_{s,i}/dt$ ), as illustrated in Figure 5-1. [13]. The mass loss rate or the reaction rate is determined by kinetic constants,  $A$  and  $E$ .

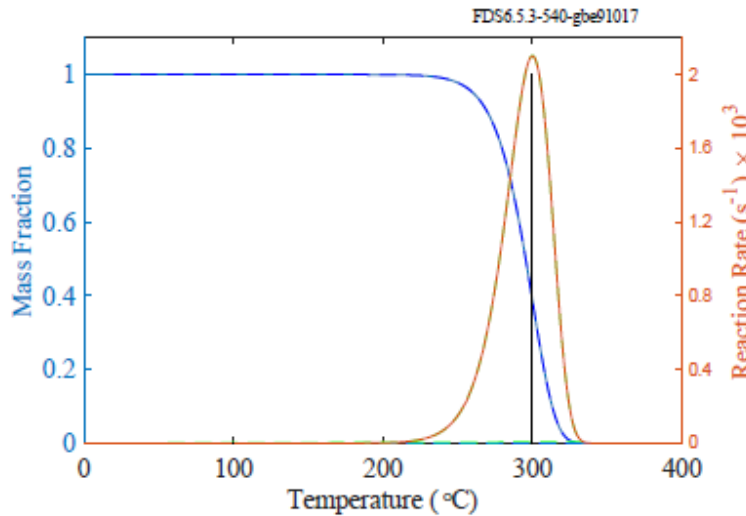


**Figure 5-1. Example mass fraction and reaction rate of a burning material**

However, the kinetic constants,  $A$  and  $E$ , are not available for most real materials. FDS provides a way to estimate the kinetic parameters. The key assumption is that the material components can undergo only one reaction, at most. Users can specify reference temperature and pyrolysis range, so the kinetics parameter can be calculated. Where this curve peaks is referred to as the reference temperature in FDS [13].

### 5.2.6 Validation of the HRRPUA Material Burning Model in FDS

The pyrolysis model in FDS requires solid fuel mixture material properties, solid product species, gas product species and most importantly reaction kinetic parameters. A series of experiments are required to quantify properties for each material, and the model accuracy is highly dependent on property estimation.

There are fewer input parameters for the HRRPUA material burning model, which requires fewer experiments. The burning rate is determined by HRRPUA, ignition temperature, and heat of vaporization control. Wood products and plastic foams were tested in the cone calorimeter by Onno and Kim [45]. These data could be used to validate the burning model in FDS. One of the materials tested in both the cone calorimeter and room corner test was plywood with a thickness of 6 mm. The material properties are given in [Table 5-1](#) [27].

**Table 5-1. Material properties of 6 mm plywood**

Material Properties	
Density (kg/m <sup>3</sup> )	550
Conductivity (W/m-K)	0.15
Specific Heat (kJ/kg-K)	1.75
Ignition T (°C)	390
Peak HRRPUA (kW/m <sup>2</sup> )	156
Heat of Evaporation (kJ/kg)	117

The parameters HRRPUA, ignition temperature, and heat of vaporization were used as model input for the HRRPUA material burning model in FDS. The peak values and time history of HRRPUA from the cone calorimeter test were used to define the burning rate once the material reaches the ignition temperature. As shown in [Figure 5-2](#), the FDS prediction in HRRPUA was consistent with the cone calorimeter data for the 50 kW/m<sup>2</sup> tests. The peak HRRPUAs of FDS prediction were within 5 percent of experimental data for the 50 kW/m<sup>2</sup> tests with the shift in time due to a delay in predicted material ignition. The comparison of mass loss rate is shown in [Figure 5-3](#). The peak values of predicted mass loss rate were 16 percent higher than the experimental data for the 50 kW/m<sup>2</sup> from Kim and Onno [45]. Overall, the profiles of mass loss rate and HRR were represented by the FDS HRRPUA material burning model, including the first and second local peaks. Note that the HRR from the material will be that prescribed independent of the exposure heat flux. Based on analysis in [Sections 2](#) and [3](#), the use of the curve at 50 kW/m<sup>2</sup> is justified for this effort due to the fact the average exposure in the corner fire configuration with the NFPA 286 burner is similar to 50 kW/m<sup>2</sup>. The time to ignition will vary based on when the material surface temperature is predicted to exceed the ignition temperature.

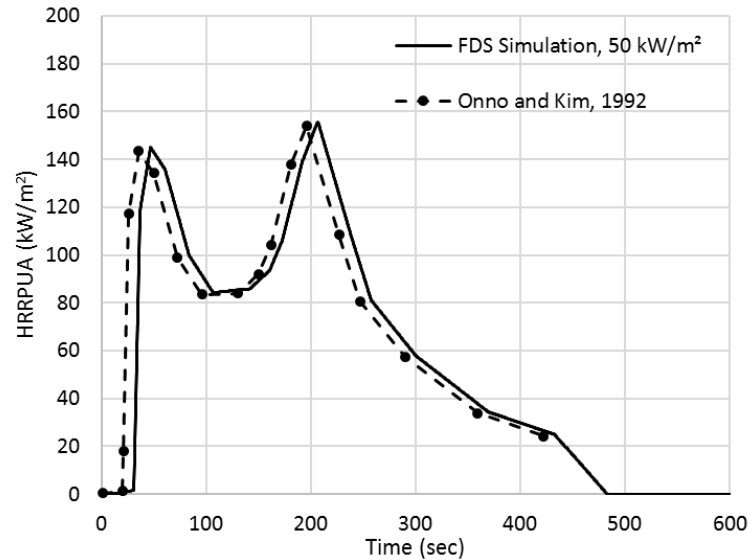


**Figure 5-2. HRR of 6 mm plywood in cone calorimeter test**

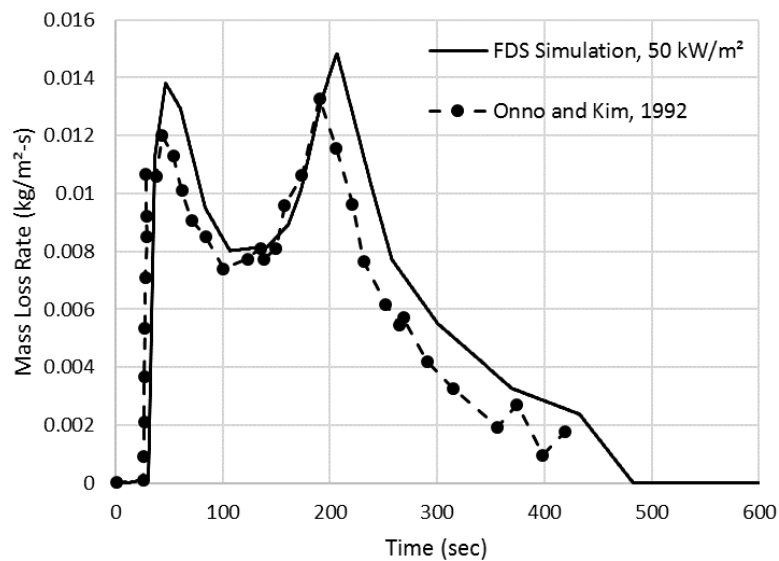


**Figure 5-3. Mass loss rate of 6 mm plywood in cone calorimeter test**

### 5.3 Fire Growth Modeling using FDS

The NFPA 286 initiating fire was found to be representative of rail car interior fires found in [Section 3](#). NFPA 286 standard room corner tests uses a room that has a similar cross section to real scale rail cars. In this study, FDS Version 6.5.2 fire growth modeling is validated using NFPA 286 standard room corner testing data. The NFPA 286 conditions are assessed and compared with those that develop in the rail car during a fire.

### 5.3.1 NFPA 286 Room Corner Test

NFPA 286 standard room test is conducted in a room with dimensions 12 ft. (3.66 m) deep, 8 ft. (2.44 m) wide and 8 ft. (2.44 m) high with a doorway having dimensions of 2.6 ft. x 6.6 ft. (0.79 m x 2.0 m) [11]. The back wall, side walls, and ceiling are lined with the combustible interior finish sample. The ignition source in the room consists of a propane sand burner, 12 in. x 12 in. (0.305 m x 0.305 m), placed flush against both walls in one of the back corners and its top surface is 0.3 m above the floor, as illustrated in [Figure 5-4](#). The burner HRR regimen is 40 kW for 5 minutes followed by 160 kW for 10 minutes for a total test duration of 15 minutes.

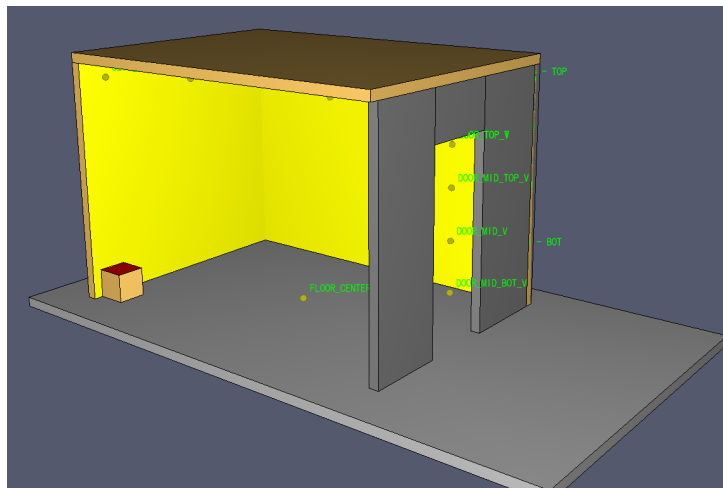


**Figure 5-4. NFPA 286 standard room corner test**

The wall containing the door was removed in some tests [19], which left the room a larger opening so more air could come into the room from outside environments. The effect of the removal of the wall containing the door was not studied. Therefore, both configurations, the NFPA 286 standard room with one door open and NFPA 286 room without door (wall removed), are considered.

### 5.3.2 Full-scale Rail Car Geometry

An exemplar intercity rail car geometry was studied in this report. The interior of the rail car is about 85 ft. (26 m) long, 10 ft. (3.1 m) wide, and 8.7 ft. (2.65 m) high over most of the car length [62]. The modeled rail car interior is shown in [Figure 5-5](#). Access to the interior is typically gained through four single panel doors, two doors on each side of the car. Each door is 6.6 ft. (2.01 m) high and 4.2 ft. (1.27 m) wide and is operated electronically. As shown in [Figure 5-5](#), the length of the rail car is larger than NFPA 286 room. The cross section is 2 ft. (0.6 m) wider and 0.7 ft. (0.2 m) higher than NFPA 286 room, but still comparable. The seating materials were assumed to be non-combustible in this study.

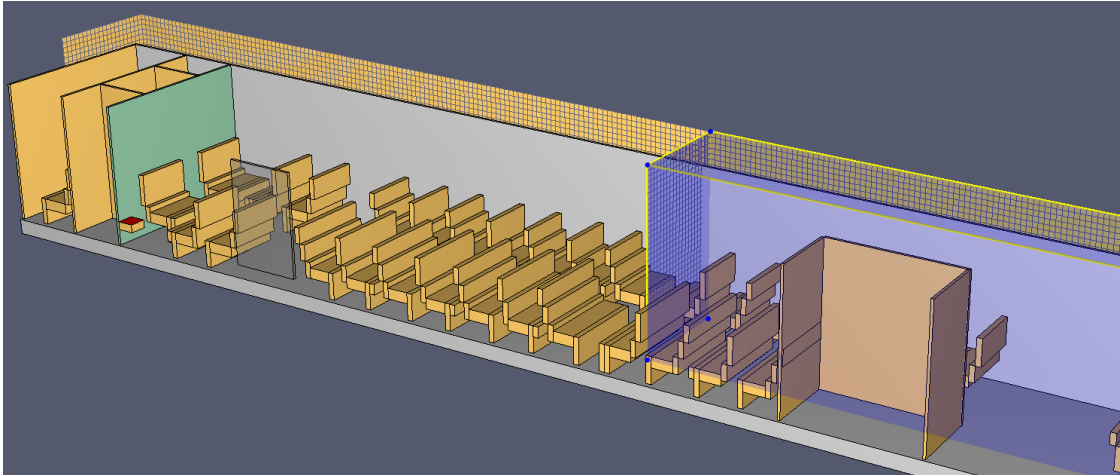


**Figure 5-5. Full scale rail car geometry with corner fire**

A burner identical to that used in NFPA 286 standard test was placed in the corner that is close to the door. The distance from top surface of the burner to the ceiling was the same as in NFPA 286 test. The door, as shown in [Figure 5-5](#), was kept open as in the NFPA 286 standard test.

### **5.3.3 Mesh Convergence Study**

A mesh convergence study was performed to demonstrate that decreasing the size of the computational mesh does not cause appreciable differences in the results [13]. To determine the appropriate mesh for this study, a mesh convergence study was conducted with a non-combustible material in a NFPA 286 standard room corner test. The ignition temperature was assumed to be 1,000 °C, which is high enough to make sure no material ignition occurred. Two different meshes were chosen to model the room corner test. In the coarse mesh, the cell size was of 4.72 in. (0.12 m) and there were 35,000 cells in total. The cell size in the fine mesh was, 2.36 in. (0.06 m), half that of the coarse mesh.

[Figure 5-6](#) presents the time history of temperature at the location 4 in. (0.102 m) below the ceiling center. The temperature reached about 120 °C within 1 minute and stayed stable as the burner HRR was kept at 40 kW. After 5 minutes, the temperature went up over 300 °C as the burner HRR was increased to 160 kW. As the material was not ignited, it did not release any heat into the room for the duration of the simulation (over 20 minutes). As a result, the gas temperature was not over 350 °C. The temperature prediction from the coarse mesh is shown in blue while the fine mesh prediction is in gray in [Figure 5-6](#). The temperature prediction using coarse and fine meshes is nearly identical. The coarse mesh was deemed sufficient for obtaining converged results for simulating the initiating fires of 40 kW and 160 kW HRRs in room corner tests. Therefore, a cell size of 4.7 in. (0.12 m) was used for all the simulations in this report.

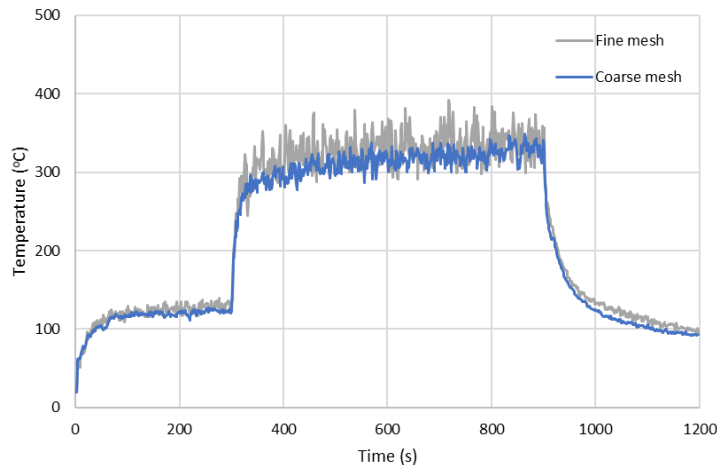


**Figure 5-6. Time history of temperature at ceiling center**

### **5.3.4 Fire Growth Modeling with Combustible Material**

As introduced in [Section 5.3.3](#), plywood with 6 mm thickness was tested in both the cone calorimeter and NFPA 286 room corner test by Onno and Kim [45] [46]. In [Section 5.3.3](#), the HRRPUA material burning model in FDS has been validated using the cone calorimeter data [45]. The 6 mm plywood was observed to ignite and cause flashover in the NFPA 286 room corner test after the burner exposure fire was increased to 160 kW [46]. The data from these tests can be used to validate the fire growth modeling using FDS. Therefore, the 6-mm thick plywood was considered in this study.

To compare the NFPA 286 conditions with those that develop in a rail car, the following cases were simulated using FDS:

- NFPA 286 standard room, with one door open
- NFPA 286 standard room with no door (wall containing door was removed)
- Rail car geometry with one side door open

The difference in geometry has been discussed in [Sections 5.4.1](#) and [5.4.2](#). The back wall, side walls, and ceilings of NFPA 286 rooms and rail car were all lined with the same material, 6 mm plywood. The material properties are given in [Table 5-1](#).

### **5.3.5 Effect of Removing Wall Containing a Door**

A comparison of the conditions that develop in the NFPA 286 test with and without a door are provided in [Figure 5-7](#) and [Figure 5-8](#). [Figure 5-7](#) presents the airflow velocity vectors along the center of the room at 360 seconds (6 minutes). It can be seen in [Figure 5-7](#) (left) that hot gas flowed out of the NFPA 286 room through the top of the open doorway. Meanwhile, cold air came in through the lower part of the door. The velocity was over 4 m/s near the top of the door. In the NFPA 286 room with the door, the temperature distribution of the center section at 360 seconds (6 minutes) is shown in [Figure 5-8](#). Even with the door open, a layer of hot gas was accumulating right below the ceiling inside the room. The gas temperature near the ceiling was over 600 °C. The



upper half of the room was occupied by hot gas with an average temperature over 300 °C, as demonstrated in [Figure 5-8](#) (left).

In the case with the NFPA 286 room with the wall removed (no door), a larger opening is present for air to flow into the room and gases to flow out as shown in [Figure 5-7](#) (right). The velocity near the top of the ceiling was less than 3 m/s, but the average velocity throughout the room was larger as compared to the case with a door. Due to the larger flow rate in and out of the room, there was less hot gas accumulation inside the room. As shown in [Figure 5-8](#) (right), only a thin layer of hot gas formed under the ceiling and the temperature was no more than 480 °C. Removal of the wall containing the door prevented hot gas from accumulating, which accelerates fire growth.

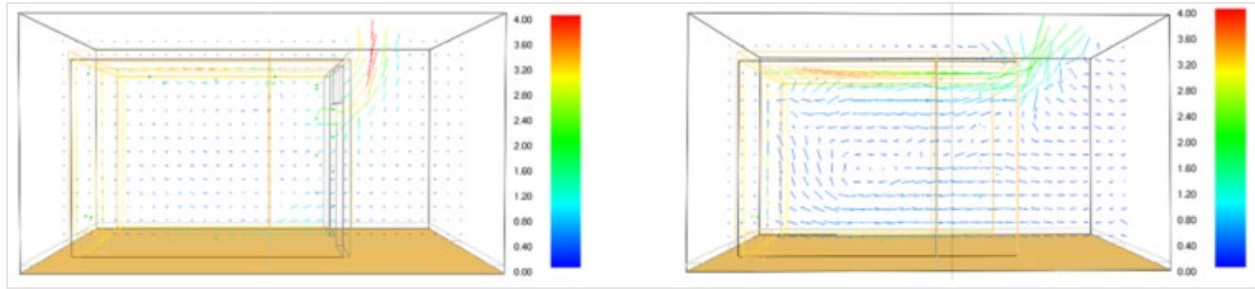


**Figure 5-7. Flow velocity of the center section of NFPA 286 rooms at 360 s (left) with door and (right) without door**

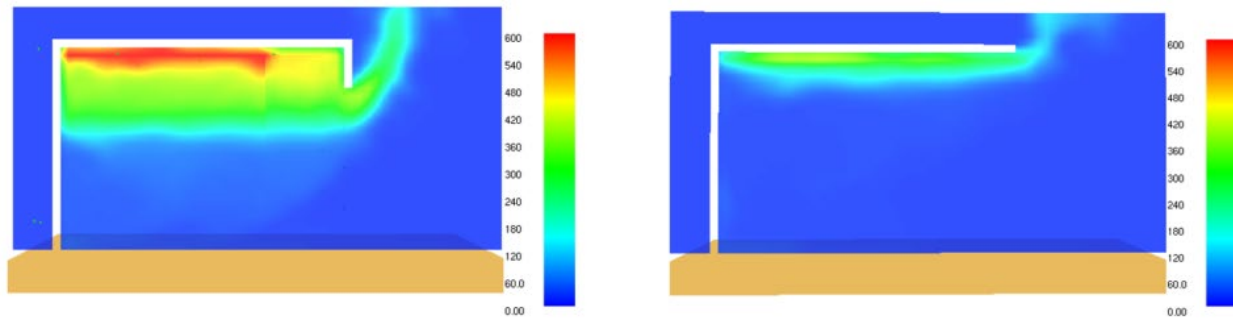


**Figure 5-8. Temperature of the center section of NFPA 286 rooms at 360 s (left) with door and (right) without door**

The inside wall temperature at 360 seconds (6 minutes) is shown in [Figure 5-9](#). The ignition temperature of plywood (390 °C) was set as the upper limit for display so the red areas represent regions where materials were ignited. The fire grew along the corner and then reached the ceiling. The accumulated hot gas layer pre-heated the ceiling materials on its way to flowing outside, causing the fire to grow from the corner directly above burner to larger areas.

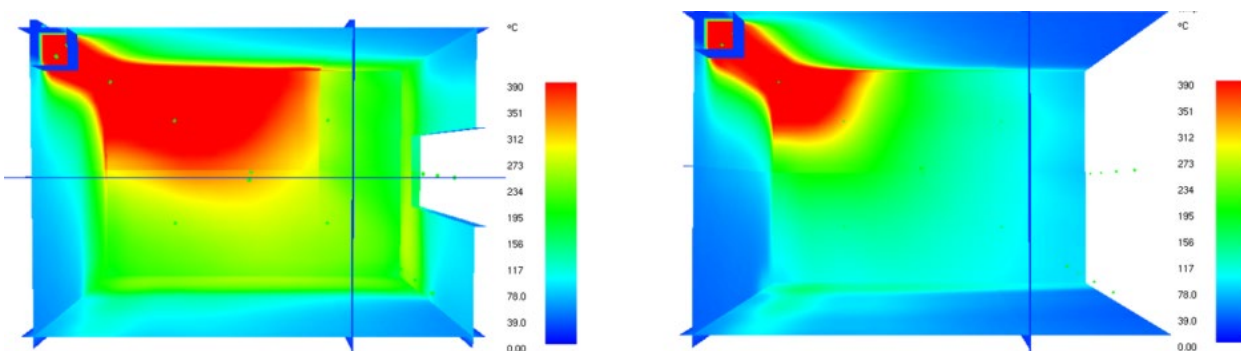


**Figure 5-9. NFPA 286 room wall temperature at 360 s (left) with door and (right) without door. View from floor looking up to the ceiling**

When the wall containing the door was removed, it took less time for the hot gas to escape and the gas temperature in the upper part of the room was lower. As a result, the ceiling material was not pre-heated as much as in the case with a door. The fire

growth in the case without a door was slower compared to the NFPA 286 room with a door, as shown in [Figure 5-9](#). After 360 seconds, the ignited material in the ceiling was only about 30 percent of that ignited in the NFPA 286 room with a door. Therefore, the NFPA 286 room corner tests without the wall containing a door are less conservative.

### 5.3.6 Fire Growth in Rail car

[Figure 5-10](#) presents the temperature distribution of the rail car center section along the longitudinal direction at 360 seconds (6 minutes). A hot gas layer was predicted to accumulate under the ceiling throughout rail car. The gas temperature near the ceiling above the burner first reached over 600 °C after 360 seconds (6 minutes). Hot gases accumulated in the upper region of the rail car interior, like in the NFPA 286 room with a door open in [Figure 5-8](#) (left). The average gas temperature in the rail car appeared to be lower than in the NFPA 286 standard room. This is because the rail car (over 80 ft. long) had a large interior space resulting in more heat loss to the boundaries and broader distribution of gases.

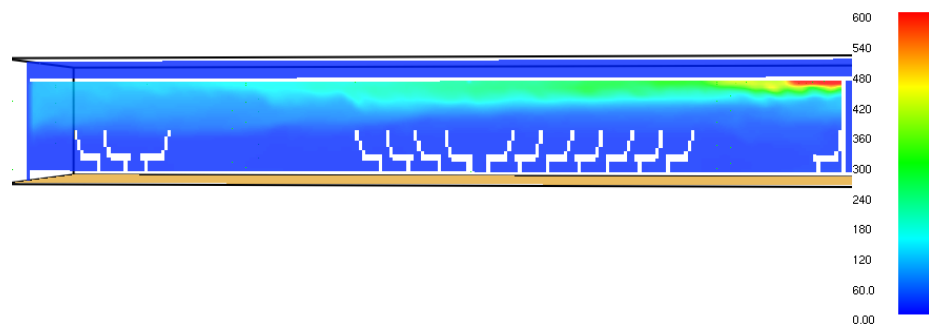


**Figure 5-10. Temperature of rail car center section at 360 seconds**

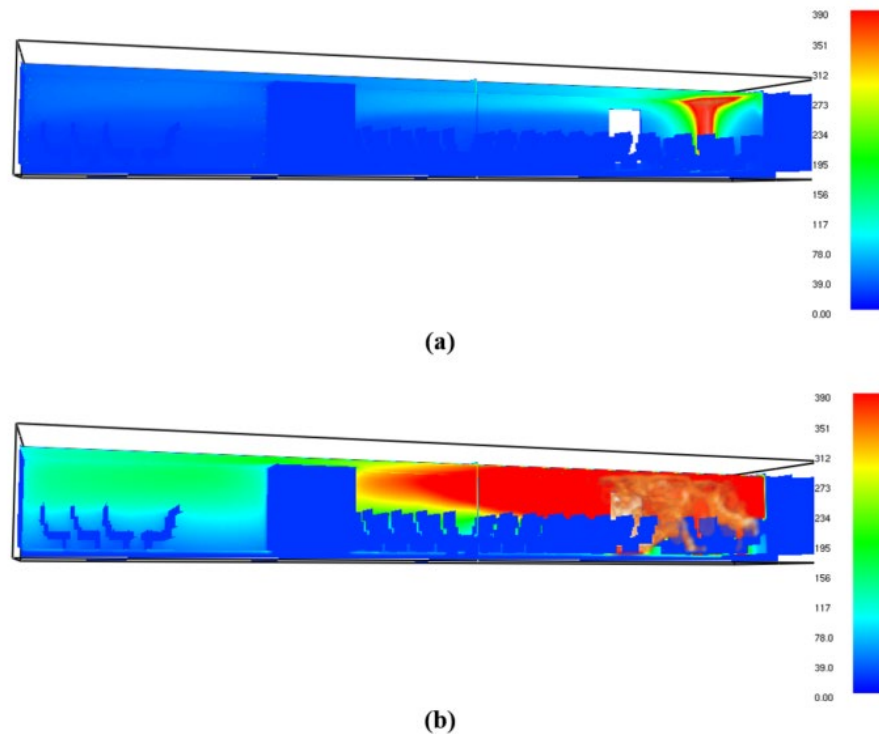


**Figure 5-11. Rail car interior wall temperature at (a) 360 s and (b) 600 seconds**

The rail car interior wall temperature at 360 seconds (6 minutes) and 600 seconds (10 minutes) is shown in [Figure 5-11](#). Again, the material ignition temperature (390 °C) was set as the upper limit for display purposes and the red areas represent regions where materials were ignited. The fire grew along the corner vertically and then to the ceiling. Hot gases were contained in the upper layer of the rail car interior. The ceiling was pre-heated so the fire grew from the ceiling corner above the burner toward the other end of rail car. After 600 seconds (10 minutes), over half of the rail car interior wall in the length direction was ignited as shown in [Figure 5-11](#) (lower).

## 5.4 Validation of FDS Models

To validate the fire growth modeling using FDS and quantify the effect of geometry on fire growth, gas temperature predictions at the center of the ceiling, total HRR and time to flashover were compared with the test data [46]. The NFPA 286 room with and without the wall containing a door are compared with those developed in a rail car during a fire.

### 5.4.1 Gas Temperature and Total HRR

As shown in [Figure 5-12](#), the gas temperature at the center of the ceiling of the NFPA 286 room with a door (orange line) increased gradually in the first 300 seconds when the HRR was 40 kW. As the HRR was increased to 160 kW, the gas temperature increased rapidly and reached over 600 °C at 360 seconds. Two NFPA 286 room corner fire tests were conducted using 6 mm plywood [46] and flashover occurred in both tests. The results of both tests are provided to demonstrate the potential variability in the data.

It took 330 seconds and 480 seconds for the gas temperature at the center of the ceiling to reach 600 °C in Test 1 and Test 2, respectively. The FDS temperature prediction was bounded by the two tests and closer to Test 1, in which the burning of plywood was more intense.

The gas temperature profile of the ceiling of the rail car (yellow line in Figure 5-12) is slightly lower but overall very similar to that of the NFPA 286 room with a door. For the case in which the wall containing the door was removed, the gas temperature (gray line in Figure 5-12) was barely over 100 °C after 300 seconds and did not reach 600 °C until 480 seconds. The gas temperature was consistently lower than that of the NFPA 286 room with a door and the rail car. These results further demonstrate that removal of the wall containing a door in NFPA 286 room tests results in non-conservative behaviors and is not recommended for rail car applications.

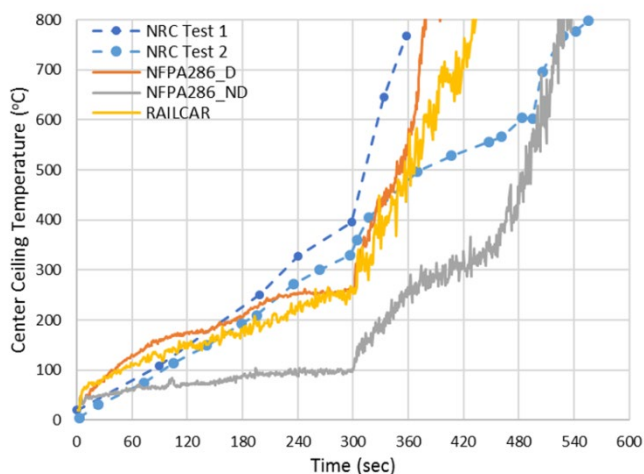


**Figure 5-12. Time history of center ceiling gas temperature in the NFPA 286 room and rail car geometries**

Figure 5-13 presents the time history of total HRR for all three cases. During the first 300 seconds, the total HRR increased slowly in all cases. When the burner HRR was increased to 160 kW at 300 seconds, the total HRR increased rapidly and reached 1 MW within 600 seconds. The HRR profile of the rail car was comparable to that of the NFPA 286 room with a door open. Both HRR curves were bounded by the measured HRRs of Test 1 and Test 2. The time history of ceiling center temperature and HRR have demonstrated that the NFPA 286 standard room with a door open is representative of rail car geometry.

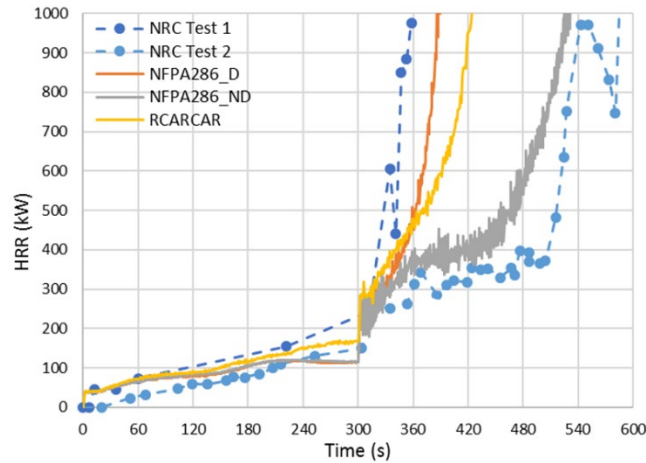


**Figure 5-13. Time history of HRR in the NFPA 286 room and rail car geometries**

#### **5.4.2 Time to Flashover**

In the NFPA 286 standard [11], flashover is defined to have occurred when two of the following are true: HRR exceeds 1 MW, heat flux at the floor exceeds 20 kW/m<sup>2</sup>, average upper layer temperature exceeds 600 °C, flames exit doorway, or a paper target on the floor auto ignites. The first three metrics were considered to calculate the time-to-flashover, as shown in [Table 5-2](#).

The average time-to-flashover of the NFPA 286 room without the wall containing a door is 26 percent longer than that of the rail car. The time-to-flashover of the NFPA 286 room with a door is 8 percent shorter than that of rail car. As a result, the NFPA 286 room with a door is a reasonably conservative representation of the rail car.

**Table 5-2. Time to flashover for the NFPA 286 room-corner test of plywood**

	Time to flashover (s)			
Criteria	NRC Test	NFPA 286 Door	NFPA 286 ND	Rail Car
Floor HF > 20 kW/m <sup>2</sup>	240–530	394	542	448
HRR > 1 MW	358–551	389	525	425
Upper layer T > 600 °C	235–485	370	504	373
Average	278–522	384	524	415

### **5.5 Section Summary**

FDS Version 6.5.2 simulated the fire growth and determined the difference in conditions that developed in the NFPA 286 room with a door, the NFPA 286 room with the wall with the door removed, and the actual rail car geometry. The HRRPUA material burning

model in FDS was validated using cone calorimeter data. It was then used in the room corner fire simulations.

Fire growth modeling using FDS was validated by comparing the results with the NFPA 286 standard room-corner fire testing. The prediction of interior gas temperature and HRR agreed well with the testing data and was bracketed by data from two tests. The fire growth starting from a room corner fire was well represented by the simulation results including flow velocity and wall temperature. The time-to-flashover was predicted and agreed well within 8 percent of the test data.

The NFPA 286 conditions were assessed and compared with those developed in a rail car during a fire. It was found that removal of the wall containing a door results in non-conservative conditions. Both gas temperature and HRR were under-estimated. Therefore, it is not recommended to remove the wall containing a door for rail car applications. The simulation results for gas temperature, HRR, wall temperature and time-to-flashover demonstrated that the NFPA 286 standard room-corner fire tests are reasonably conservative and well represent the fire behaviors that develop in rail car with one door open. These modeling results suggest that the NFPA 286 standard room corner test is representative of conditions that would develop inside of a rail car. Additional sensitivity studies are recommended to evaluate the effects of fire location inside of the rail car, number of rail car doors opened, and additional interior finish materials on the fire growth inside of real rail cars compared to that in NFPA 286.

## 6. Cone Calorimeter Testing of Rail Car Interior Materials

---

In order to develop HRR based fire safety performance criteria based on small-scale test data such as those obtained from the ASTM E1354 cone calorimeter test [60], a connection between the large-scale material contribution to fire growth and small-scale test data needs to be established. It is necessary to have data at both scales to adequately evaluate the suitability of HRR from the cone calorimeter as a fire performance parameter for evaluation of fire safety in passenger rail cars.

There have been limited studies [27] [45]–[49] that have related the behavior in the large-scale NFPA 286 room-corner fire test with small-scale test data such as those obtained from the ASTM E1354 cone calorimeter. The majority of these studies have focused on building products [45]–[49] with only one study by the NASFM [27] focused on materials used in rail car transportation applications. The NASFM report [27] (“Recommended Fire Safety Practices for Rail Transit Materials Selection”) contains results for rail car lining materials for both NFPA 286 room-corner test [11] and ISO 5660-1 cone calorimeter test [63].

In the HRR database established in [Section 2](#) identified that there is a lack of HRR data on rail car materials that also underwent large-scale fire tests, namely the NFPA 286 room-corner fire test [11]. The lack of HRR data on rail car materials has prompted efforts in this research to collect both small-scale ASTM E1354 cone calorimeter test data and large-scale NFPA 286 room-corner fire test data on rail car interior materials.

The work in this section is focused on determining the fire performance parameters of seven representative rail car materials at the small-scale using the ASTM E1354 cone calorimeter test. The materials selected for testing are applicable to interior finish in passenger rail cars. These materials were obtained in a bulk lot, so that the same materials could be tested in the large-scale room corner fire tests. Cone calorimeter tests were conducted on these materials, and standard test data on ignition, HRR, and other fire properties are presented herein. Furthermore, a series of ASTM E162 radiant panel tests were also conducted, which serve as a basis for comparison to the existing requirements.

### 6.1 Methodology

#### 6.1.1 Cone Calorimeter Tests

The cone calorimeter fire test is used to measure and describe the response of materials to heat and flame under controlled laboratory conditions. The test may be used to determine the ignitability, HRR, mass loss rate, effective heat of combustion, and visible smoke development of materials. A schematic of the apparatus is provided in [Figure 6-1](#).



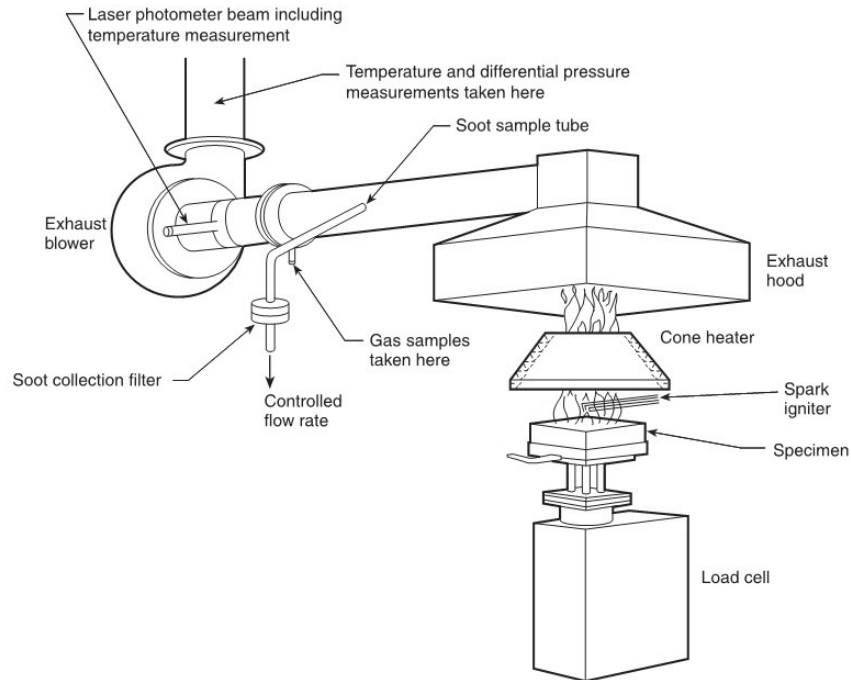


**Figure 6-1. ASTM E1354 cone calorimeter test apparatus (image reproduced from the SFPE Handbook of Fire Protection Engineering [8])**

In the cone calorimeter test, a small specimen is placed in a tray, which is then positioned on a load cell (to measure the mass of the specimen) below a conical electric heating element. This cone heater exposes the top surface of the specimen to a calibrated incident heat flux. As the specimen thermally decomposes under this external heating, vapors rise through an electric spark igniter and exhaust into a duct. If the mixture of vapors in the heated region is flammable, ignition may occur. In this case, the spark igniter is removed, and the specimen is permitted to burn until the appropriate end-of-test criterion is met.

Temperature and differential pressure in the exhaust duct are measured, and the flow rate of gases in the duct is calculated. As the specimen burns, gases in the duct are sampled, and the volume concentrations of oxygen, carbon dioxide, and carbon monoxide are measured. Based on the principle of oxygen consumption calorimetry, the HRR of the specimen is computed. Effective heat of combustion is calculated from the measured mass loss and heat release of the specimen. The obscuration of light along a path traversing the diameter of the duct is measured by a laser photometer, and specific extinction area is calculated as a measure of smoke development.

Since the cone calorimeter test involves a small specimen, which is inherently representative of a larger material in end-use, rate results are normalized by the exposed area of the specimen. These include:

- Heat release rate per unit area (HRRPUA)
- Total heat release per unit area (THRPUA)
- Mass loss rate per unit area (MLRPUA)

In the work conducted in this section of the research, cone calorimeter tests were conducted in accordance with test standard ASTM E1354. Samples were obtained for a number of materials (as outlined in the following section), and specimens were prepared to the required specifications: 0.10 m by 0.10 m (3.9 in by 3.9 in) in area, and a thickness indicative of the end-use configuration. Specimens were wrapped in a single layer of aluminum foil, shiny side toward the specimen, covering the sides and bottom.

The standard specimen holder is constructed from 2.4 mm (0.1 in) thick stainless steel, and has inside dimensions measuring approximately 0.101 m by 0.101 m (4.0 in by 4.0 in), by 23 mm (0.9 in) deep. The standard retainer frame, alternatively denoted the “edge frame,” fits over the sample holder and reduces the exposed area of the specimen to 88.4 cm<sup>2</sup> (13.7 in<sup>2</sup>). The use of the retainer frame is recommended in ASTM E1354 for testing of building products in the cone calorimeter,<sup>1</sup> and required in ISO 5660-1 with the exception of materials that melt or require other specialized considerations.<sup>2</sup> Given this, the retainer frame was adopted here (materials selected for study did not exhibit melting behavior). The specimen holder was filled with refractory ceramic fiber insulation, the specimen placed on top, and the retainer frame placed over the specimen holder, pressing flush against the exposed surface of the specimen. An assembled specimen, holder, and retainer frame are shown in [Figure 6-2](#).

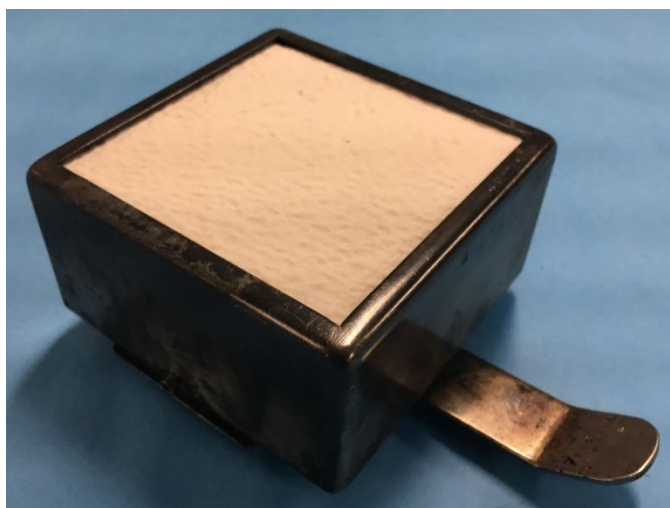


**Figure 6-2. Specimen prepared in accordance with ASTM E1354 using the retainer frame**

The standard spacing of 25 mm (1.0 in) between the exposed surface of the specimen and the bottom plate of the cone heater was used in most cases; when intumescent<sup>3</sup> or delamination threatened contact between the specimen surface and the spark igniter, spacing was increased to 60 mm (2.4 in) as stipulated in the standard test method [1], [64]. When the spacing was adjusted, the cone heater was re-calibrated to achieve the

---

<sup>1</sup> Refer to ASTM E1354-17, section X1.11, “Specimen Mounting Methods” [1].

<sup>2</sup> Refer to ISO 5660-1:2015, section 8.3.2, “Specimen Preparation” [64].

<sup>3</sup> Intumescent describes the act of abnormal swelling or enlarging, typically a result of heating.

same level of irradiance at the center of the specimen. Note that in the present work, delamination occurred in some composite specimens as a result of pressure buildup between the layers.

Ignition tests were conducted on samples by measuring the time to ignition under a selection of different heat flux values. In this manner, critical heat flux (CHF) was determined as the heat flux value below which ignition of a sample is not expected to occur within 20 minutes of exposure. CHF was determined in accordance with Annex A3 of ASTM E1354-17 [1].

Cone calorimeter tests were conducted at three levels of incident heat flux:  $25 \text{ kW}\cdot\text{m}^{-2}$ ,  $50 \text{ kW}\cdot\text{m}^{-2}$ , and  $75 \text{ kW}\cdot\text{m}^{-2}$ . If the CHF of the sample was determined to be greater than  $25 \text{ kW}\cdot\text{m}^{-2}$ ,  $35 \text{ kW}\cdot\text{m}^{-2}$  was used instead. Tests ended according to the appropriate end-of-test criterion; in the present work, this criterion was taken to be two minutes following the ceasing of flaming combustion (that is, the presence of visible flames of the exposed surface).

Pertinent results from the cone calorimeter tests include:

- Time to sustained flaming (occurrence of sustained flames on the exposed surface)
- Time to flame-out (ceasing of visible flames on the exposed surface)
- Time to end-of-test (selected per ASTM E1354 criteria)
- Total mass loss:
  - Over the entire test
  - From ignition to flame-out
- MLRPUA:
  - Average from 10 percent to 90 percent of the ultimate mass loss
  - Average from the start to the end of the test; and
  - Average from ignition to flame-out
- HRRPUA:
  - Peak over the entire test
  - Average from ignition to ignition plus 60 seconds
  - Average from ignition to ignition plus 180 seconds
  - Average from ignition to ignition plus 300 seconds
  - Average from the start to the end of the test; and
  - Average from ignition to flame-out
- THRPUA:
  - From the start to the end of the test; and
  - From ignition to flame-out

- Average effective heat of combustion:
  - From the start to the end of the test; and
  - From ignition to flame-out
- Average specific extinction area:
  - From the start to the end of the test; and
  - From ignition to flame-out

### **6.1.2 Radiant Panel Tests**

The radiant panel test is intended to measure and compare the surface flammability of materials when exposed to a prescribed level of radiant heat. Radiant panel tests were conducted in accordance with test standard ASTM E162, and a schematic of the test apparatus is given in [Figure 6-3](#). Samples are ignited at the top of the panel and the flame is then allowed to spread downward.

The radiant panel test apparatus consists of a 0.305 m (12 in.) by 0.457 m (18 in.) radiant panel, with a 0.152 m (6 in.) by 0.457 m (18 in.) specimen positioned in front, at an incline of 30 degrees to the vertical surface of the panel. The panel is fueled by a propane and air mixture, and an acetylene and air fueled pilot burner is positioned such that it impinges upon the top edge of the specimen. The specimens are wrapped in aluminum foil on the unexposed sides and backed with 6.4 mm (0.25 in.) of high density inorganic reinforced cement board. Specimens are retained in a specimen holder by a sheet of 25.4 mm (1 in.) hexagonal steel wire mesh (20 AWG) over the exposed face.

In each test, the temperature of gases in the exhaust stack above the exposed specimen is measured, and from these a Heat Evolution Factor (HEF) is computed. Additionally, the times at which the flame front spreads past distance markers are measured, and from these a Flame Spread Factor (FSF) is calculated. Finally, the Radiant Panel Index (RPI) is computed to be the product of HEF and FSF. In this test series, four tests were conducted on each sample, and the reported result is the average RPI for the four tests.

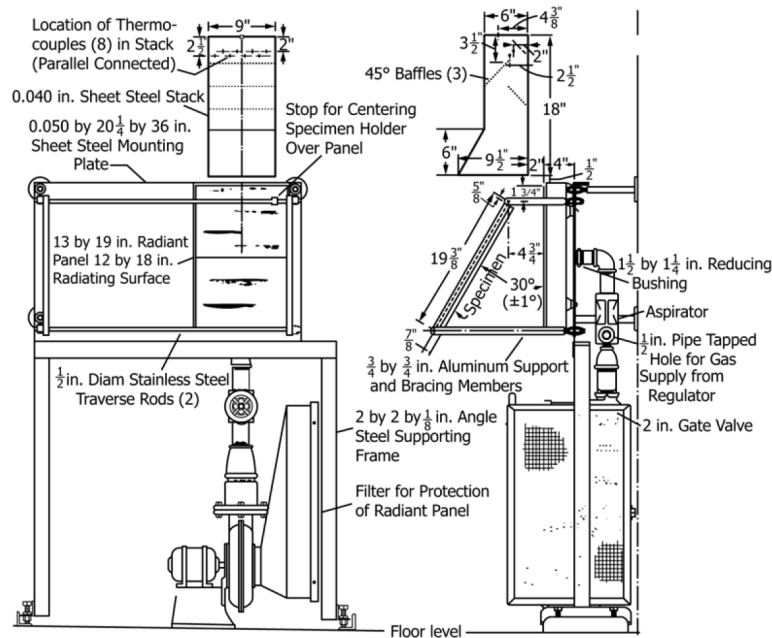


**Figure 6-3. ASTM E162 radiant panel test apparatus (image reproduced from test standard ASTM E162 [65])**

## 6.2 Materials Selection and Test Matrix

### 6.2.1 Materials Selection

For this test series, seven different materials representative of those commonly used in passenger rail cars were obtained in bulk lots. Samples were selected for cone calorimeter tests, radiant panel tests, and room corner tests. The samples selected and their intended end-uses in passenger rail car applications are described in [Table 6-1](#).

**Table 6-1. Description and end-use of tested samples**

Sample ID	Description and End-Use
Sample 1	Opaque thermoplastic material, nominally 3.81 mm (0.150 in.) thick, used for seat backs, wall panels, window masks, partitions, and ceiling panels.
Sample 2	Composite material consisting of a layer of plywood sandwiched between layers of aluminum, nominally 12.7 mm (0.500 in.) thick, used for wall panels, ceiling panels, and closets.
Sample 3	Composite material consisting of a layer of balsa wood sandwiched between layers of aluminum, nominally 15.9 mm (0.625 in.) thick, used for wall panels, ceiling panels, and closets.
Sample 4	Translucent thermoplastic material 4.5 mm (0.177 in.) thick, used for light fixtures.
Sample 5	Opaque thermoplastic material, nominally 4.75 mm (0.187 in.) thick, used for seat backs, wall panels, window masks, partitions, and ceiling panels.
Sample 6	Fiberglass material, nominally 7.0 mm (0.275 in.) thick, used for wall lining, window masks, and seat components.
Sample 7	Fiberglass material, nominally 3.27 mm (0.128 in.) thick, used for wall lining.

### 6.2.2 Cone Calorimeter Tests

Cone calorimeter tests were conducted at the Jensen Hughes laboratory, located in Baltimore, MD. Duplicate or triplicate testing was conducted at three levels of incident heat flux for each sample. Samples tested in duplicate were sufficiently repeatable to warrant two tests. CHF was also determined, which required six additional tests per sample (calorimetry was not performed during CHF tests). The test matrix for the primary cone calorimeter test series is provided in [Table 6-2](#).

**Table 6-2: Test matrix for the primary cone calorimeter test series**

Sample ID	Number of Tests Conducted at Each Heat Flux				CHF	Total Number of Tests
	25 kW/m <sup>2</sup>	35 kW/m <sup>2</sup>	50 kW/m <sup>2</sup>	75 kW/m <sup>2</sup>		
Sample 1	3		3	3	6	15
Sample 2		3	3	3	6	15
Sample 3		3	3	3	6	15
Sample 4	3		3	3	6	15
Sample 5	2		2	2	6	12
Sample 6	2		2	2	6	12
Sample 7		2	2	2	6	12

In addition to the primary test series, a preliminary series of tests was conducted on Sample 1 for the purpose of investigating the impact of various specimen configuration options. Due to the atypical burning behavior of the sample, it was necessary to determine the most suitable configuration based on the available options within the confines of the ASTM E1354 test method. Tests were conducted without the retainer frame, with the retainer frame, with the retainer frame and a wire grid (all at a spacing of 25 mm (1 in.) and heat flux of 50 kW/m<sup>2</sup>). Additionally, a test was conducted with the retainer frame and using a dynamic adjustment of the load cell platform (an effort to maintain 25 mm (1 in.) spacing between the intumescent surface of the specimen and the bottom of the cone heater). A detailed list of all cone calorimeter tests conducted is provided in [Appendix A](#).

### 6.2.3 Radiant Panel Tests

Radiant panel tests were conducted in accordance with test standard ASTM E162 [65] at external laboratories that routinely perform this testing. Due to scheduling, radiant panel tests for Sample 7 were conducted SGS Govmark.<sup>4</sup> The remaining samples were tested at the Commercial Testing Company.<sup>5</sup> Four specimens were tested for each sample. A detailed list of all radiant panel tests conducted is provided in [Appendix B](#).

---

<sup>4</sup> SGS Govmark, 96 Allen Boulevard., Farmingdale, NY 11735-5626.

<sup>5</sup> Commercial Testing Company, 1215 S Hamilton Street, Dalton, GA 30720.

## 6.3 Results and Discussion

### 6.3.1 Cone Calorimeter Preliminary Test Series

Prior to conducting the primary cone calorimeter test series, it was necessary to establish the test protocols that would be adopted and to keep these consistent for the entire test series. Special consideration is warranted for samples that exhibit delamination, intumescing, warping, excessive char formation, etc. The materials selected in the present work [Table 6-1](#) include laminated composites and fire-retarded thermoplastics, so intumescing and delamination were expected.

As previously stated, delamination occurs when pressure builds up between layers of an unrestrained composite sample. In some cases, if the pressure buildup is very large or occurs rapidly, violent delamination may occur. Such events can cause damage to the spark igniter and may result in the sample contacting the cone heater, either of which is cause for invalidation of the test. It is noted in ISO 5660-3 (the ISO equivalent of ASTM E1354) that “laminated products require some form of edge sealing to ensure that the burning process used in the cone calorimeter reflects that found in practice” [66]. Two solutions are suggested: use of the retainer frame or sealing the edges of laminate materials using impermeable cements. In addition to reducing non-representative exposure and mass transport effects, the retainer frame provides physical resistance to delamination, preventing layers of the composite material from expanding toward the igniter and cone heater. Use of the retainer frame is favored for this type of sample; however, a question remained as to the influence of the frame on the heat release and ignition propensity of the materials. Therefore, its use was investigated in the present work.

The wire grid is an optional accessory that is intended to prevent (or restrict) materials from intumescing out of the retainer frame, which can occur for some types of thermoplastic materials. An unfortunate consequence of this accessory is that it greatly impacts the exposure (partially obstructing the surface of the specimen), the rate and uniformity of vapor production, and ignitability of the material [66]. For this reason, the wire grid accessory is not often used in practice. Despite this, it does effectively contain some types of intumescing materials within the sample holder, so its use was investigated in the present work. [Figure 6-4](#) shows the sample tray, retainer frame, and wire grid accessory assembled.





**Figure 6-4. Specimen prepared with retainer frame and wire grid**

Both ISO 5660-1:2015 and ASTM E1354-17 provide that two different spacings between the top of the specimen and the bottom surface of the cone heater are acceptable: 25 mm (1.0 in) and 60 mm (2.4 in) [1], [64]. When it is expected that a specimen will intumesce or warp so as to contact the igniter or cone heater, even when the retainer frame is used, then it is recommended to lower the position of the specimen. This method is generally preferred to the use of the wire grid, in practice [66]. When the spacing is increased to 60 mm (2.4 in), the cone heater is re-calibrated so as to deliver the same target heat flux to the center of the specimen as was the case at 25 mm (1.0 in) spacing. Another option that is sometimes used in practice, although not mentioned in ASTM E1354-17, is to begin the test at a spacing of 25 mm (1.0 in) and to dynamically lower the position of the specimen tray as the exposed surface of the specimen rises, maintaining a constant separation distance. This process is controlled manually (the Jensen Hughes lab incorporates a screw jack to facilitate adjustment of the specimen tray), and subject to some associated error. The intent with this process is to maintain a constant heat flux on the exposed surface of the specimen as it rises. It must be noted that this will only be the case if it rises uniformly—for materials that rise predominantly in the center or warp nonuniformly, the suitability of this approach is questionable.

In order to assess the suitability of these alternative test protocols, a small series of tests were conducted on Sample 1 at  $\text{kW/m}^2$  in various configurations:

- At 25 mm (1.0 in.) spacing, without the retainer frame, without the wire grid ([Figure 6-7](#))
- At 25 mm (1.0 in.) spacing, with the retainer frame, without the wire grid ([Figure 6-6](#))
- At 25 mm (1.0 in.) spacing, with the retainer frame, with the wire grid ([Figure 6-5](#))
- Dynamically adjusting the spacing to maintain a constant separation distance of approximately 25 mm (1.0 in.) between the underside of the cone heater and the rising surface of the specimen, with the retainer frame, without the wire grid

Images are shown below for each of the first three cases (constant 25 mm [1 in.] spacing). [Figure 6-5](#) shows that the wire grid was ineffective in containing the



intumescent material—in fact, the material pressed up through the grid. From this, it was decided not to use the wire grid accessory.



**Figure 6-5. Preliminary test of Sample 1 with the retainer frame and the wire grid**



**Figure 6-6. Preliminary test Sample 1 with the retainer frame and without the wire grid**

[Figure 6-6](#) shows the behavior of the specimen with the retainer frame, and [Figure 6-7](#) without the retainer frame (and no wire grid). The retainer frame notably reduced the amount of intumescent and warping of the specimen. Therefore, it was decided to adopt the use of the retainer frame moving forward.

[Figure 6-8](#) shows the HRRPUA for the four tests in this preliminary test series. The red (retainer frame) and green (no retainer frame) traces in [Figure 6-8](#) show that the addition of the retainer frame did not significantly delay ignition time (the difference was about 3 seconds which is within the repeatability of the test). The addition of the retainer frame decreased HRRPUA in the initial 2 minutes by about 10 percent, increased HRRPUA in the subsequent 4 minutes by about 30 percent, and reduced the total burn

time by about 2 minutes. The average HRRPUA over the entire test was 124.3 kW/m<sup>2</sup> without the retainer frame and 110.0 kW/m<sup>2</sup> with the retainer frame, a difference of 12 percent.



**Figure 6-7. Preliminary test of Sample 1 without the retainer frame or the wire grid**

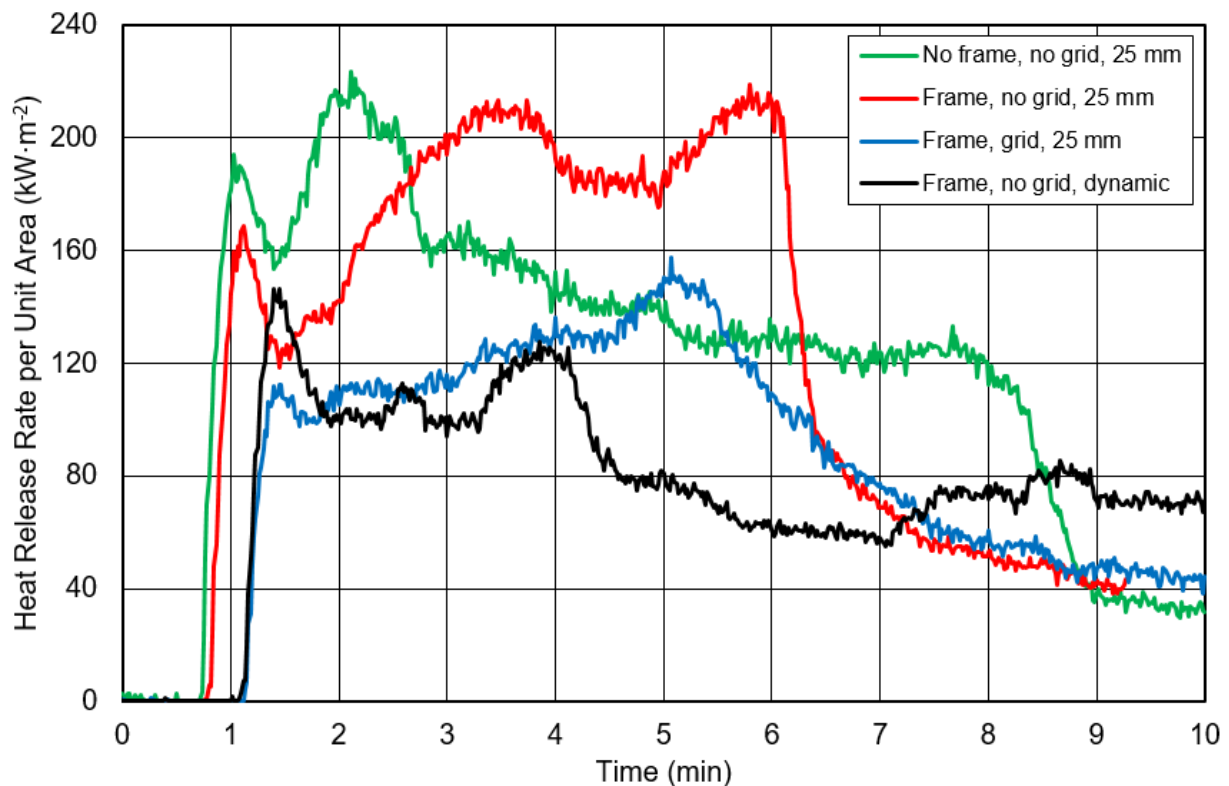


**Figure 6-8: HRRPUA of Sample 1 at 50 kW/m<sup>2</sup> in various configurations**

The red (retainer frame) and blue (retainer frame and grid) traces in Figure 6-8 show that the addition of the wire grid to the retainer frame setup caused ignition time to increase from 46 to 66 seconds. The average HRRPUA of the specimen was

61.5 kW/m<sup>2</sup> with the wire grid, a difference of 67 percent compared to the HRRPUA of 124 kW/m<sup>2</sup> for the specimen with just the retainer frame.

The average HRR (for the first 3 minutes,  $\dot{Q}_{180}''$ ) of the four tests shown in [Figure 6-8](#) were, 175 kW/m<sup>2</sup> (no frame, no grid), 165 kW/m<sup>2</sup> (frame, no grid), 110 kW/m<sup>2</sup> (frame, grid), and 106 kW/m<sup>2</sup> (frame, no grid, dynamic). As outlined in the ASTM E1354 test standard, the repeatability of the test in the calculation of average HRR (for the first 3 minutes following ignition) using a baseline of 175 kW/m<sup>2</sup> is 29.8 kW/m<sup>2</sup> (23.3 + 0.037  $\dot{Q}_{180}''$  given by [1]). It means that the probability is 95 percent that the average HRR result for the first 3 minutes of the second test will fall between 204.8 kW/m<sup>2</sup> and 145.2 kW/m<sup>2</sup>. Assuming a similar relationship for average heat release over the flaming duration, it is clear that the addition of the retainer frame produced a difference in average HRRPUA that was within the repeatability of the instrument, while the addition of the wire grid and retaining frame was not.

The black trace shows the HRRPUA for the case in which dynamic spacing was used. The results were similar to the case of the wire grid and retainer frame resulting in a delayed ignition time and a significantly lower average HRRPUA (55.1 kW/m<sup>2</sup>) compared with No Frame and Frame No Grid. It was also noted that the surface of the specimen did not rise uniformly, undergoing both warping and intumescing; therefore, it was decided that the dynamic adjustment method was not suitable.

Based on these results, it was decided to adopt the use of the retainer frame and constant spacing of 25 mm (1.0 in) for the primary test series; spacing would be increased to 60 mm (2.4 in) only when contact with the igniter became imminent.

### **6.3.2 Cone Calorimeter Primary Test Series**

An overview of results from this test series is provided in [Table 6-3](#), this includes:

- Peak heat release rate per unit area (HRRPUA<sub>peak</sub>) over the entire test for each heat flux tested
- Average heat release rate per unit area from ignition to flame-out (HRRPUA<sub>avg,flaming</sub>) for each heat flux tested
- Average effective heat of combustion (EHC<sub>avg</sub>) over the entire test for each heat flux tested
- Critical heat flux (CHF), determined to within the nearest 1 kW/m<sup>2</sup> for an exposure time of 20 minutes

**Table 6-3. Summary of cone calorimeter test results for each sample**

Sample ID	HRRPUA <sub>peak</sub> (kW/m <sup>2</sup> )			HRRPUA <sub>avg, flaming</sub> (kW/m <sup>2</sup> )			EHC <sub>avg</sub> (kJ/g)			CHF (kW/m <sup>2</sup> )
	25 (35)	50	75	25 (35)	50	75	25 (35)	50	75	
Sample 1	100.1	214.2	254.6	29.0	159.5	185.7	15.88	21.36	21.21	22.5
Sample 2	(180.0)	198.8	274.8	(65.3)	66.6	101.0	(7.88)	9.89	12.02	23.5
Sample 3	(87.3)	152.7	190.2	(21.0)	31.7	61.5	(7.82)	10.92	12.99	24.5
Sample 4	580.6	978.4	1437.2	253.7	477.0	699.3	24.83	24.85	25.59	5.5
Sample 5	121.8	223.7	321.6	71.2	124.0	163.4	19.13	24.22	24.26	24.5
Sample 6	8.3	136.6	167.6	2.4	101.6	108.9	2.13	17.36	20.15	21.5
Sample 7	(53.6)	129.0	171.6	(30.4)	54.0	86.3	(10.7)	21.01	21.7	31.5

[Appendix B](#) contains detailed test results for each sample at each heat flux, including averages for repeat tests and plots of HRR and mass over time. [Figure 6-9](#) shows a plot of the HRR for all materials, and [Figure 6-10](#) shows that same information with the vertical axis truncated (for clarification).

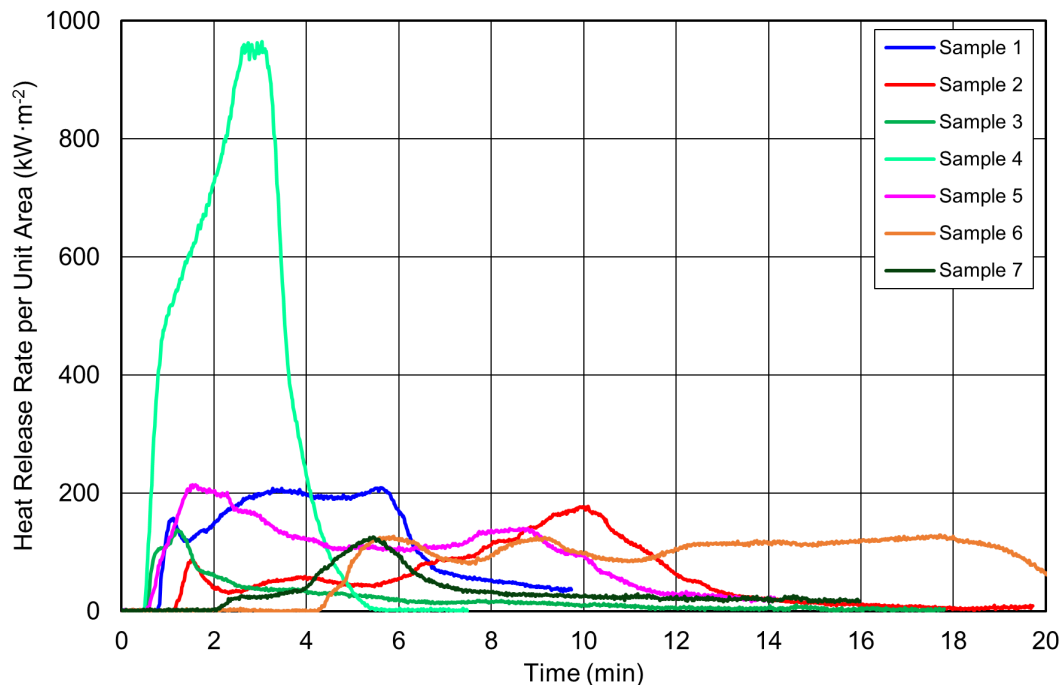


**Figure 6-9. HRRs for the materials tested in the study (refer to [Table 6-1](#) for descriptions of each sample)**

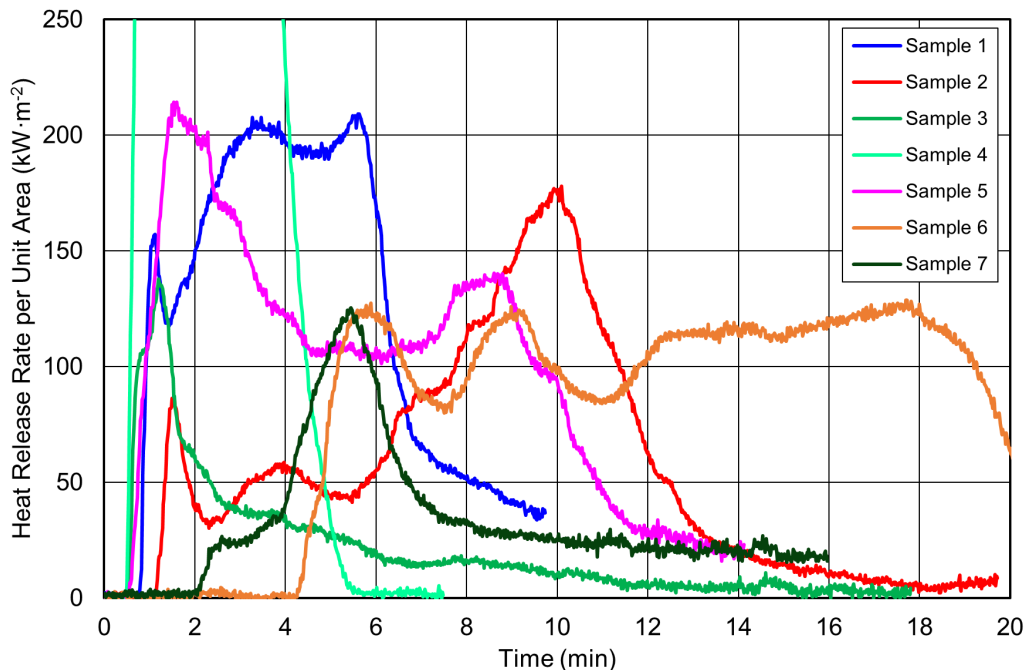


**Figure 6-10. HRRs for the materials tested in the study, truncated (refer to [Table 6-1](#) for descriptions of each sample)**

The results show that both HRR and effective heat of combustion, in general, increased with greater incident heat flux values. CHF was the highest for Sample 7 and lowest for Sample 4. Sample 4 had the highest average HRR, which was 4 to 10 times greater than the other samples. Samples 6 and 7 had the lowest HRRs.

Sample 6 exhibited a unique behavior compared to the other samples. At all heat flux values the samples readily ignited, after which flame extinction followed in less than 60 seconds as a layer of char built up on the surface of the samples. Per ASTM E1354, the spark igniter was reinserted within 5 seconds of flame extinction. For tests conducted at 50 kW/m<sup>2</sup> and 75 kW/m<sup>2</sup>, re-ignition subsequently occurred; however, for tests conducted at 25 kW/m<sup>2</sup>, the specimen did not reignite. This behavior was consistent across repeat tests.

Samples 1 and 5 exhibited significant intumescing as they burned, rising into the internal region of the cone heater (no contact with the heating coil was made). At the low heat flux, this intumescent behavior would have caused interference with the spark igniter; therefore, these tests were conducted with 60 mm (2.4 in.) spacing.

Samples 2, 3, and 7 exhibited a delamination behavior, along with a characteristic “popping” sound as the top layers delaminated under heat exposure. Following this event, flammable vapors from the underlying material and/or adhesives vaporized, eventually progressing to ignition.

For all samples, tests conducted at exposures of 50 kW/m<sup>2</sup> and 75 kW/m<sup>2</sup> produced results which were consistent between repeat tests, with ignition times, HRR peaks, and average effective heats of combustion in good agreement test-to-test. However, tests conducted at 25 kW/m<sup>2</sup>–35 kW/m<sup>2</sup> (near the CHF for each sample) yielded greater

variability in ignition times and HRRs for some samples. For example, Sample 2 when tested in triplicate at 35 kW/m<sup>2</sup> resulted in ignition times varying from 336 to 762 seconds, and correspondingly average HRRPUA varying from 43.7 kW/m<sup>2</sup> to 125.2 kW/m<sup>2</sup>. In contrast, this same material tested at 75 kW/m<sup>2</sup> resulted in ignition times varying from 22 to 28 seconds, and average HRRPUA varying from 95.4 kW/m<sup>2</sup> to 104.5 kW/m<sup>2</sup>.

These results demonstrate that the response of these materials in low-exposure fire conditions is less certain, and more difficult to quantify, than their response in high-exposure conditions. This is primarily a consequence of the complex nature of solid material ignition. Of note, results at 50 kW/m<sup>2</sup> exposures or greater are traditionally used in fire performance assessments based on cone calorimeter results [1].

### 6.3.3 Radiant Panel Tests

Results from the radiant panel tests are summarized in [Table 6-4](#) (refer to [Appendix B](#) for detailed results).

**Table 6-4. Summary of radiant panel test results for each sample**

Sample ID	FSF	HEF	I <sub>s</sub>	I <sub>s</sub> (Rounded)
Sample 1	1.30	2.23	2.89	5
Sample 2	1.76	9.28	16.69	15
Sample 3	1.51	4.87	7.21	5
Sample 4	4.50	40.42	181.45	180
Sample 5	1.55	3.25	5.34	5
Sample 6	1.07	4.12	4.43	5
Sample 7	1.00	1.58	1.58	0

Note: FSF= flame spread factor, HEF= heat evolution factor, I<sub>s</sub>= radiant panel index

Of the samples tested, only Sample 4 exhibited a noteworthy behavior, having an I<sub>s</sub> that was 12 to 36 times greater than that of the other samples. These results indicate that Sample 4 represents the greatest hazard from the perspective of surface flammability of the samples considered, under the controlled conditions of the test. This material was described to be usable for signage, in floor lighting, lighting, illuminated poster boxes, etc. However, its flame spread rating exceed the I<sub>s</sub> of 100 for materials used for light diffusers (NFPA 130, Section 8.4) [3]. This would limit its application inside of a rail car to 1 ft<sup>2</sup> per foot of car length.

## 6.4 Section Summary

A series of ASTM E1354 cone calorimeter tests were conducted on seven different rail car interior finish materials. An initial assessment included the appropriate method for testing the samples in the cone calorimeter. It was found that the use of the retainer frame provided a test scenario which is more suitable for the evaluation of the response to fire of these materials in their end-use configuration, notably reducing the amount of intumescenting and warping of the specimens, yet still producing results within the expected repeatability of the test. Furthermore, it was found that dynamic adjustment of spacing and the adoption of the wire grid accessory significantly affected the results;

therefore, these techniques are not recommended for cone calorimeter testing of these materials.

A set of cone calorimeter and radiant panel test data was developed for seven different samples of materials used in passenger rail cars. These data were added to the existing database and used along with large-scale testing (e.g., fire resistance furnace, or realistic fire exposures) to evaluate predictive models being used to develop performance requirements for materials used in passenger rail cars.

It was found that testing of these materials at exposures of 25 kW/m<sup>2</sup> and 35 kW/m<sup>2</sup> (near the CHF) produced results of varying consistency, and in some cases well beyond the range of expected repeatability of the test. On the other hand, testing at 50 kW/m<sup>2</sup> and 75 kW/m<sup>2</sup> produced consistent results across repeat tests. Therefore, it is recommended that future testing of rail car interior components be conducted at exposures of 50 kW/m<sup>2</sup> and greater. This will ensure not only repeatable and reliable results, but also data which are of relevance to performance-based modelling.



## 7. NFPA 286 Room-corner Testing of Rail Car Interior Materials

---

A lack of HRR data on rail car materials to provide a connection of material performance between small-scale testing and large-scale performance has prompted tasks to collect both small-scale ASTM E1354 cone calorimeter test data and large-scale NFPA 286 room-corner fire test data on rail car interior materials. In this section, the results of seven materials tested in NFPA 286 room-corner tests are provided to evaluate their potential for flame spread and contribution to the fire growth including gas temperature rise and overall HRR. The results for the ASTM E1354 cone calorimeter tests on these same materials are provided in the [Section 6](#). The combination of the small and large-scale test data will provide validation data for fire growth models that will be used to develop small-scale HRR requirements. This section provides the HRR data, gas temperatures, and combustion products generated during the large-scale NFPA 286 room-corner fire tests with the seven materials lining the room.

### 7.1 Experimental Approach

#### 7.1.1 Test Overview

A series of NFPA 286 standard room-corner fire tests was conducted to quantify the performance of seven different interior finish materials that could be used on rail cars. In the U.S., the NFPA 286 [11] room-corner test is the common standard large-scale test used to measure the contribution of interior finish materials on fire growth, mainly HRR and upward flame spread. The room is 2.4 m wide by 3.6 m long by 2.4 m high (8 ft. x 12 ft. x 8 ft.) and has an open doorway 2.0 m (79.5 in.) in height and 0.78 m (37.5 in.) in width. In this test series, the lining materials were installed on the ceiling and walls. A propane gas burner measuring 0.3 m x 0.3 m (12 in. x 12 in.) was placed in one of the back corners, in contact with the walls. The HRR for the burner was 40 kW for 5 minutes, and then 160 kW for 10 minutes. These regimes correspond to roughly 0.72 m and 1.5 m flame heights (2.4 ft. and 4.9 ft.), respectively.

The overall HRR from the burner and the interior finish were measured using a hood calorimeter system as shown in [Figure 7-1](#). Gas temperatures were measured near the ceiling and at the top of the door, and the heat flux to the floor was also measured. The onset of flashover, which is when a fire is transitioning to a fully-developed fire where large surface areas of combustibles inside the room would be expected to ignite, was determined using the criteria set forth in NFPA 286. Flashover was determined to occur if two of five criteria were met. These criteria were 1) gas temperatures exceeding 600 °C (1,112 °F), 2) flame extending outside of the door, 3) overall HRR measuring 1 MW (3.4E6 Btu/hr), 4) heat flux to the floor exceeding 20 kW/m<sup>2</sup> (105 Btu/(min ft<sup>2</sup>)), or 5) ignition of a crumpled paper target on the floor.

The HRR during the test was measured using oxygen consumption calorimetry with the hood collection system shown in [Figure 7-1](#). Using the measured mass flow rate of exhaust gases and the concentrations of oxygen, carbon dioxide and carbon monoxide, the HRR can be calculated using Thorton's rule which states that 13.1 MJ of energy are produced per 1 kg of oxygen consumed [67].



The mass flow rate of combustion gases was determined by measuring the stack temperature and pressure drop across an orifice plate. A gas analyzer measures the concentration of oxygen (O<sub>2</sub>), carbon dioxide (CO<sub>2</sub>), and carbon monoxide (CO). In addition, the smoke production was also measured using a light extinction system in the duct.

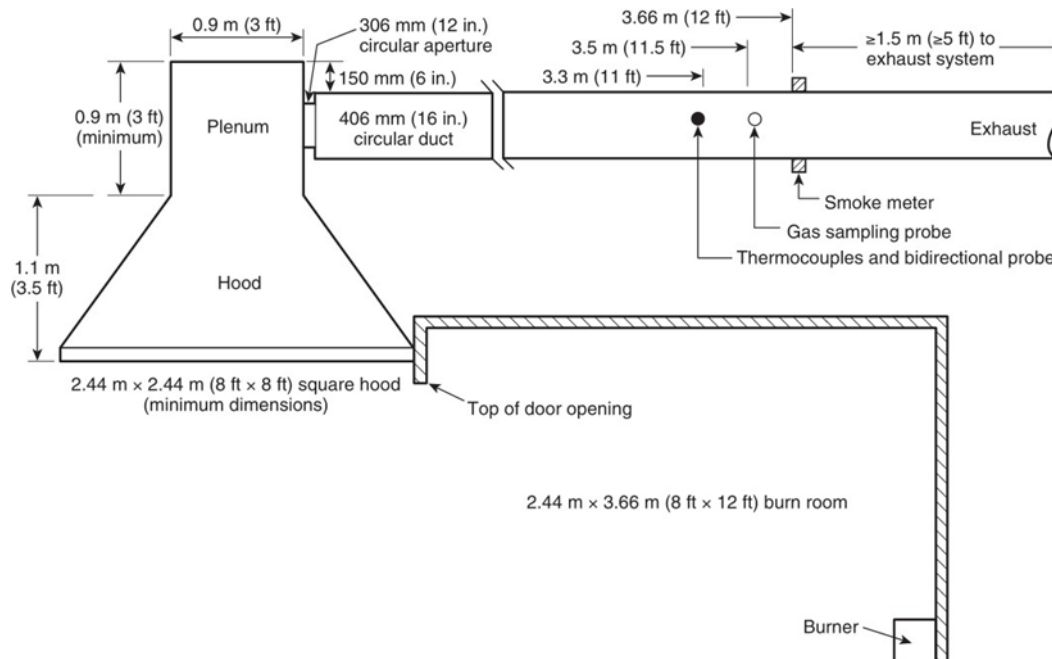


**Figure 7-1. NFPA 286 room configuration with hood and instrumentation (image source NFPA 286) [11] with HRR measured using the hood calorimeter (side view)**

### 7.1.2 Materials Tested

Table 7-1 lists the seven materials which were tested in the NFPA 286 room-corner test in this study. In each test, the material was installed on two side walls, the back wall, and the ceiling. A total of 352 sq. ft. (32.7 m<sup>2</sup>) of material was required for each test. Successfully tested materials mounted to both the walls and ceiling would approve them for use in any location within the rail car. Note that the standard also provides an option to test materials on the walls only or on the ceiling only; however, this would restrict the use of this material to those locations within a rail car.

Materials tested included a range of compositions that are typical of those used in rail car applications. Sandwich composites, consisting of aluminum or steel skins bonded to a wood core material, are commonly used for ceiling panels, bulkheads, and doors in passenger rail cars. Thermoplastics are used for a variety of small and large components, including seatbacks, window masks, windscreens, and luggage compartments. Fiberglass-reinforced polymers (FRPs) are commonly used for seat components and wall linings.

Care was taken during testing to arrange the samples in a way most applicable to end usage installation. The sandwich composite materials (Samples 2 and 3) had a decorative melamine facing on the aluminum skin, and this decorative finish was

exposed. The Sample 6 material likewise had a smooth gel-coat surface finish and was mounted so that this surface was exposed. The Thermoplastic 1 material had a polyvinylidene fluoride (PVDF) surface finish, and this was the exposed surface during testing. The other thermoplastic and FRP materials were constructed so that both sides were the same.

**Table 7-1. Samples selected for testing**

Sample ID	Description and End Use
Sample 1	Thermoplastic 1, opaque light gray thermoplastic material, nominally 3.81 mm (0.150 in.) thick, with polyvinylidene fluoride (PVDF) coating. Used for seat backs, wall panels, window masks, partitions, and ceiling panels.
Sample 2	Sandwich Composite 1, composite material consisting of a layer of plywood sandwiched between layers of aluminum, nominally 12.7 mm (0.500 in.) thick. Decorative melamine facing on exposed side. Used for wall panels, ceiling panels, and closets.
Sample 3	Sandwich Composite 2, composite material consisting of a layer of balsa wood sandwiched between layers of aluminum, nominally 15.9 mm (0.625 in.) thick. Decorative melamine facing on exposed side. Used for wall panels, ceiling panels, and closets.
Sample 4	Thermoplastic 3, translucent thermoplastic material 4.5 mm (0.177 in.) thick, used for light fixtures.
Sample 5	Thermoplastic 2, opaque dark gray thermoplastic material, nominally 4.75 mm (0.187 in.) thick, used for seat backs, wall panels, window masks, partitions, and ceiling panels.
Sample 6	FRP 1, fiberglass reinforced plastic material, nominally 7.0 mm (0.275 in.) thick. Composite composed of chopped fiberglass mat with polyester-type resin with fire retardant additives and gel coat. Commonly used for wall lining, window masks, seat components.
Sample 7	FRP 2, fiberglass reinforced plastic material, nominally 3.27 mm (0.128 in.) thick, used for wall lining components.

Sample ID	Description and End Use
Sample 1	Thermoplastic 1, opaque light gray thermoplastic material, nominally 3.81 mm (0.150 in.) thick, with polyvinylidene fluoride (PVDF) coating. Used for seat backs, wall panels, window masks, partitions, and ceiling panels.
Sample 2	Sandwich Composite 1, composite material consisting of a layer of plywood sandwiched between layers of aluminum, nominally 12.7 mm (0.500 in.) thick. Decorative melamine facing on exposed side. Used for wall panels, ceiling panels, and closets.
Sample 3	Sandwich Composite 2, composite material consisting of a layer of balsa wood sandwiched between layers of aluminum, nominally 15.9 mm (0.625 in.) thick. Decorative melamine facing on exposed side. Used for wall panels, ceiling panels, and closets.
Sample 4	Thermoplastic 3, translucent thermoplastic material 4.5 mm (0.177 in.) thick, used for light fixtures.
Sample 5	Thermoplastic 2, opaque dark gray thermoplastic material, nominally 4.75 mm (0.187 in.) thick, used for seat backs, wall panels, window masks, partitions, and ceiling panels.
Sample 7	FRP 2, fiberglass reinforced plastic material, nominally 3.27 mm (0.128 in.) thick, used for wall lining components.

### 7.1.3 Experiment Description

The testing was performed at SGS Govmark<sup>6</sup> from December 11, 2017, to December 14, 2017. The test room was constructed of cinder blocks, and the ceiling of 2x6 studs lined with 5/8 in. drywall. One test was performed with each material sample. Each day before testing, the room was calibrated with a 160-kW burner HRR for 10 minutes with the burner located inside the room. The calibration factors were assessed to ensure that the new calibration factor was not more than 5 percent different than one obtained the previous day as required by the standard.

The material samples were obtained or modified to fit into 4 ft. by 8 ft. panels. These panels were affixed to the ceiling by using drywall screws. The ceiling panels were also drilled for the seven thermocouples which protrude from the ceiling during the test.

The attachment method for the walls varied based on the material configuration. For the first two tests (Sample 6 and Sample 1), the material was screwed directly into steel studs with self-tapping screws. The sandwich composite panels were not screwed, but were placed directly in contact with the cinder block walls. Sample 4 and 5 materials, as well as Sample 7, were screwed to 5/8 in. drywall that was mounted onto steel studs. This wall panel configuration for the thermoplastic and FRP materials is shown in [Figure 7-2](#). The sandwich composites were not attached to any drywall or studs on the walls. The wall panels were held in place using spreader bars, with flanges screwed to the exposed material. This support method configuration is shown in [Figure 7-3](#) for Sample 6.

The testing was performed in accordance with NFPA 286. The materials were conditioned in the testing room for at least 50 minutes before commencement of the burn. The testing room was kept within a temperature range of 20 °C ±10 °C (68 °F ± 18 °F). Temperatures, HRR, and floor heat flux were monitored during the test, and operators observed conditions in the room. Flashover was determined to occur if two of the five metrics were met [11]: 1) ceiling temperature above 600 °C, 2) HRR over 1 MW, 3) heat flux to gage on floor over 20 kW/m<sup>2</sup>, 4) ignition of paper target on floor, or 5) flame extended from doorway to room.

Tests ran a maximum of 15 minutes, with the 0.3 m by 0.3 m burner providing a 40 kW HRR for the first 5 minutes, and 160 kW for the remaining 10. The testing was terminated upon occurrence of flashover. Two or three garden hoses were used to extinguish the fire upon completion of the tests, regardless of the result of the test (flashover or not).

---

<sup>6</sup> SGS Govmark, 96 Allen Blvd., Farmingdale, NY 11735-5626, United States.



**Figure 7-2. Thermoplastic three wall panels screwed to 5/8-inch drywall sandwich with steel studs**

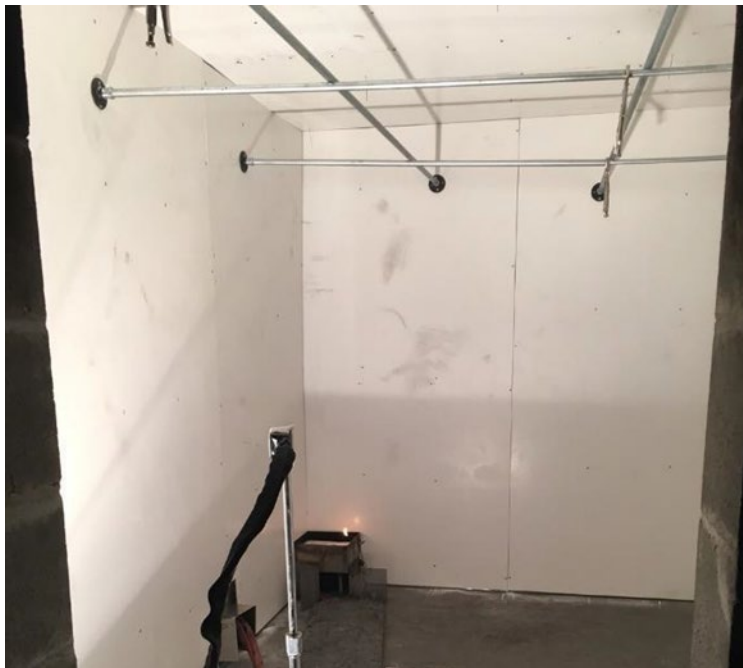


**Figure 7-3. Sample 6 setup. Spreader poles held the wall panels in place, with flanges screwed to the material**

## 7.2 Results

### 7.2.1 Overall Material Performance

Table 7-2 contains the results from the NFPA 286 room-corner testing. Four out of the seven materials caused flashover thereby failing in the room-corner test. The results for peak HRR (kW) and total heat released (MJ) include the burner HRR, which is 40 kW for the first 300 seconds (5 minutes), and then 160 kW for 600 seconds (10 minutes) making the total test duration 900 seconds (15 minutes). The heat released by the propane burner is 108 MJ for a test which proceeds until the end of the 160 kW burner regime. The test was stopped if flashover was determined to occur, so the values for total heat release (THR) for materials which caused flashover are usually lower due to the shorter test duration. For example, Sample 7, which did not cause flashover, had a 4 MJ contribution from the lining, but a THR of 112 MJ. Sample 2, conversely, ran for 560 seconds until flashover occurred and the heat release from the linings was 38 MJ while the THR was 92 MJ.

**Table 7-2. Sample NFPA 286 test results**

Sample ID	Description	Flashover Time (s)	Peak Upper Layer Temperature (°C)	Peak Heat Release Rate (kW)	Total Heat Released (MJ)	Lining Contribution Heat Release (MJ)
Sample 1	Thermoplastic 1	No flashover	440	240	122	14
Sample 2	Sandwich Composite 1	560	757	653	92	38
Sample 3	Sandwich Composite 2	383	714	931	59	34
Sample 4	Thermoplastic 3	190	682	1,016	65	57
Sample 5	Thermoplastic 2	No flashover	499	271	136	28
Sample 6	FRP 1	576	832	766	123	67
Sample 7	FRP 2	No flashover	414	191	112	4

### 7.2.2 Test Observations

A log of events that occurred was recorded for each test. These logs are displayed in [Table 7-3–Table 7-9](#). Official test reports are included in [Appendix C.1](#). Data plots are contained in [Appendix C.2](#), and photos of the testing are included in [Appendix C.3](#).

Of the four materials which cause flashover, the Thermoplastic 2 material was the only one to cause flashover within the 5 minute 40 kW burner regime. This material caused room flashover in about 3 minutes and was difficult to extinguish compared to the other materials which caused flashover. The other three materials which caused flashover were composite materials. The two sandwich composites both caused flashover. Flashover occurred within 2.5 minutes of ramping the HRR to 160 kW for test with Sample 3, which had a light balsa core. For Sample 2, which had a denser plywood core, and Sample 6, flashover occurred at about 4.5 minutes after ramping to the 160 kW burner HRR.

The two thermoplastics which did not cause flashover (Samples 1 and 5) both experienced significant material deformation resulting in holes and material collapse on both the walls and ceiling. Limited intumescent behavior was observed for the material on the walls near the burner. During both tests material fell directly on the sand burner, and this temporarily provided additional fuel. The loss of materials from the wall and ceiling limited the flame spread to the area very near the burner. The lack of flame spread resulted in a lower overall HRR. Upon increasing the HRR to 160 kW, the upper layer temperature rose to 330–430 °C. This was a sufficient temperature to cause the material to yield under its own weight, and fall from the ceiling. This falling material was in a taffy-like semi-solid state. Most of the ceiling material fell from the surface away from the flames limiting its ignition and contribution to the fire.

The second fiberglass material, Sample 7, did not flashover and had the best performance of all the materials in the study. Very little of the material burned, and no collapse or yielding was observed. The material which was left blackened/charred but limited burning occurred. No flame spread was observed.

HRR plots are shown for the seven materials in [Figure 7-4–Figure 7-10](#). For almost all the materials, the contribution to the HRR during the 40-kW regime was minimal. Only with the Sample 4 material was the contribution significant, and this material caused the room to develop to flashover conditions within the first 5 minutes of the test.

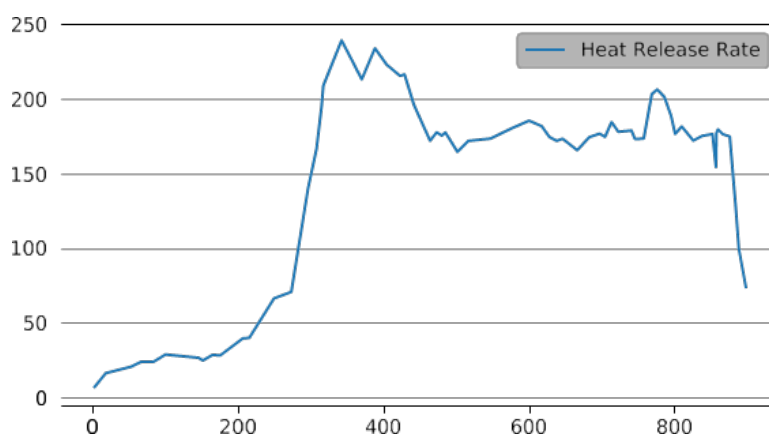


**Figure 7-4. NFPA 286 test HRR vs. time for Sample 1**

**Table 7-3. Test log for Sample 1**

Time	Event
35 s	Wall browning
45 s	Material deformation/warping
100 s	Wall ignition
120 s	Smoky upper gas layer
160 s	Panel burn-through, fall away
200 s	Material falling on burner
264 s	More, larger chunks of material falling on burner

Time	Event
300 s	Increase burner HRR to 160 kW
374 s	Ceiling falling
465 s	Extinguish under burner with squirt from water hose
530 s	Material falls on/near heat flux gage
820 s	Last ceiling panel collapse
900 s	End test, extinguish, no flashover

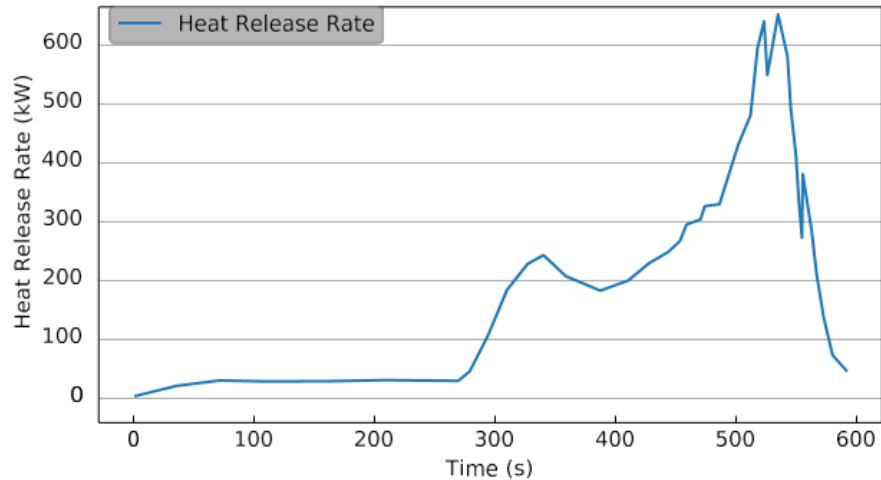


**Figure 7-5. NFPA 286 test HRR vs. time for Sample 2**

**Table 7-4. Test log for Sample 2**

Time	Event
45 s	Wall browning
57 s	Wall ignition
120 s	4.5–5 ft. flame height, wall brown in corner, but no lateral flame spread
227 s	Smoky upper layer
298 s	Ramp to 160 kW
300 s	Ceiling, wall ignition in corner
310 s	Consistent flame impingement on ceiling
350 s	Ceiling browned on far panel in corner
426 s	Outer layer on ceiling failed, ignition of plywood
510 s	Wall burning away from corner, thick smoke in room
560 s	Flashover (temps, flame out door)
566 s	Stop test, extinguish

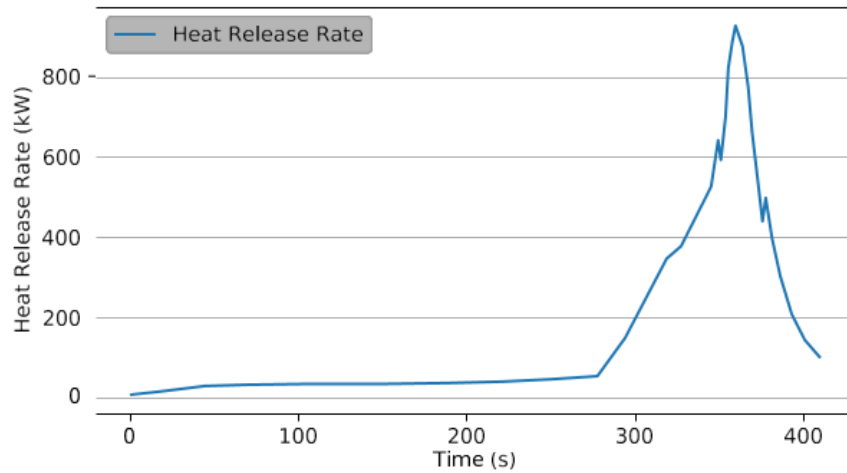


**Figure 7-6. NFPA 286 test HRR vs. time for Sample 3**

**Table 7-5. Test log for Sample 3**

Time	Event
25 s	Melamine facing/glue crackling and popping
45 s	Wall browning
55 s	Wall Ignition
120 s	Light smoke upper layer
150 s	Fire under pot extinguished with squirt from water hose, bottom of panel burning on sidewall near burner
180 s	Extinguish flame under pot again
210 s	Extinguish flame again
300 s	160 kW HRR, flames on ceiling, increased popping sound
375 s	Fire ignites walls, thick black smoke
383 s	Flame out door, flashover



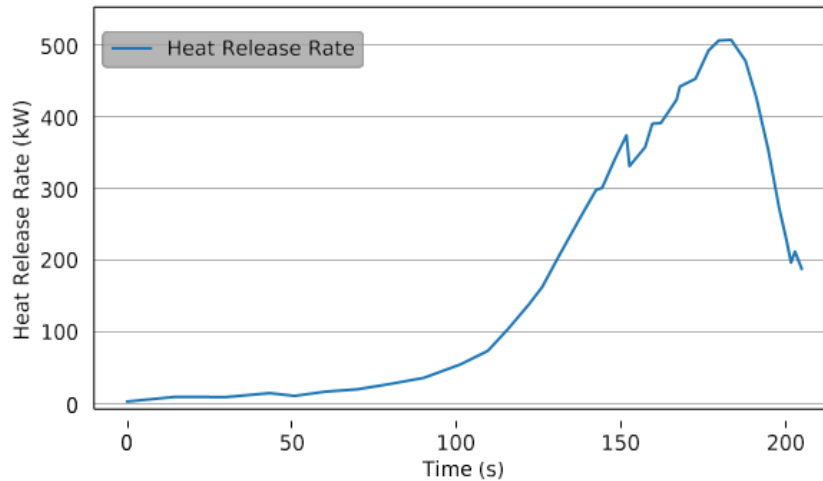


**Figure 7-7. NFPA 286 test HRR vs. time for Sample 4**

**Table 7-6. Test log for Sample 4**

Time	Event
35 s	Wall ignition
60 s	Minimal wall browning, some glistening of material on back wall
90 s	Flames on ceiling (which is fail according to NFPA 286)
150 s	Thick black smoke
175 s	Flame out door
190 s	Extinguish, flashover
220 s	Finally extinguished

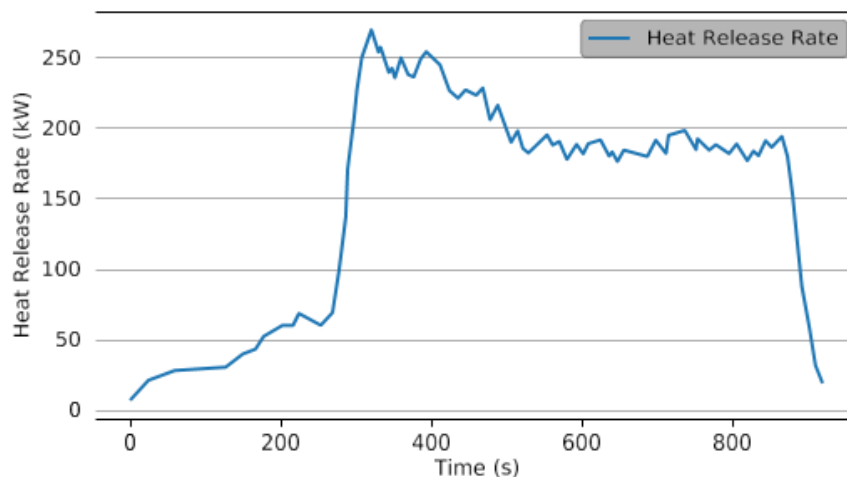


**Figure 7-8. NFPA 286 test HRR vs. time for Sample 5**

**Table 7-7. Test log for Sample 5**

Time	Event
44 s	Wall ignition
76 s	Smoky upper layer
100 s	5 ft. max flame height (sporadic)
180 s	Material falling, collapsing in corner near burner
210 s	Black smoke coming out doorway
230 s	Lots of material falling on burner
300 s	160 kW burner HRR
340 s	Ceiling material falling, wall material burning
380 s	Chunks falling off ceiling, material yielding
430 s	Material that was burning under gas burner extinguished with squirt from water hose
770 s	Chunks falling from ceiling farthest from burner
900 s	End test, extinguish, no flashover

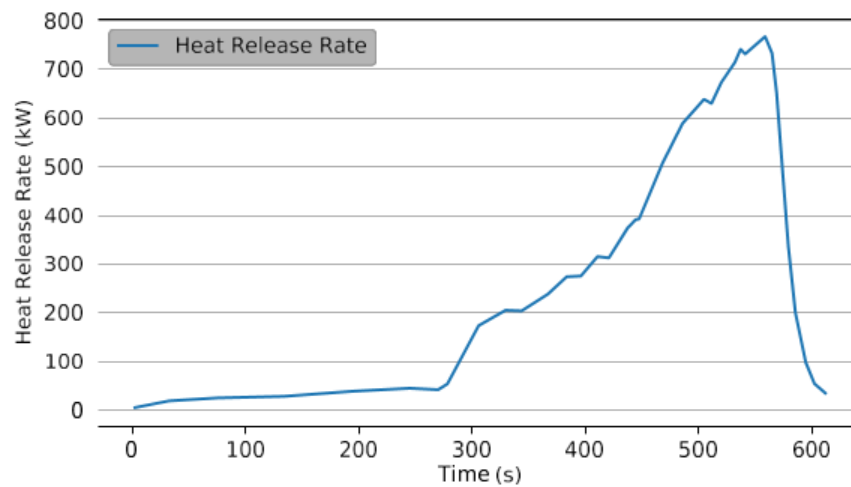


**Figure 7-9. NFPA 286 test HRR vs. time for Sample 6**

**Table 7-8. Test log for Sample 6**

Time	Event
20–30 s	Material started browning on walls, delamination
180 s	Flame height about 5 ft. max
195 s	Wall ignition next to burner
240 s	3 ft. layer height
300 s	Ramp to 160 kW
450 s	Back wall burning
560 s	Paper target ignition
576 s	Flame out doorway
589 s	End test, extinguish

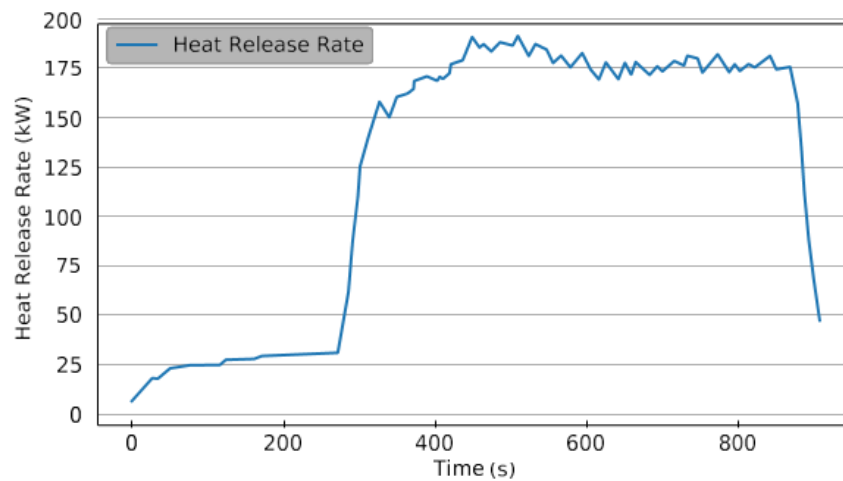


**Figure 7-10. NFPA 286 test HRR vs. time for Sample 7**

**Table 7-9. Test log for Sample 7**

Time	Event
40 s	Crackling/popping sound
63 s	Wall browning, minimal ignition if any
110 s	Light smoke in upper layer
149 s	Blackened wall material in corner
285 s	About 4.5 ft. flame height
295 s	Ramp to 160 kW
360 s	Light smoke issuing from between panels near corner
460 s	Ceiling ignition on edge of panels
900 s	Stop test, no flashover, minimal ignition

### **7.3 Section Summary**

NFPA 286 room-corner testing was performed for seven material samples that are typical of those that may be used on rail cars. This testing used the standard fire exposure of 40 kW for 300 seconds (5 minutes) followed by 160 kW for 600 seconds (10 minutes), for a total test duration of 900 seconds (15 minutes). Out of the seven materials, four caused the room to flashover. The best performing material was Sample 7, which did not cause flashover and stayed in place during the test. Samples 1 and 5 did not cause flashover, but exhibited substantial yielding and collapse from the walls and ceiling. The three other composite materials caused flashover in the 160-kW burner regime. Sample 4 caused flashover within 190 seconds during the 40-kW burner regime.

The materials used in the work for this report were also tested in the cone calorimeter per ASTM E1354 and the flame spread apparatus per ASTM E162. The combined data from large and small-scale testing will be used to validate fire growth models which will be used to develop small-scale fire performance requirements for interior finish materials based on further analysis with the validated empirical model.

## 8. Validation of FDS and Empirical Model in Predicting Rail Car Lining Fire Growth Contribution

---

An empirical flammability model which correlates parameters from cone calorimeter testing to NFPA 286 room corner testing was developed and calibrated in [Section 4](#). This method uses HRR, ignitability, and burning duration data from the cone calorimeter test to predict whether the material will cause flashover in a room-corner test. However, test data at both scales were not available for materials used in passenger rail cars.

Testing was performed on seven materials in both the cone calorimeter (ASTM E1354) and the room-corner test (NFPA 286) summarized in [Sections 6](#) and [7](#), respectively. The resulting data and analysis are used to validate the empirical modeling approach in this study. This validated flammability model can develop effective performance criteria for screening hazardous materials. In addition, FDS results were compared with room-corner test experimental data to validate its use to support developing requirements as needed.

### 8.1 Empirical Flammability Model

The flammability model developed in [Section 4](#) is an empirical model which has been used to predict flashover from material flame spread in full-scale room environments. This model was originally developed by Qunitiere, Harleroad, and Hasemi [41], Mowrer and Williamson [42], and Beyler et al. [43] based on flame spread theory. It describes the propensity of a material to cause flame spread in a full-scale compartment, based on material flammability parameters from a small-scale test. The flammability parameter is defined as

$$F = 0.01 \dot{Q}'' - t_{ig}/t_{bd} \quad (8-1)$$

where  $\dot{Q}''$  is the average HRR per unit area in kW/m<sup>2</sup>,  $t_{ig}$  is the time to ignition in seconds, and  $t_{bd}$  is the burn duration, also in seconds. These variables are obtained from cone calorimeter tests performed at 50 kW/m<sup>2</sup> heat flux. The constant 0.01 represents the flame height correlating factor, and its units are m<sup>2</sup>/kW.

The flammability parameter relates small-scale test parameters to flame spread potential in full-scale room-corner experiments. There are two main components to this equation. The first,  $\dot{Q}''$ , represents the contribution to flame spread from the burning material. A high value of the average HRR indicates a high propensity for flame spread. The second component,  $t_{ig}/t_{bd}$ , is a ratio between the ignition resistance and the duration of burning. A large ignition resistance and short burning duration can decrease the size of the burning region leading to material burnout.

Beyler et al. [43] stated that the theoretical development of the model implies a critical flammability parameter of 1.0, which separates materials which will cause accelerating flame spread. Due to material preheating and differences in initiating fires and compartment configurations, a realistic critical flammability parameter is lower. In comparison of tests from different studies, Beyler et al. [43] found that materials having  $F < 0$  would not cause flashover in the ISO 9705 room-corner test (source fire of 100 kW

for 10 minutes followed by 300 kW for 10 minutes), but mixed results occur when  $0 < F < 0.2$ . Lattimer and Sorathia [44] found similar results; however, they stated the range being  $0 < F < 0.5$  where there would be mixed results. For NFPA 286 which has a smaller source fire (40 kW for 5 minutes followed by 160 kW for 10 minutes), a flammability parameter threshold value of  $F < 0.6$  was found to correlate with existing NFPA 286 room-corner test results, as introduced in [Section 4](#). It was recommended that more data should be obtained to further validate the flammability parameter threshold for NFPA 286.

## 8.2 Evaluation of Empirical Model Predictions

### 8.2.1 New Test Data Summary

Seven materials were tested by Jensen Hughes for the purpose of validating models that will be used to guide the determination of appropriate fire safety performance requirements of interior finish materials on passenger rail cars. This will include validating the empirical model for predicting flashover in NFPA 286 and FDS for more detailed predictions of fire growth in the NFPA 286 room-corner test. The materials were tested in the cone calorimeter according to ASTM E1354, radiant panel tests according to ASTM E162, and the room-corner test according to NFPA 286. [Table 8-1](#) contains the materials which were included in the program. A variety of material types were selected, including fiberglass reinforced plastics (FRPs), sandwich composite materials (composed of metal facings with a wood core), and polymers.

**Table 8-1. Material samples selected for testing**

Sample ID	Description and End-Use
Sample 1	Opaque thermoplastic material, nominally 3.81 mm (0.150 in.) thick, with polyvinylidene fluoride (PVDF) coating. Used for seat backs, wall panels, window masks, partitions, and ceiling panels.
Sample 2	Composite material consisting of a layer of plywood sandwiched between layers of aluminum, nominally 12.7 mm (0.500 in.) thick. Decorative melamine facing on exposed side. Used for wall panels, ceiling panels, and closets.
Sample 3	Composite material consisting of a layer of balsa wood sandwiched between layers of aluminum, nominally 15.9 mm (0.625 in.) thick. Decorative melamine facing on exposed side. Used for wall panels, ceiling panels, and closets.
Sample 4	Translucent thermoplastic material 4.5 mm (0.177 in.) thick, used for light fixtures.
Sample 5	Opaque thermoplastic material, nominally 4.75 mm (0.187 in.) thick, used for seat backs, wall panels, window masks, partitions, and ceiling panels.
Sample 6	Fiberglass reinforced plastic material, nominally 7.0 mm (0.275 in.) thick. Composite composed of chopped fiberglass mat with polyester-type resin with fire retardant additives and gel coat. Commonly used for wall lining, window masks, seat components.
Sample 7	Fiberglass reinforced plastic material, nominally 3.27 mm (0.128 in.) thick, used for wall lining components. Woven glass fabric with phenolic resin.

The results for small and large-scale tests are presented in the previous [Sections 6](#) and [7](#). [Table 8-2](#) contains a selection of test results as well as the flammability parameters calculated from the cone calorimeter data tested at 50 kW/m<sup>2</sup>. Four out of the seven materials caused flashover in the NFPA 286 room-corner test. Six of these materials

currently qualify for use in passenger rail cars with a passing ASTM E162 radiant panel index (RPI) of less than 20., except Sample 4 which had a RPI of 180.

**Table 8-2. Small and large-scale fire tests results for materials with flammability parameter calculated from ASTM E1354 data at 50 kW/m<sup>2</sup>**

Sample ID	Average HRR (kW/m <sup>2</sup> )	Ignition time (s)	Burn duration (s)	Flammability Parameter <i>F</i>	NFPA 286 time to flashover (s)	NFPA 286 peak HRR (kW)
Sample 1	160	48	393	1.47	No flashover	240
Sample 2	67	70	937	0.59	560	653
Sample 3	32	33	684	0.27	383	931
Sample 4	477	26	294	4.68	190	1,016
Sample 5	124	34	623	1.19	No flashover	271
Sample 6	102	269	1,020	0.75	576	766
Sample 7	54	171	556	0.23	No flashover	191

As summarized in [Section 7](#), three samples did not cause flashover in the room-corner test, which include an FRP material, Sample 7, as well as two transportation-grade fire-retardant thermoplastics, Samples 1 and 5. Sample 7 had excellent performance in the cone calorimeter with an average HRR of less than 54 kW/m<sup>2</sup>. Samples 1 and 5 had moderate HRR and short ignition times in small-scale testing but did not cause flashover. However, these materials were observed to deform and fall from the surface during the room-corner test resulting in different from expected large-scale performance. Conversely, Sample 3 and Sample 4 had very good small-scale performance resulting in flashover in the room-corner test. This material had the aluminum facesheet debond during the fire test, exposing the core material which resulted in flashover.

### 8.2.2 Empirical Model Calibration

Data acquired from testing of actual interior passenger rail cars enables the evaluation of the empirical model predictions. In [Section 4](#), a critical flammability parameter of 0.6 was identified as a value which appropriately separated materials which caused flashover in the NFPA 286 test from those which did not. [Figure 8-1](#) contains a plot of the time to flashover and corresponding flammability parameters for materials tested by JENSEN HUGHES. These data are also listed in [Table 8-2](#). Half of the materials performed as expected in terms of flashover prediction by the empirical model, while the other half did not. Some of these materials which had flammability parameters of less than 0.6 caused flashover while others that had a flammability parameter greater than 0.6 resulted in no flashover. The differences in performance compared with the empirical model predictions can be explained through the material behavior in large scale.

Samples 2 and 3 were aluminum-faced sandwich composite materials whose flammability parameters are both less than the threshold value ( $F < 0.6$ ). Sample 2 had a plywood core while Sample 3 had balsa. During cone calorimeter testing the aluminum facing delaminated but stayed intact. As a result, the escaping flammable gases burned.

However, the aluminum facing shielded for the wood core from direct radiation. These sandwich composite materials had better than average performance in the cone calorimeter, with Sample 2 and Sample 3 having flammability parameters of 0.59 and 0.27, respectively. However, in the room-corner test these materials caused flashover. During the room-corner tests the aluminum facing experienced burn-through and delamination, exposing the core material to the fire. This accelerated the fire growth ultimately resulting in flashover. This material response was not predicted by the cone calorimeter test, even when the sample was placed in the vertical orientation.

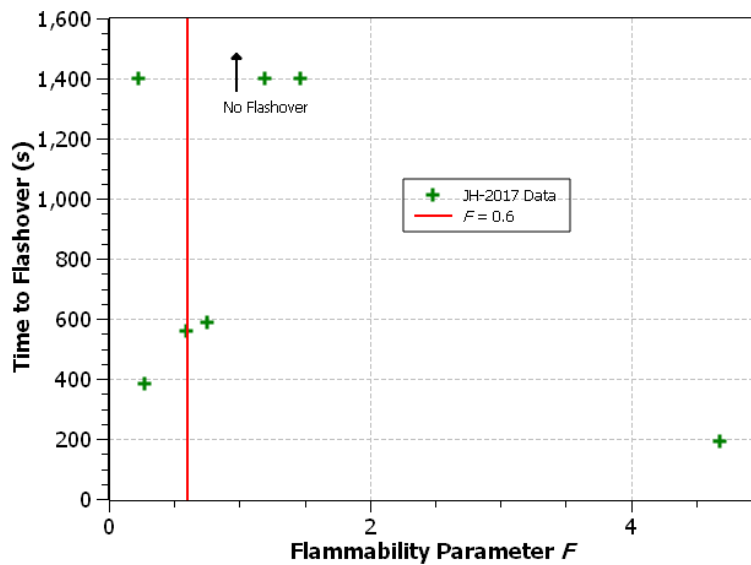


**Figure 8-1. Comparison of time to flashover and flammability parameter for newly tested materials**

Samples 1 and 5 (thermoplastics), in the current study, had flammability parameters of 1.19 and 1.47 but did not cause flashover in the room-corner test. These were modern thermoplastics which designed specifically for use in the mass transit industry. Although in the cone calorimeter the materials had high HRR results relative to the other materials in the study, during the room-corner test most of the installed material fell from the upper portion of the walls and the ceiling without being ignited. Essentially, this removed the potential for flame spread.

True evaluation of these materials as relating to the flammability model would require the materials to stay in place during the test. However, the goal of testing is to ensure an adequate level of fire safety performance for materials in end use applications. The results from the room-corner test indicate that these materials provide this level of safety. For some materials, a full-scale room-corner test may be necessary to assess the potential for flame spread.

### 8.2.3 Effectiveness of Empirical Model

Figure 8-2 contains the building material data previously used as well as the data from the current test program. A flammability parameter of -1 signifies a material which did not ignite in the cone calorimeter. Two materials tested by Kim and Onno [45], polystyrene and polyurethane, did not ignite in the cone calorimeter and were assigned



$F = -1$ . Both materials had significant collapse in the cone calorimeter resulting in no ignition at  $50 \text{ kW/m}^2$ . In the room-corner test, polystyrene melted away from the flames and did not result in flashover while the polyurethane deformed but remained sufficiently in place to support flame spread and ultimately cause flashover. Overall, the approach of using the flammability parameter to correlate room-corner test performance assumes that the material stays in place and does not experience significant differences in physical response compared to the cone calorimeter test. In general, the model works well in predicting these types of materials that stay in place but may not be predictive if there are material failures or other physical changes.

The materials from the study by NASFM [27] were also included in this plot. The flammability parameter was calculated using the average HRR and time to ignition reported in the NASFM report with an estimated burnout time from similar materials in the rail car material database established in [Section 2](#). The two materials selected were a Nomex® rail car panel (aluminum-Nomex®-aluminum composite) and a plywood rail car panel (aluminum-plywood-aluminum composite) [27], similar in construction to the sandwich composites tested by Jensen Hughes. Based on database information from [Section 2](#), the Nomex panel had an aluminum honeycomb core and was estimated to have a burnout time of 352 seconds while the plywood panel was estimated to have a burnout time of 620 seconds.

Note that materials with a flammability parameter of  $0.6 < F < 0.9$  are borderline materials. These materials have a wide range of times to flashover, from no flashover to flashover occurring over 300 seconds after the burner is increased to 160 kW. These materials require additional investigation using detailed modeling with FDS to determine what their performance may be inside a rail car.

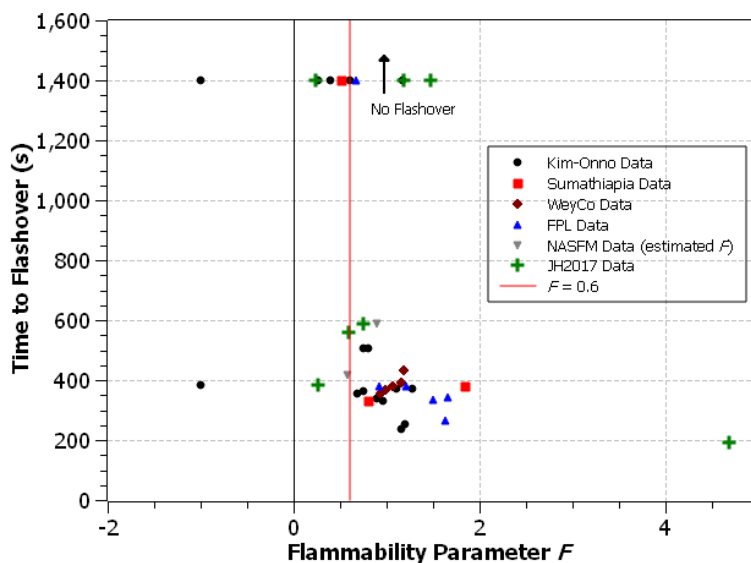


**Figure 8-2. Time to flashover in the NFPA 286 room-corner test versus flammability parameter for all available materials [27], [45]–[48], [68]**

[Figure 8-3](#) contains a plot of the flame spread index versus flammability parameter for the previously established rail car material database. The materials tested by Jensen Hughes are also included. The results show that only 30 percent of materials that pass

the ASTM E162 test with a flame spread index of less than 35 have a flammability parameter of less than 0.6. Additional qualification tests, such as the NFPA 286 room-corner test, may be necessary to qualify materials which have better large-scale performance than indicated by the small-scale cone calorimeter data.

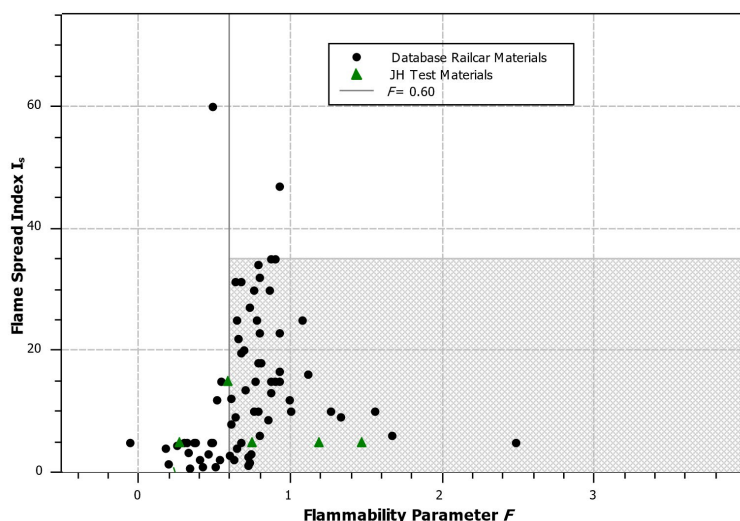


**Figure 8-3. Flammability parameter versus ASTM E162 flame spread index of database rail car materials**

### 8.3 FDS Modeling of Room-corner Tests

During the room-corner tests, some unexpected behaviors were observed. In the tests of Samples 1 and 5, materials were observed to fall off before they ignited. The aluminum facesheet of Samples 2 and 3 (sandwich composite materials) experienced burn-through and delamination, which enabled easier fire spread across the underlying wood surface. To study such behaviors and their effects on flashover prediction, the fire growth modeling using FDS developed and validated in the previous [Section 5](#) was used to simulate the room-corner tests of all seven samples. More building materials were also modeled and the results are presented in [Appendix D](#).

In the FDS modeling, a HRRPUA material burning model was used. The peak values and time history of HRRPUA from the 50 kW/m<sup>2</sup> cone calorimeter tests ([Section 6](#)) were used to define the burning rate. The prediction in HRR of the room and center ceiling temperature is presented and compared with experimental data ([Section 7](#)).

#### 8.3.1 Sample 1

The NFPA 286 room-corner test of Sample 1 (thermoplastic) was modeled, with and without considering the materials falling. In the first case, the materials are assumed to stay in place during the test. Flashover was predicted to occur after 800 seconds, when the total HRR reached 1 MW and the center ceiling temperature was above 600 °C as shown in [Figure 8-4](#).

In the second case, the materials are assumed to fall off when the unexposed surface reached 80 °C, the estimated glass transition temperature of Sample 1 material. This

glass transition temperature was the average glass transition temperature of Polymethyl methacrylate (PMMA) and Polyvinyl chloride (PVC) [67], which are the two base polymers of the thermoplastic. Substantial portions of the material placed along the wall corner and on the ceiling above the burner fell as can be seen in Figure 8-5, which was also observed at the end of the test. Circled areas in the Figure 8-5 shows where the material fell from the ceiling. Since the materials fell before they were ignited, the HRR did not increase as much as when the materials were assumed to stay in place, as shown in Figure 8-4.

During the room-corner test of Sample 1, it was observed that some material fell onto the burner and ignited. That could explain why the measured HRR and center ceiling temperature during the test are higher than the model prediction.

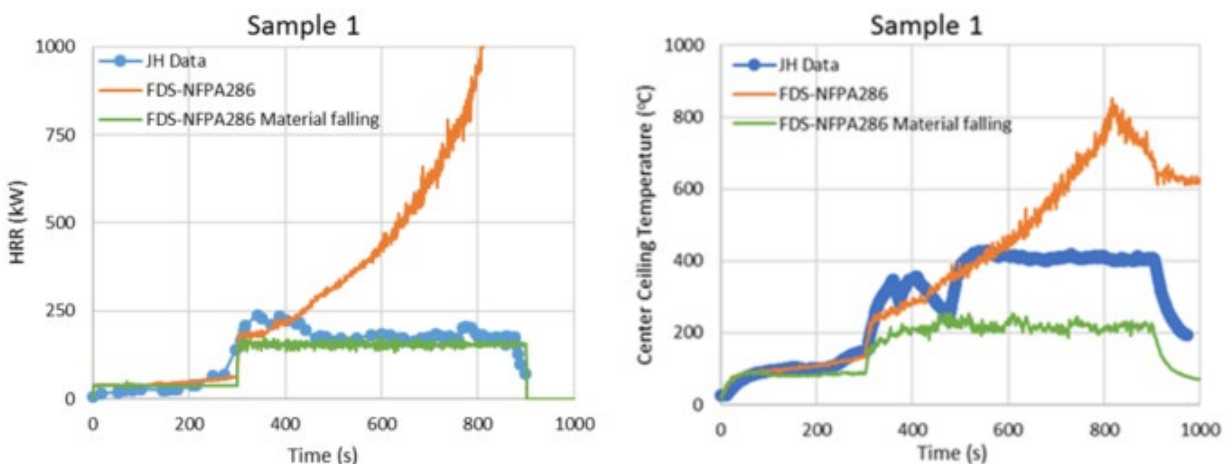


**Figure 8-4. Effect of material falling on flashover prediction for sample 1: (left) HRR and (right) ceiling center temperature**

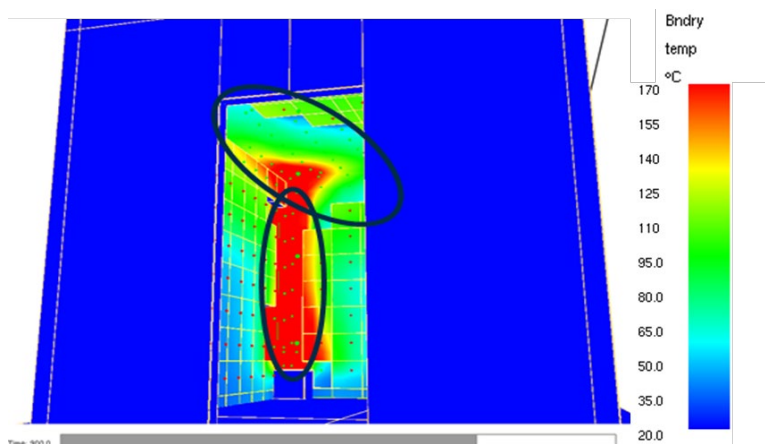


**Figure 8-5. Simulation of Sample 1 materials falling at time of 900 second**

### 8.3.2 Sample 2

The fire growth modeling was also performed based on the Sample 2 NFPA 286 room-corner test. Sample 2 is an aluminum-faced sandwich panel with plywood core. Figure

8-6 presents the comparison of HRR and center ceiling temperature. In the first case, the aluminum facesheet is assumed to stay in place during the test. No flashover was predicted because the facesheet protected the plywood core from igniting.

In the second case, the aluminum facesheet was assumed to fail (delaminate and fall off) when the epoxy adhesive between facesheet and core reached its glass transition temperature of 80 °C [69]. After the facesheet was predicted to fall from the surface, the 50kW/m<sup>2</sup> cone calorimeter test data for plywood [45] was used as HRRPUA material burning model for the boundary. The failing of the facesheet exposed the plywood core making it easier to ignite and spread flame across the surface. As a result, flashover was predicted to occur consistent with experimental observation. The predictions of the time history of HRR and center ceiling temperature have similar profiles compared with the experimental data, as shown in Figure 8-6. Note that the test was terminated right after flashover occurred in the test at 566 seconds.

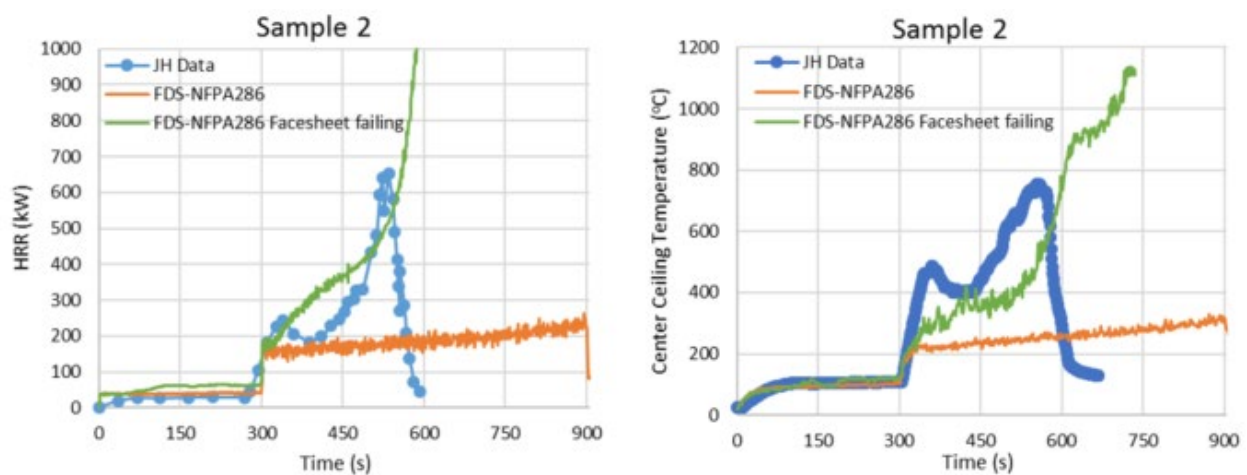
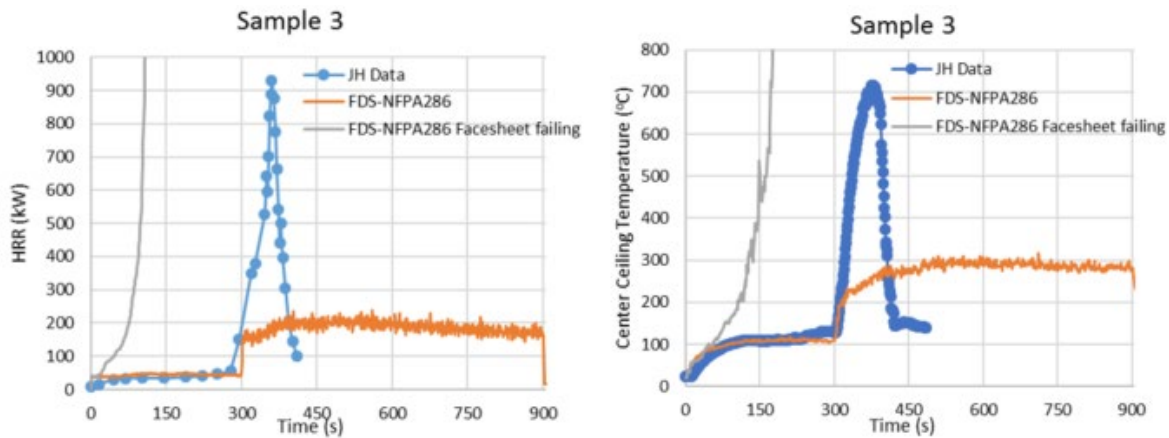


**Figure 8-6. Effect of facesheet failing on flashover prediction for Sample 2 (left) HRR and (right) ceiling center temperature**

### 8.3.3 Samples 3–7

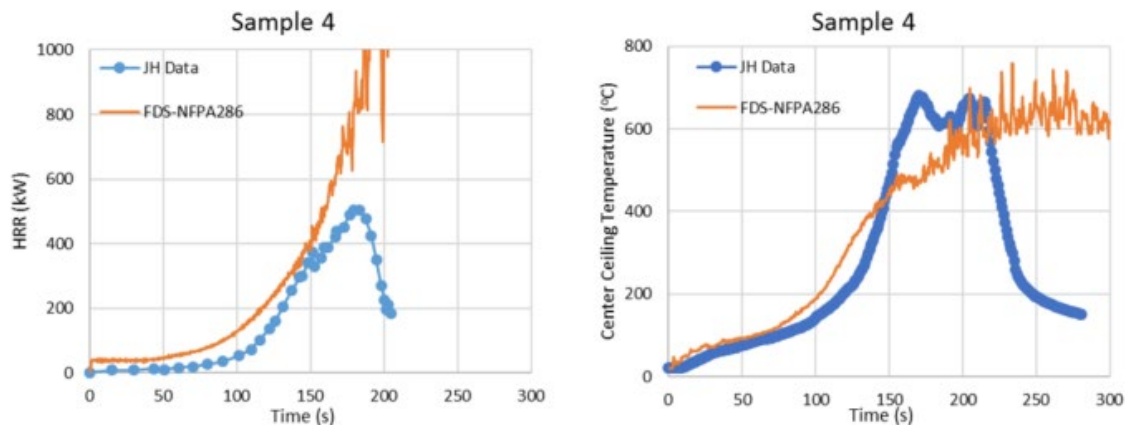
The FDS simulations of the NFPA 286 room-corner tests on Samples 3–7 are presented in this section.

Figure 8-7 depicts the time history of HRR and center ceiling temperature of Sample 3, which is a composite material consisting of a layer of balsa wood sandwiched between layers of aluminum. In the FDS simulation, the aluminum facesheet is assumed to stay in place during the test, and no flashover was predicted. During the test, it was observed that the aluminum facesheet delaminated and the fire burned through the facesheet of the corner wall panel and the middle ceiling panel also delaminated (Section 7). Flashover occurred at 383 seconds. When the model included the facesheet delamination using the method previously described for Sample 2, the predictions also resulted in the lining material causing the room to reach flashover similar to the experimental data. The model predictions are also conservative relative to the experimental data, likely due to not having measured the HRR of the actual core material.



**Figure 8-7. Time history of HRR (left) and center ceiling temperature (right) of Sample 3 tested in NFPA 286 room**

Figure 8-8 presents the time history of HRR and center ceiling temperature of Sample 4, a translucent thermoplastic material. The test was terminated at 190 seconds when the flashover occurred. In the FDS simulation, flashover was predicted to occur at 195 seconds which agrees with the experimental data.

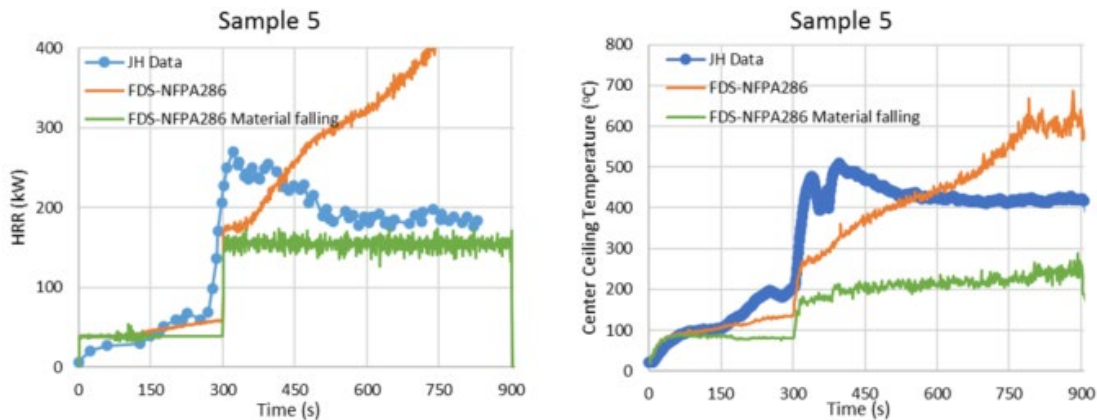


**Figure 8-8. Time history of HRR (left) and center ceiling temperature (right) of Sample 4 tested in NFPA 286 room**

Figure 8-9 presents the time history of HRR and center ceiling temperature of Sample 5, an opaque thermoplastic material. Flashover did not occur during the test, but materials were observed to fall from the wall and ceiling. When the materials were assumed to stay in place, flashover was not predicted to occur but the HRR and center ceiling temperature were predicted to keep increasing after the HRR of the burner was increased to 160 kW. Similar to the method used for Sample 1, the material falling from the surface was modeled to occur when the unexposed surface temperature reached the estimated glass transition temperature of 145 °C. This glass transition temperature is that of polycarbonate [67], which is the base polymer for this material. When materials falling from the surface was accounted for in the FDS model, the model predicted no flashover which is similar to that observed in the testing, see Figure 8-9. The predicted HRR and center ceiling temperature were lower than the test data, likely due to not

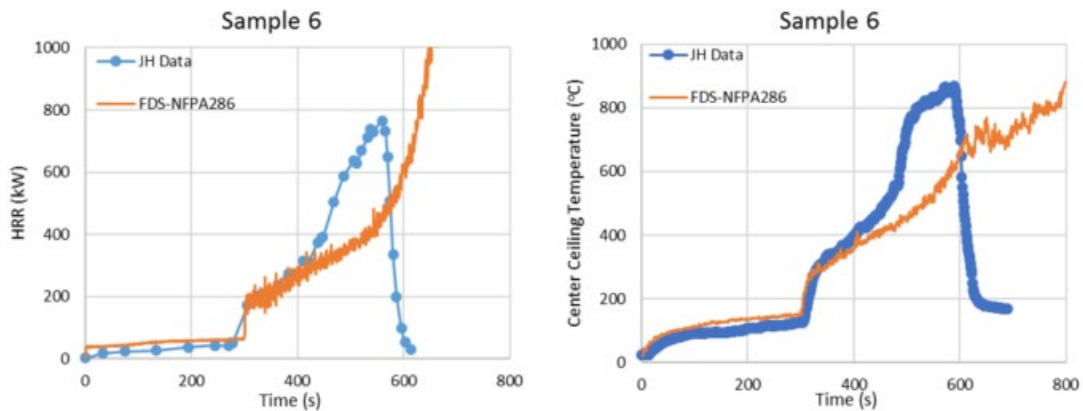


having the material ignited on and around the burner, which was observed in the testing.



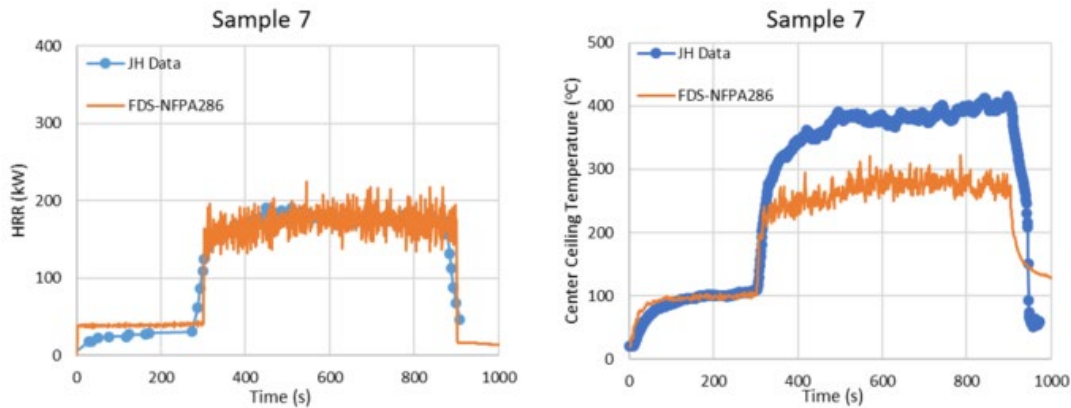
**Figure 8-9. Time history of HRR (left) and center ceiling temperature (right) of Sample 5 tested in NFPA 286 room**

Figure 8-10 contains the time history of HRR and center ceiling temperature of Sample 6, which is a fiberglass reinforced plastic material. In the test, flashover occurred at 576 seconds when the flames were observed to exit doorway. In the FDS simulation, flashover was also predicted to occur. The predicted time to flashover, determined using HRR and center ceiling temperature, is about 100 seconds later than the experimental data.



**Figure 8-10. Time history of HRR (left) and center ceiling temperature (right) of Sample 6 tested in NFPA 286 room**

Figure 8-11 contains the time history of HRR and center ceiling temperature of Sample 7, which is also a fiberglass reinforced plastic material. In the test, flashover did not occur. The FDS simulation also predicted no flashover. The prediction in HRR agreed with the experimental data, while the predicted center ceiling temperatures were about 100 °C lower than experimental data.



**Figure 8-11. Time history of HRR (left) and center ceiling temperature (right) of Sample 7 tested in NFPA 286 room**

From the fire growth modeling results of room-corner tests, it was found that the facesheet failing of sandwich composite panels exposed their core materials to the heat source for easier flame spread, which caused flashover to occur. For some modern thermoplastics, flashover was precluded from occurring because the materials fell off before igniting in the room-corner tests. These behaviors can be captured using FDS if the failure behavior is known; however, a large-scale room-corner test may be necessary to accurately predict the fire performance of these materials.

#### 8.4 Section Summary

The fire test data on interior finish materials developed as part of this research effort was used to validate models to support developing the HRR-based flammability requirements for interior finish materials on passenger rail cars. The data were compared with the predictions from the empirical model that determines the occurrence of flashover due to the lining material as well as the CFD model FDS that predicts more detailed fire growth. Both models were determined to be able to predict the behavior of materials that remained attached to the boundary surfaces during the large-scale NFPA 286 room-corner fire test. However, some materials delaminated or had facesheet failures that resulted in performance not expected based on small-scale cone calorimeter test data.

A flammability parameter threshold of  $F < 0.6$  was determined to be the appropriate value for screening the occurrence of flashover due to a lining material. Materials with a flammability parameter of  $0.6 < F < 0.9$  may be borderline and require additional modeling to determine their behavior in larger spaces, such as a rail car seating area. Failure of materials, such as falling from the surface or delamination, may cause conditions that accelerate or decelerate fire growth. This cannot be predicted using the flammability parameter.

FDS predictions of the room-corner tests were in good agreement with the HRRs and gas temperatures measured during the NFPA 286 tests. For the thermoplastic materials, the modeling needed to include the potential for material fall off based on its glass transition temperature. For sandwich composite materials, a delamination failure potential had to be included that allowed the possibility for the facesheet to fall off

exposing the core material directly to the fire. With these effects included, good agreement between the models and data was achieved.

Both the flammability parameter empirical model and FDS were demonstrated to be capable of generally predicting the performance of materials in large scale. As a result, they can be used to support development of the heat release based requirements for interior finish.



## 9. Development of HRR Requirements for Rail Car Interior Materials

---

Currently, NFPA 130 [3] and 49 CFR Part 283.103 [4] generally use two standard test methodologies for rail car interior finish material flammability and smoke emission acceptance. These are the ASTM E162 [6] “radiant panel” test and the ASTM E662 [5] “smoke density chamber” test. A HRR based test is considered to provide a more practical and valuable alternative to the current standards for determining the fire safety performance of materials. The most widely used test for determining the HRR performance characteristics of materials is the bench-scale cone calorimeter test, as specified in ASTM E1354 [60]. The focus of this section is to determine HRR-based performance criteria based on the ASTM E1354 cone calorimeter test standard for rail car interior finish materials.

In NFPA 130 and the 49 CFR Part 238.103, interior finish is broken down by material function on the rail car as shown in [Table 9-1](#). As seen in the table and further described in the notes for each material function (not shown), there may be special requirements and testing for particular materials based on their function. The focus of the work presented in this report is on the materials that are enclosed in the box in [Table 9-1](#). Other than the seating and the floor coverings, these materials comprise a large surface area inside the rail car. Seating assembly and floor coverings already have appropriate, modern fire tests and requirements. NFPA 130 requires a complete seat assembly (including cushions, fabric layers, and upholstery) be tested according to ASTM E1537 using the pass/fail criteria of California Technical Bulletin 133 [3]. The other interior finish materials not considered in this work were cushioning, fabrics, windows, elastomers, and sealants/ adhesives. These are special classes of materials where the fire safety behavior, physical performance, and end-use configuration all need to be considered, but were outside the scope of this effort. Electric cabling and wiring were considered in a separate effort with the current minimum fire safety testing requirements determined to be adequate.

**Table 9-1. NFPA 130 [3] material fire performance criteria table<sup>7</sup>**

Category	Function of Material	Test Method	Performance Criteria
Cushioning	All individual flexible cushioning materials used in seat cushions, mattresses, mattress pads, armrests, crash pads, and grab rail padding	ASTM D3875	$I_s \leq 25$
		ASTM E862	$D_p(1.5) \leq 100$ $D_p(4.0) \leq 175$
Fabrics	Seat upholstery, mattress ticking and covers, curtains, draperies, window shades, and woven seat cushion suspensions	14 CFR 25, Appendix F, Part I (vertical test)	Flame time $\leq 10$ sec Burn length $\leq 6$ in.
		ASTM E862	$D_p(4.0) \leq 200$
Other vehicle components	Seat and mattress frames, wall and ceiling lining and panels, seat and toilet shrouds, toilet seats, trays and other tables, partitions, shelves, opaque windscreens, combustible signage, end caps, roof housings, articulation bellows, exterior shells, nonmetallic skirts, battery case material, and component boxes and covers	ASTM E162	$I_s \leq 35$
		ASTM E862	$D_p(1.5) \leq 100$ $D_p(4.0) \leq 200$
	Thermal and acoustical insulation	ASTM E162	$I_s \leq 25$
		ASTM E862	$D_p(4.0) \leq 100$
	HVAC ducting	ASTM E162	$I_s \leq 25$
		ASTM E862	$D_p(4.0) \leq 100$
	Floor covering	ASTM E848	$CRF \geq 5 \text{ kW/m}^2$
		ASTM E862	$D_p(1.5) \leq 100$ $D_p(4.0) \leq 200$
	Light diffusers, windows, and transparent plastic windscreens	ASTM E162	$I_s \leq 100$
		ASTM E862	$D_p(1.5) \leq 100$ $D_p(4.0) \leq 200$
Elastomers	Adhesives and sealants	ASTM E162	$I_s \leq 35$
		ASTM E862	$D_p(1.5) \leq 100$ $D_p(4.0) \leq 200$
	Window gaskets, door gaskets, intercar diaphragms, seat cushion suspension diaphragms, and roof mats	ASTM C1166	Flame propagation $\leq 100 \text{ mm (4 in.)}$
		ASTM E862	$D_p(1.5) \leq 100$ $D_p(4.0) \leq 200$
Wire and cable	All	See 8.6.7.1.1.1 through 8.6.7.1.3.	See 8.6.7.1.1.1 through 8.6.7.1.3
Structural components	Flooring, other	ASTM E119	Pass

Study applies to these materials

## 9.1 Flammability Parameter Based HRR Requirements

The empirical flammability parameter model was validated with test data from the small-scale cone calorimeter and the NFPA 286 room-corner test. These results and the

<sup>7</sup> ASTM E162 might not be suitable for materials that exhibit flaming, running or dripping because the test apparatus is not designed to accommodate this kind of burning behavior.

validation effort were described in [Sections 6, 7, and 8](#). The flammability parameter ( $F$ ) is defined as

$$F = 0.01 \dot{Q}'' - t_{ig}/t_{bd} \quad (9-1)$$

where  $\dot{Q}''$  is the average HRRPUA in kW/m<sup>2</sup>,  $t_{ig}$  is the time to ignition in seconds, and  $t_{bd}$  is the burn duration, also in seconds. These variables are obtained from cone calorimeter tests performed at 50 kW/m<sup>2</sup> heat flux. The constant 0.01 represents the flame height correlating factor, and its units are m<sup>2</sup>/kW.

The model predicts that the material will most likely cause flashover if its flammability parameter is greater than 0.6, and will not if less than 0.6. Materials with values near this critical flammability parameter have varied performance. These results are shown in [Figure 9-1](#), which contains all the data from both the calibration and validation efforts.

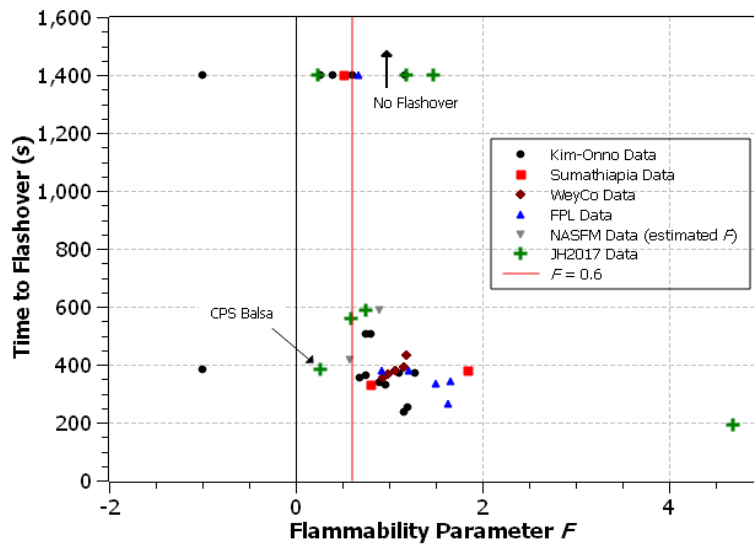


**Figure 9-1. Predicting flashover with the empirical flammability model. The critical flammability parameter of  $F=0.6$  delineates materials which are likely to cause flashover from those that will not**

The materials in the region  $0.6 < F < 0.9$  have more varied performance and for the materials that do cause flashover the time to reach flashover conditions is longer. All the materials with  $F < 0.9$  did not cause flashover before the ramp-up to 160 kW burner HRR.

Some test results were not predicted by the model, and these were indicative of a physical response in the large scale which was not manifested in the small scale. For the composite sandwich panels, the degradation and failure of the facesheet exposed the underlying plywood during the room-corner test and caused its performance to be worse than predicted by the empirical model. In the cone calorimeter the facesheet remained intact. Conversely, in the large scale the polymer materials melted away and collapsed to the floor of the room. No flashover occurred due to this response, even though it was predicted using the models. These examples of model limitations are present when using small scale data to predict large scale response.

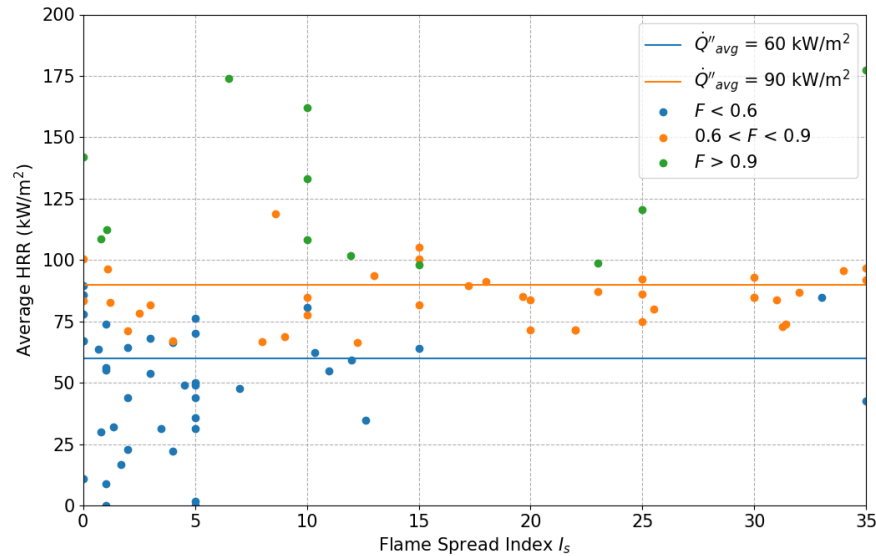
### 9.1.1 Critical Flammability Parameter Based Requirements

The critical flammability parameter of 0.6 most effectively screens out poor performing materials. If the  $t_{ig}/t_{bd}$  term in the model is set to 0, the resulting HRR requirement would be  $Q''_{avg} = 60 \text{ kW/m}^2$  (the test average HRR). This second term in the model is the ignitability and heat release capacity term. For the term to be 0, either the time to ignition is very small ( $t_{ig} \approx 0$ ) or the burning duration is long ( $t_{bd} \rightarrow \infty$ ). These are conservative conditions.

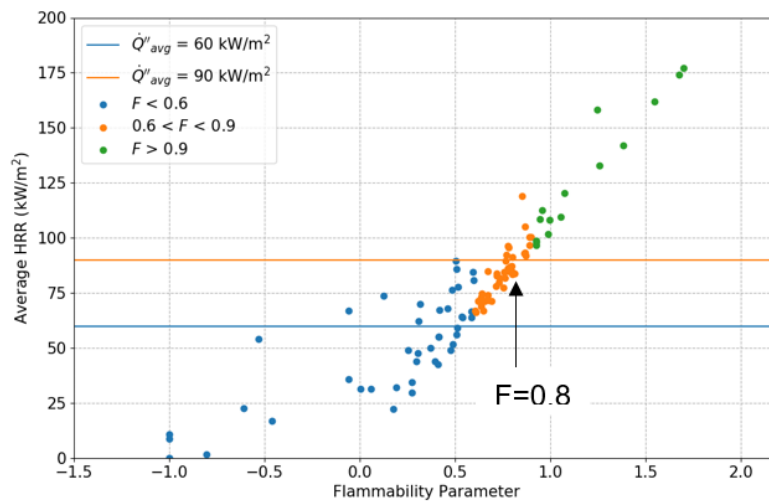
Likewise, a flammability parameter of 0.9 yields a requirement for HRR of  $Q''_{avg} = 90 \text{ kW/m}^2$  (test average). Overall this requirement may not be conservative enough, especially for small spaces. Figure 9-2 and Figure 9-3 show an evaluation of these initial requirements using materials in the passenger rail car material database.

Figure 9-2 shows the comparison of average HRR with flame spread index. The materials with  $F < 0.6$ ,  $0.6 < F < 0.9$ , and  $F > 0.9$  are shaded distinct colors. Generally, the best performing materials (those with  $F < 0.6$  and  $Q''_{avg} < 60 \text{ kW/m}^2$ ) also have an ASTM E162 flame spread index  $I_s < 15$ . Materials with  $F < 0.6$  have excellent flammability performance (i.e., not expected to cause flashover in the NFPA 286 room-corner test or in a rail car); however, to accept all these currently acceptable materials the HRR requirement would need to be set to  $Q''_{avg} = 90 \text{ kW/m}^2$ . A HRR requirement of  $Q''_{avg} = 90 \text{ kW/m}^2$  also accepts materials with a flammability parameter as high as  $F = 0.8$ . Also, with this requirement 30 percent of materials with  $I_s < 35$  are screened out. In Figure 9-3,  $Q''_{avg} < 90 \text{ kW/m}^2$  accepts all materials with  $F < 0.6$ , and also materials with flammability parameters up to 0.8

If the HRR requirement is set to  $Q''_{avg} < 60 \text{ kW/m}^2$ , no materials are accepted that have a  $F > 0.6$  (i.e., have the potential to cause flashover in NFPA 286 or in a rail car). However, this level also screens out 37 percent of materials with  $F < 0.6$ . It also screens out 74 percent of materials currently accepted for use in rail cars with  $I_s < 35$ . Therefore, it was concluded that this level of HRR requirement may be overly restrictive.



**Figure 9-2. Comparison of passenger rail car materials with flammability parameters of 0.6 and 0.9 with initial requirements**



**Figure 9-3. Flammability parameter and average HRR for passenger rail car materials.  $\dot{Q}''_{avg} < 90 \text{ kW/m}^2$  accepts all materials with  $F < 0.6$**

### 9.1.2 Data Analytics Clustering Requirements

To further evaluate the rail car material database established in [Section 2](#), clustering was performed to group the materials. K-means clustering [70] was done using five parameters based on cone calorimeter test data. These were the flammability parameter ( $F$ ), average HRR ( $\dot{Q}''_{avg}$ ), peak HRR ( $\dot{Q}''_{peak}$ ), time to ignition ( $t_{ig}$ ), and the total heat released (THR). The K-means algorithm groups materials into clusters of equal variance in the multidimensional space. Five clustering groups were used. The clustering groups are shown in [Figure 9-4](#).

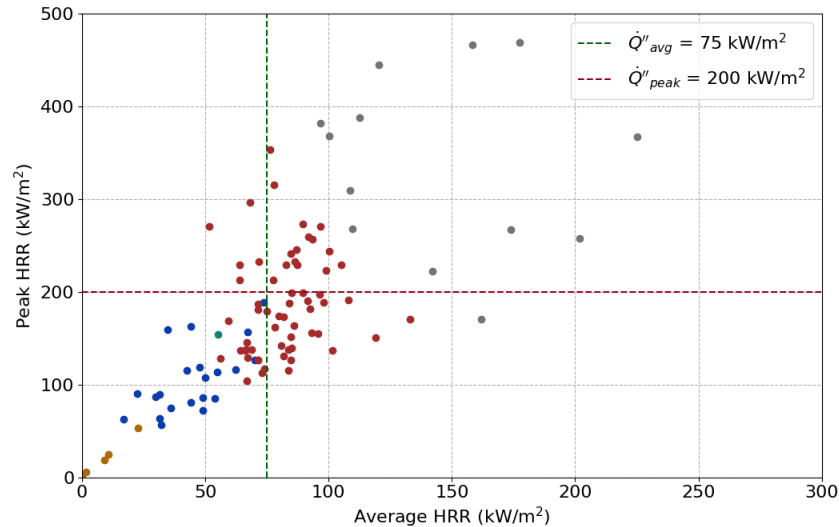


**Figure 9-4. K-means clustering on database of passenger rail car materials**

Three best performing material groups of the five cluster groups are accepted by  $Q''_{avg} < 75 \text{ kW/m}^2$  and  $Q''_{peak} < 200 \text{ kW/m}^2$  (see the yellow, green, and blue symbols in [Figure 9-4](#)). The yellow symbols represent the best performing group, which only contained four materials. The blue group in [Figure 9-4](#) had most of the better performing materials, and the criteria necessary to define this group as acceptable are  $Q''_{avg} < 75 \text{ kW/m}^2$  and  $Q''_{peak} < 200 \text{ kW/m}^2$ . The peak HRR is used in many standards for material acceptance. The other parameters used in the clustering were less useful in setting requirements due to a number of factors. The time to ignition was highly variable, even within the same material group. The total heat released was less variable, but this parameter varies for the same material if the thickness is changed. The peak and average HRR were therefore found to be the most effective parameters for setting criteria limits. Using values of  $Q''_{avg} < 75 \text{ kW/m}^2$  and  $Q''_{peak} < 200 \text{ kW/m}^2$ , these criteria would accept 77 percent of the materials in the database which exhibit  $F < 0.6$ .

[Figure 9-5](#) shows the material database with lines drawn at  $Q''_{avg} = 75 \text{ kW/m}^2$  and  $F = 0.75$ , which is the flammability parameter. As previously mentioned, materials that cause flashover conditions in the range  $0.6 < F < 0.9$  have longer times to flashover in the NFPA 286 test and flashover occurred after the burner was increased to 160 kW. Using  $Q''_{avg} < 75 \text{ kW/m}^2$  only as the HRR requirement does allow some materials with a peak HRR of greater than 200 kW/m<sup>2</sup> to be considered acceptable. Flammability parameter of 0.75 may be sufficient to screen out poor performing materials. Conversely, there are several materials with  $Q''_{avg} > 75 \text{ kW/m}^2$  that have a borderline flammability parameter ( $0.6 < F < 0.9$ ). Additional modeling of materials with borderline flammability parameter is needed to determine how these materials perform in a rail car to assess their performance in the end-use application. This is done in the next [Section 9.1.3](#).

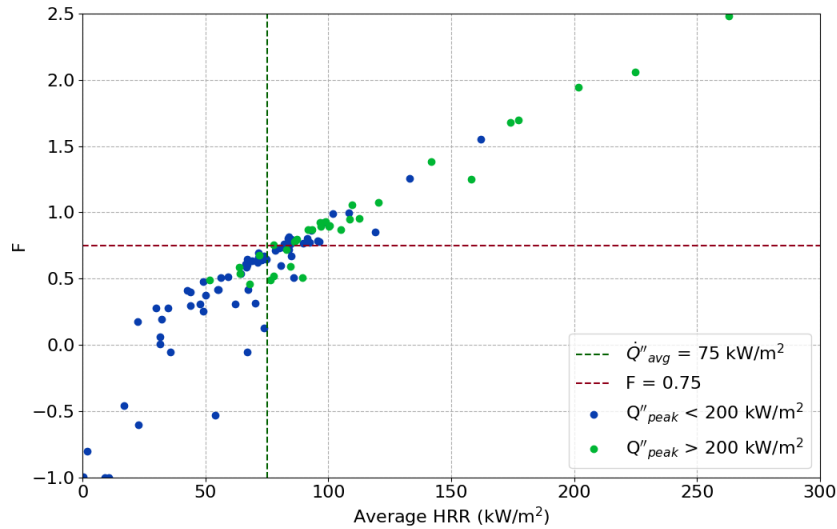


**Figure 9-5. Evaluating material database with requirements for average and peak HRR**

### 9.1.3 Refinement Based on Borderline Material Evaluation

A series of fire growth simulations were performed to evaluate the performance of borderline materials ( $0.6 < F < 0.9$ ) in a rail car. Some of this modeling was previously performed, but this was mostly on materials that had a flammability parameter of  $F > 1.0$ . Similar to the previous work, FDS simulations were performed to quantify the fire growth in a NFPA 286 test room as well as a rail car seating area with a side door open. The walls and ceiling were all lined with the material of interest.

Materials were selected which had flammability parameters ranging from 0.68 to 0.96, and the cone calorimeter data for these materials were input into the FDS model to account for the ignition, flame spread, and HRR contribution of the material lining. The predictions of the occurrence of flashover from the simulations are provided in [Table 9-2](#). While most of these materials caused flashover in the NFPA 286 room corner test, no flashover was predicted by the model in the rail car geometry due to the larger volume of the rail car. [Figure 9-6](#) and [Figure 9-7](#) contain plots of the HRR curves from the FDS simulations for two of the rail car materials used in the NFPA 286 and rail car geometries. From these results, it can be seen that in the larger rail car spaces flashover is less likely to occur even if materials have a flammability parameter in the range of  $0.6 < F < 0.9$ . As a result, using a flammability criterion of  $F < 0.75$  (which provides some margin) would be appropriate to support determining a HRR requirement for lining materials.

**Table 9-2. FDS results for materials in NFPA 286 and rail car geometries**

F	Material	NFPA 286 Flashover	Rail car Flashover
0.68	NRC Plywood 1991	Yes	No
0.69	Rail car Ceiling Panel	Yes	No
0.75	Rail car Wall Lining	No	No

F	Material	NFPA 286 Flashover	Rail car Flashover
0.75	JH Sample 6 (FRP)	Yes	No
0.80	NRC Plywood 1990	Yes	No
0.89	Rail Car Toilet Room Lining	Yes	No
0.90	NRC Plywood	Yes	Yes
0.96	NRC Plywood	Yes	Yes

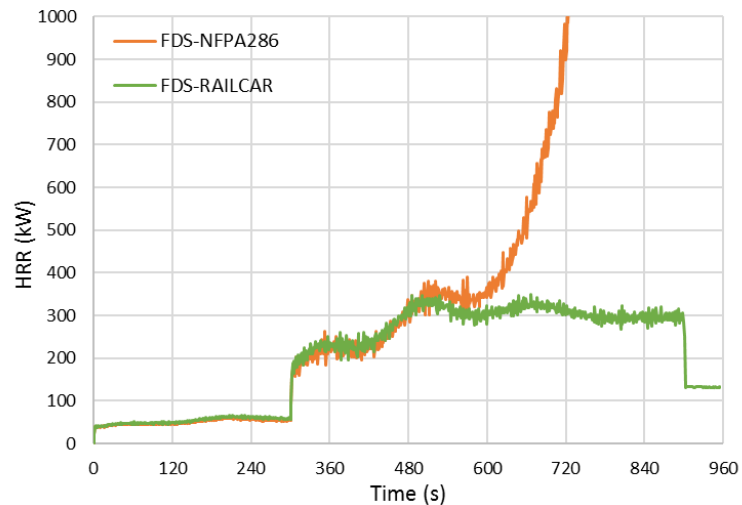


**Figure 9-6. FDS simulation result for rail car ceiling lining material with flammability parameter of 0.69**

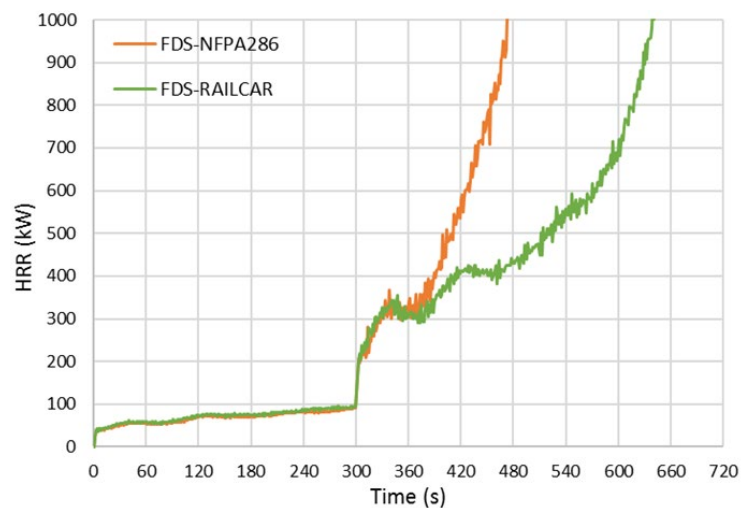


**Figure 9-7. FDS simulation result for rail car toilet room lining material with flammability parameter of 0.89**



## 9.2 Evaluation Using EN-45545-2 HRR Requirements

European standard EN-45545-2 specifies two small scale tests for assessing flammability [2]. The first is ISO-5658-1, which is a lateral ignition and flame spread test (LIFT). The other test is the ISO 5660-1, which is equivalent to the ASTM E1354 cone calorimeter test. Requirements for materials are based on operation and design categories. From the operation category and design category, a HL assessed in [Table 9-3](#) specifies the running time before stopping and minimum average speed at which a train must operate to be in a certain Operation Category (OC). Additionally, in OC 1, the train must stop in a location of safe egress with minimum delay. For OC 2, the vehicles may operate in underground sections, in tunnels, and/or on elevated structures, with side evacuation routes available. Stations must be available that offer a place of safety for passengers, reachable within a short running time. OC 3 has the same requirements as OC 2, except that stations may be reachable within a long running time. For OC 4, vehicles operate in underground sections, tunnels, and/or on elevated structures, but without side evacuations available. Stations and rescue stations for safe egress must be reachable within a short running time.

[Table 9-4](#) contains a matrix defining the hazard level of the vehicle, which depends on the operational category and design category. Design categories include standard vehicles, vehicles forming part of an automatic train with no emergency staff on board, double decked vehicles, and sleeping cars. These hazard levels are then used to define the requirements for the component materials.

**Table 9-3. Operation category definitions from EN 45545-2**

Operation Category	Running Time	Minimum Average Speed infrastructure subject to the Directive	Minimum Average Speed infrastructure not subject to the Directive
OC 1	Vehicles may stop with minimum delay	Not applicable. See 5.2.1, Note 2	No requirement
OC 2	4 min.	80 km/h (50 mph)	No requirement
OC 3	15 min.	80 km/h (50 mph)	No requirement
OC 4	4 min.	No requirement	No requirement

**Table 9-4. Hazard level matrix for qualifying materials in train vehicles**

Operation Category	Design Category			
	N: Standard Vehicles	A: Vehicles forming part of an automatic train having no emergency trained staff on board	D: Double decked vehicle	S: Sleeping and couchette vehicles
1	HL1	HL1	HL1	HL2
2	HL2	HL2	HL2	HL2
3	HL2	HL2	HL2	HL3
4	HL3	HL3	HL3	HL3

The test type and requirements for a given component depend on the hazard level. Most materials have a requirement for critical flux at extinguishment (CFE) from the ISO 5658-1 LIFT test. Other materials have requirements for heat release from ISO 5660-1. Materials with requirements for ISO 5660-1 are tested at either 25 or 50 kW/m<sup>2</sup>. Most interior vertical or horizontal downward facing surfaces are tested at 50 kW/m<sup>2</sup> due to the higher propensity to spread flame in these configurations.

The requirements for materials tested in the ISO 5660-1 cone calorimeter are based on a maximum average rate of heat emission (MARHE). The average rate of heat emission (ARHE) is a curve calculated from the cumulative integral of the HRR curve, and the MARHE is the maximum point on this curve. The ARHE curve is integrated from the start of the test, thus the time to ignition is somewhat incorporated in this calculation. [Figure 9-8](#) and [Figure 9-9](#) show the relation of MARHE to average HRR for two sample materials. In [Figure 9-8](#), MARHE is lower than average HRR due to the long time to ignition and the smaller initial HRR; whereas, in [Figure 9-9](#), MARHE is higher than average HRR due to the short time to ignition and the larger initial HRR.

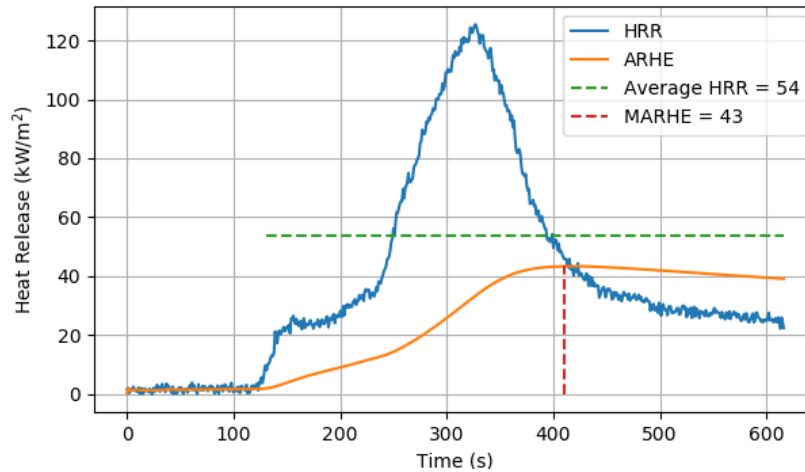


**Figure 9-8. Comparison of MARHE and average HRR for Sample 3 cone calorimeter test**

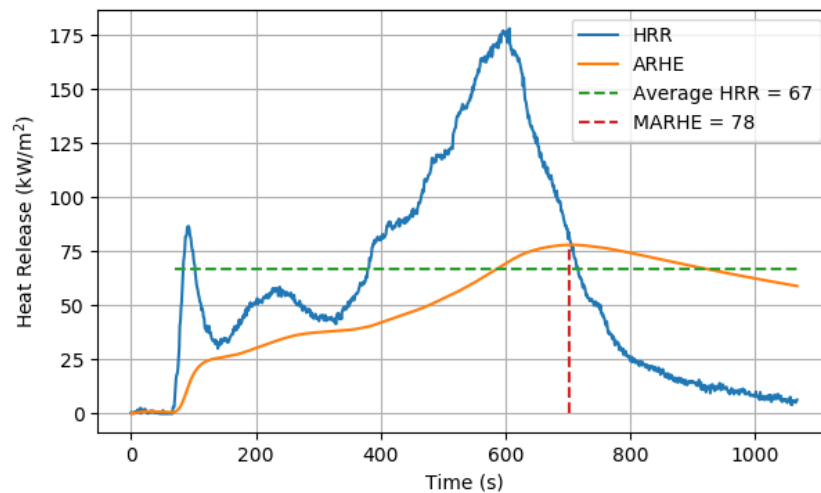


**Figure 9-9. Comparison of MARHE and average HRR for Sample 2**

Material component requirements based on the ISO 5660-1 cone calorimeter at 50 kW/m<sup>2</sup> are listed in [Table 9-5](#). Those that are tested at 25 kW/m<sup>2</sup> are in [Table 9-6](#), which are less stringent due to the testing being performed at a lower heat flux level. The MARHE requirement for most interior finish in HL2 is 90 kW/m<sup>2</sup>, while for HL3 it is 60 kW/m<sup>2</sup>. These materials are mostly rigid linings used on the rail car interior. Seat shells have a MARHE requirement of 90 kW/m<sup>2</sup> for HL1. The interior linings mainly have no requirement for MARHE for HL1, but do have a requirement for minimum CFE from the ISO 5658-1 test. These range from 13 to 20 kW/m<sup>2</sup> for most interior linings.

**Table 9-5. Requirements for material sets according to hazard levels. All testing done in ISO 5660-1 at 50 kW/m<sup>2</sup>**

SET	COMPONENTS	MARHE REQUIREMENT FOR HL1	MARHE REQUIREMENT FOR HL2	MARHE REQUIREMENT FOR HL3
R1	Interior walls, partitions, doors, insulation, ceiling panels, luggage racks, gangways, bellows, window frames, curtains, air ducts, display screens, tables	No requirement	90 kW/m <sup>2</sup>	60 kW/m <sup>2</sup>
R2	Interior upward facing table surfaces, limited area surfaces	No requirement	No requirement	90 kW/m <sup>2</sup>
R6	Seat shell	90 kW/m <sup>2</sup>	90 kW/m <sup>2</sup>	60 kW/m <sup>2</sup>
R7	Exterior walls, bellows, air ducts, arc-splash barrier	No requirement	90 kW/m <sup>2</sup>	60 kW/m <sup>2</sup>
R11	Arc-resistant insulation materials(A)	90 kW/m <sup>2</sup>	90 kW/m <sup>2</sup>	60 kW/m <sup>2</sup>
R12	Arc-resistant insulation materials(B)	60 kW/m <sup>2</sup>	60 kW/m <sup>2</sup>	60 kW/m <sup>2</sup>
R17	Cab housing	No requirement	90 kW/m <sup>2</sup>	60 kW/m <sup>2</sup>

**Table 9-6. Requirements for material sets according to hazard levels. All testing done in ISO 5660-1 at 25 kW/m<sup>2</sup>**

SET	COMPONENTS	MARHE REQUIREMENT FOR HL1	MARHE REQUIREMENT FOR HL2	MARHE REQUIREMENT FOR HL3
R5	Air filters	50 kW/m <sup>2</sup>	50 kW/m <sup>2</sup>	50 kW/m <sup>2</sup>
R8	Roof, containers mounted on roof	No requirement	50 kW/m <sup>2</sup>	50 kW/m <sup>2</sup>
R9	Suspension air bags, wheel sets, brakes, tires, metal/rubber units	90 kW/m <sup>2</sup>	90 kW/m <sup>2</sup>	60 kW/m <sup>2</sup>
R19	Staff seats (upholstery and back/base shell)	75 kW/m <sup>2</sup>	50 kW/m <sup>2</sup>	50 kW/m <sup>2</sup>
R20	Loose upholstery items (bed clothes, curtains, blankets, pillow, sheets)	50 kW/m <sup>2</sup>	50 kW/m <sup>2</sup>	50 kW/m <sup>2</sup>
R21	Upholstery, armrests, head rests, mattresses	75 kW/m <sup>2</sup>	50 kW/m <sup>2</sup>	50 kW/m <sup>2</sup>

### 9.2.1 EN 45545-2 MARHE and Flammability Parameter Requirements

The results from the validated flammability model and the initial requirements for  $Q''_{avg}$  were compared to the EN-45545 MARHE requirements for interior finish. Data from the material database which included HRR curves were used. Both the MARHE and the flammability parameter contain an ignitability component, and these metrics are correlated. Figure 9-10 shows the comparison between MARHE and flammability parameter.

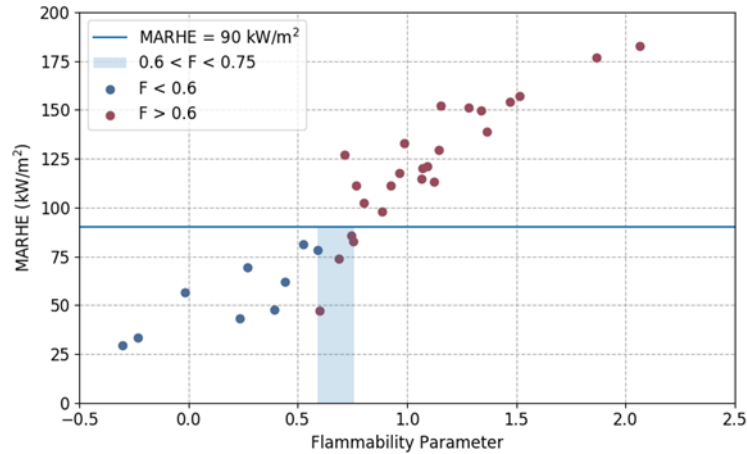


**Figure 9-10. MARHE and flammability parameter comparison. Requirement  $\text{MARHE} < 90 \text{ kW/m}^2$  accepts all materials with  $F \leq 0.75$**

From the FDS computational analysis, materials with  $F < 0.75$  are not expected to cause flashover in the larger spaces of a rail car geometry. Materials which meet the MARHE requirement of  $90 \text{ kW/m}^2$  also have  $F \leq 0.75$ , and thus should be appropriate for general use in large spaces of rail cars. The MARHE requirement of  $90 \text{ kW/m}^2$  does screen out 8 percent of materials which have  $F < 0.75$ . Materials which have  $\text{MARHE} < 60 \text{ kW/m}^2$  also have  $F < 0.6$ . These materials are not expected to flashover in the smaller spaces similar to the NFPA 286 room.

Figure 9-11 contains a comparison of the initial requirements for average HRR with those specified in EN 45545-2. Using  $\dot{Q}''_{\text{avg}} < 90 \text{ kW/m}^2$  to screen materials rejects those which would be accepted by  $\text{MARHE} < 90 \text{ kW/m}^2$ . Some ignition resistant materials which pass  $\text{MARHE} < 90 \text{ kW/m}^2$  may fail  $\dot{Q}''_{\text{avg}} < 90 \text{ kW/m}^2$ . These materials, circled in red, have longer time to ignition. The average HRR does not capture this aspect of flammability, while the MARHE does.

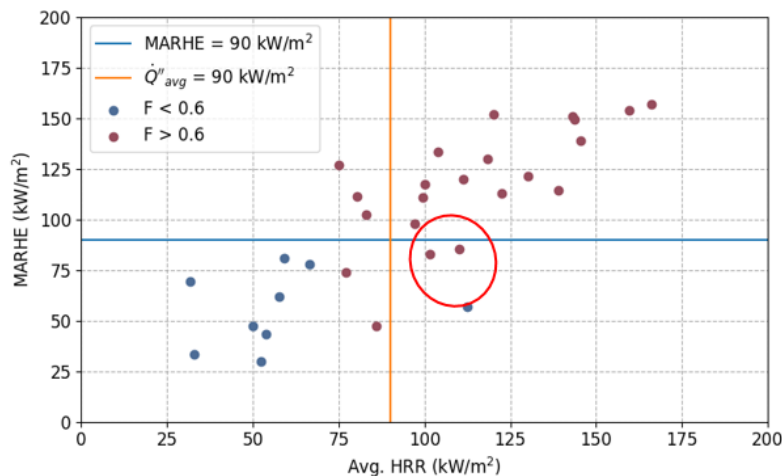


**Figure 9-11. Comparison of initial requirements with those specified in EN 45545-2**

### 9.3 Database Evaluation of Potential Requirements

To evaluate the effectiveness of the various potential HRR requirements, an analysis of the rail car material database was performed to determine the fraction of materials that would be deemed acceptable when different criteria are applied. The results of this analysis are shown in Table 9-7. All HRR related data in the table were from cone calorimeter tests at 50 kW/m<sup>2</sup>. For materials in the general seating area, the requirements  $Q''_{avg} < 60 \text{ kW/m}^2$ ,  $Q''_{avg} < 75 \text{ kW/m}^2$ , and  $Q''_{avg} < 75 \text{ kW/m}^2$  and  $Q''_{peak} < 200 \text{ kW/m}^2$  screen out 20 percent or more of materials with  $F < 0.75$ . As a result, these requirements are likely too restrictive. A HRR requirement of  $Q''_{avg} < 90 \text{ kW/m}^2$  appears to be appropriate based on flammability performance in a rail car (i.e., accepts all materials with  $F < 0.75$ ), except it screens out 23 percent of materials with MARHE  $< 90 \text{ kW/m}^2$ . This would also reject 30 percent of materials with ASTM E162 flame spread index  $I_s < 35$ . A requirement based on a MARHE  $< 90 \text{ kW/m}^2$  was found to accept most (92 percent) materials with an  $F < 0.75$  and would be in alignment with the EN standard. Although a full set of data is not available on this, based on the similar  $Q''_{avg} < 90 \text{ kW/m}^2$  data set, the MARHE  $< 90 \text{ kW/m}^2$  criterion would be expected to reject approximately 30 percent of materials with ASTM E162 flame spread index of  $I_s < 35$ . The use of the EN requirement of MARHE  $< 90 \text{ kW/m}^2$  would also be beneficial to rail car manufacturers since they could use their material supply chain that meets EN standards. A MARHE  $< 60 \text{ kW/m}^2$  appears to be overly restrictive since it rejects over 44 percent of materials with  $F < 0.6$ , which would not be expected to cause flashover in small spaces.

**Table 9-7. Fraction of materials which pass selected HRR requirements**

Rail car data without MARHE	$I_s < 35$		$F < 0.6$		$F < 0.75$		$F < 0.9$		MARHE $< 90 \text{ kW/m}^2$		MARHE $> 90 \text{ kW/m}^2$	
Data with MARHE												
Requirement (kW/m <sup>2</sup> )	Accept	Reject	Accept	Reject	Accept	Reject	Accept	Reject	Accept	Reject	Accept	Reject
$Q''_{avg} < 60$	26%	74%	63%	37%	44%	56%	32%	68%	54%	46%	0%	100%
$Q''_{avg} < 75$	48%	52%	86%	14%	80%	20%	58%	42%	62%	38%	0%	100%
$Q''_{avg} < 90$	70%	30%	100%	0%	100%	0%	86%	14%	77%	23%	14%	86%
$Q''_{avg} < 75, Q''_{peak} < 200$	43%	57%	77%	23%	72%	28%	52%	48%	62%	38%	0%	100%
MARHE $< 90$	No data	No data	100%	0%	92%	8%	76%	24%	-	-	-	-
MARHE $< 60$	No data	No data	56%	44%	46%	54%	35%	65%	-	-	-	-

## 9.4 Section Summary

Based on the table found in NFPA 130 and 49 CFR § 238.103, Appendix B, the flammability requirements developed in this report to replace the ASTM E162 requirements only apply to the materials in the red box provided in [Table 9-1](#). Based on the evaluation in this research, the following conclusions were reached.

Cone calorimeter tests conducted at 50 kW/m<sup>2</sup> should be used for material evaluation. An average HRR requirement of  $Q''_{avg} < 90 \text{ kW/m}^2$  works best with existing ASTM E1354 reported data. It screens out 23 percent of EN 45545-2 materials; however, it is potentially problematic with rail car manufacturers since this could affect their EN-compliant material supply chain.

It was found that MARHE < 90 kW/m<sup>2</sup> based on EN 45545-2 requirements accepts all materials with  $F < 0.6$  and 92 percent of materials with  $F < 0.75$ . No flashover is expected in large rail car spaces (seating area) for these materials. Based on other data, approximately 70 percent of materials tested with ASTM E162 with  $I_s < 35$  are expected to meet this but validation is needed. EN operation and design categories are different than those in the U.S. This requirement would start to harmonize U.S. and EN standards allowing manufacturers to maintain supply chains.

MARHE < 60 kW/m<sup>2</sup> based on EN 45545-2 requirements (HL2/HL3) accepts 56 percent  $F < 0.6$  and 46 percent of  $F < 0.75$  materials. No flashover is expected for these materials in smaller spaces (sleeping areas, bathrooms) similar to the NFPA 286 standard room. More data will be needed to determine if this requirement is overly restrictive.

ASTM E162 might not be suitable for materials that exhibit flaming running or dripping because the test apparatus is not designed to accommodate this kind of burning behavior. Cone calorimeter tests in a horizontal configuration cannot be used to evaluate the flaming droplet hazard. In EN 45545-2, the ISO 5658-2 (ASTM E1321) LIFT is used for such hazard evaluation.

Small-scale tests may not capture all large-scale behaviors. It was observed that aluminum facesheet debonding resulted in worse behavior in the NFPA 286 room corner fire test compared with the small-scale cone calorimeter test. Layered materials would need to demonstrate that facesheet fall-off would not result in poorer performance. One option would be to ensure that each material in the layer meets the flammability performance requirements as well as the assembly. Thermoformed materials that melt away resulted in better behavior in the NFPA 286 room corner fire test than expected from the small-scale test. Therefore, an option for large-scale room corner fire testing of a material should be provided to demonstrate material performance.

## 10. Calorimeter Tests on Seating Assemblies for Model Validation

---

To support future modeling, large-scale calorimeter tests were performed for three types of seating assemblies inside a NFPA 286 standard room with inert wall and ceiling linings. The testing results including gas temperature rise, combustion product generation, and overall HRR provide validation data and input for the empirical model and FDS fire growth model that were developed in this research to predict fire growth inside of rail cars. These models will be used to demonstrate the fire performance of materials meeting the proposed HRR-based performance requirements in their end-use environment.

### 10.1 Experimental Approach

#### 10.1.1 Test Overview

A series of large-scale calorimeter fire tests were conducted to quantify the performance of three different seating assemblies that currently meet the NFPA 130 [3] requirements for use on passenger rail cars. The tests were conducted in a NFPA 286 standard room [11], which is 2.4 m wide by 3.6 m long by 2.4 m high (8 ft. x 12 ft. x 8 ft.) and has a doorway with 2.0 m (79.5 in.) height and 0.78 m (37.5 in.) width. In each test, two identical full seating assemblies were placed on the floor against the side wall, as shown in [Figure 10-1](#).

The test configuration was developed based on the recommended Fire Scenario #1 in ASTM E2061 [71] for fire hazard assessment of rail transportation vehicles, which is an exposure fire between or under two interior seating assemblies. In these tests, a propane gas burner measuring 0.3 m x 0.3 m (12 in. x 12 in.) was used as the initiating exposure fire, which was placed between two seating assemblies against the side wall. The HRR for the burner was 40 kW for 5 minutes and then 160 kW for 10 minutes for a total exposure duration of 15 minutes. This is the same burner and HRR regimen recommended in NFPA 286 [11]. If flashover was not reached during the 15 minutes, the seating test articles could continue to burn until the fire was measured to be in the decay stage of the fire and close to burning out.

Gas temperatures were measured near the ceiling and at the top of the door. Heat flux to the floor was also measured at the center of the room. Fire spread along the seats was recorded in video. The overall HRR from the burner and the seating assemblies was measured using oxygen consumption calorimetry with a hood collection system as illustrated in [Figure 10-1](#). Using the measured mass flow rate of exhaust gases and the concentrations of oxygen, carbon dioxide and carbon monoxide, the HRR can be calculated using Thorton's rule which states that 13.1 MJ of energy are produced per 1 kg of oxygen consumed [67]. The mass flow rate of combustion gases was determined by measuring the stack temperature and pressure drop across an orifice plate. A gas analyzer measured the concentration of oxygen (O<sub>2</sub>), carbon dioxide (CO<sub>2</sub>), and carbon monoxide (CO). In addition, the smoke production rate was measured using a light extinction system in the duct.



### 10.1.2 Materials Tested

Table 10-1 lists the three samples of seating assemblies which were tested in this study. In each test, two identical full seating assemblies were placed on the floor near the side wall as shown in Figure 10-1. Samples tested include a range of typical seating assemblies used in passenger cars from different rail operators. Samples 1 and 2 were seating assemblies from commuter passenger rail cars that were in service. As a comparison, a transit rail car seating assembly was chosen to be Sample 3. The overall dimensions of the samples are listed in Table 10-1. In the testing setup, assemblies were configured in a way consistent with their end-use installation, as shown in Figure 10-2.

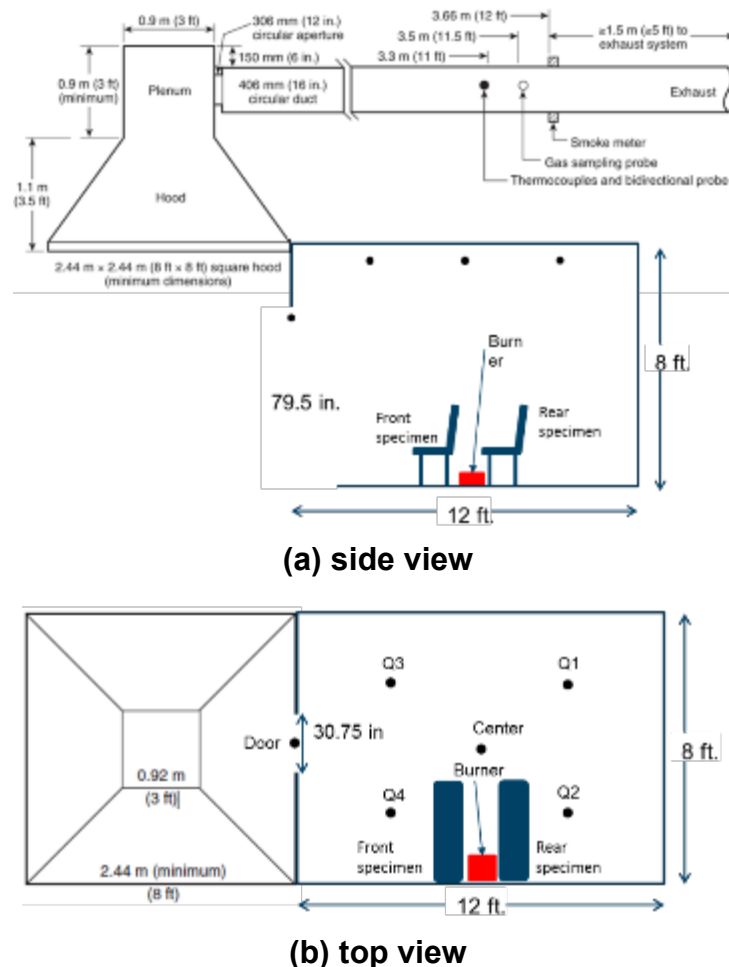


Figure 10-1. Test room configuration with hood and instrumentation with HRR measured using the hood calorimeter

**Table 10-1. Samples selected for testing**

<b>Sample ID</b>	<b>Description</b>	<b>Dimension</b>
Sample 1	Full (commuter passenger rail car) seating assembly with metal frame, cushioned double seat, arm rests and on both sides and cushioned back support with covering shell.	L: 36.5 in, D: 26 in, H: 44.75 in
Sample 2	Full (commuter passenger rail car) seating assembly with metal frame, cushioned double seat, cushioned back support, and end shells on both sides.	L: 37.5 in, D: 28 in, H: 47.25 in
Sample 3	Full (transit passenger rail car) seating assembly with metal frame with end shells, two back-to-back cushioned double seats, arm rests on the aisle side.	L: 38.75 in, D: 48 in, H: 38.5 in



**Sample 1**



**Sample 2**



**Sample 3**

**Figure 10-2. Setup of the samples in the room before testing**

## **10.2 Experiment Description**

The walls of the testing room at SGS Govmark were constructed of cinder blocks lined with  $\frac{5}{8}$  in. drywall, and the ceiling of 2x6 studs lined with  $\frac{5}{8}$  in. drywall. Each test was performed with one type of seating assembly inside the room. The hood calorimeter was calibrated with 160 kW burner HRR for 10 minutes with the burner located inside the room before each test. The seating assembly samples were conditioned in the testing room before commencement of the burn, and the testing room was within a temperature range of  $20\text{ }^{\circ}\text{C} \pm 10\text{ }^{\circ}\text{C}$  ( $68\text{ }^{\circ}\text{F} \pm 18\text{ }^{\circ}\text{F}$ ). Temperatures, HRR, and floor heat flux were monitored during the test, and operators observed conditions in the room.

The 0.3 m (0.012 in) by 0.3 m (0.012 in) burner exposure fire burned for a maximum of 15 minutes, with a 40 kW HRR for the first 5 minutes, and 160 kW for the remaining 10 minutes. The fire was permitted to burn until it was determined to have decayed to a point close to burn-out or until flashover conditions were reached (to prevent damage to the instrumentation used in the testing room). If either of these conditions was reached, the fire was extinguished.

## 10.3 Results

### 10.3.1 Overall Sample Performance

The results from the calorimeter tests are summarized in [Table 10-2](#). One out of the three samples of seating assemblies caused flashover. The results for peak HRR (kW) and total heat released (MJ) include the burner HRR, which was 40 kW for the first 300 s (5 min.) and then 160 kW for 600 s (10 min.). The heat released by the propane burner is 108 MJ for a test which proceeds until the end of the 160 kW burner regime. The test was stopped if flashover was determined to occur, so the values for total heat release (THR) for seating assemblies which caused flashover are usually lower due to the shorter test duration. For example, Sample 3, which did not cause flashover, had a THR contribution of 32 MJ from the seating assemblies but a THR of 140 MJ. Sample 1, conversely, ran for 460 s until flashover occurred and the THR contribution from the seating assemblies was 64 MJ while the overall THR was 93 MJ.

**Table 10-2. Sample full seating assembly calorimeter test results**

Sample ID	Flashover Time (s)	Peak Upper Layer Temperature (F)	Peak Heat Release Rate (kW)	Total Heat Release (MJ)	Seating assembly Contribution Total Heat Release (MJ)
Sample 1	460	1,420 (771 °C)	739	93	64
Sample 2	No flashover	1,069 (576 °C)	435	275	167
Sample 3	No flashover	822 (439 °C)	391	140	32

### 10.3.2 Test Observations

A log of events were recorded for each test. These logs are displayed in [Table 10-3](#), [Table 10-4](#), and [Table 10-5](#). The HRR plots are given in [Figure 10-3](#), [Figure 10-4](#), and [Figure 10-5](#). Official test reports from SGS Govmark are included in [Appendix E.1](#). Data plots are contained in [Appendix E.2](#), including gas temperatures, gas concentrations, floor heat flux, and rate of smoke release. Photos of the testing are included in [Appendix E.3](#), which are all available separate from the report.

**Table 10-3. Test log for seating assembly Sample 1**

Time	Event
0 s	Test starts; Burner turned on, 40 kW
25 s	Back of the front seat ignites
150 s	Rear seat cushion ignites
185 s	Materials/flames falling onto floor between two seats
210 s	Entire seat cushion and front surface of the rear seat burns
300 s	Ramp to 160 kW
370 s	Back of the front seat burns through
415 s	Half of the seat cushion of the front seat burns
440 s	Entire seat cushion of the front seat burns
460 s	Flames across the ceiling
465 s	Flames out doorway
466 s	End test, extinguish

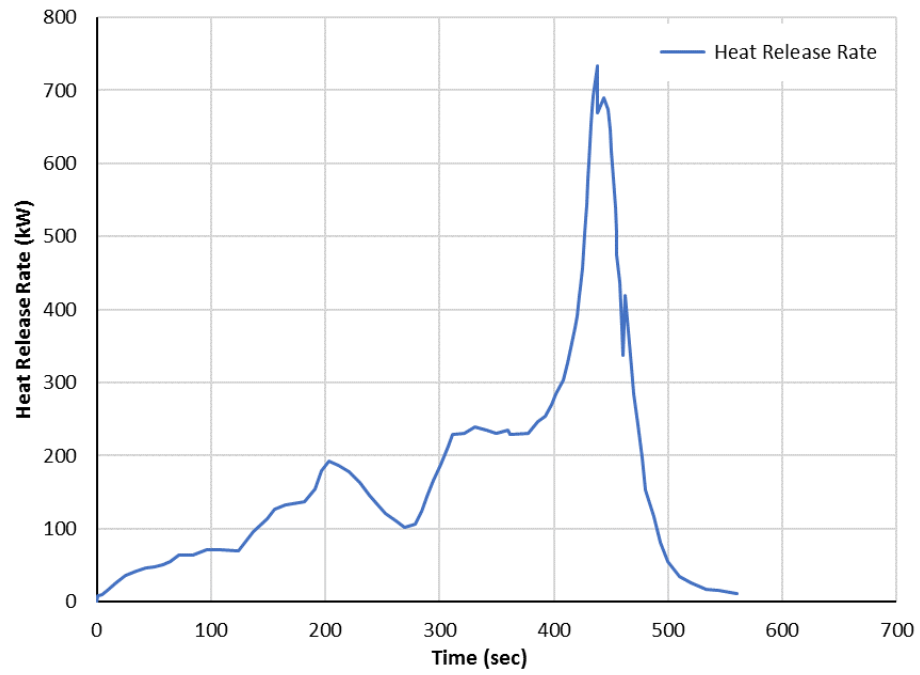


**Figure 10-3. HRR vs. time for seating assembly Sample 1**

**Table 10-4. Test log for seating assembly Sample 2**

<b>Time</b>	<b>Event</b>
0 s	Test starts; Burner turned on, 40 kW
20 s	Seat cushion of the rear seat ignites
95 s	Unstable flames are observed from the back (near the wall) of the front seat
185 s	Back of the front seat burns
245 s	Camera moved outside doorway
300 s	Ramp to 160 kW
320 s	Back cushion of the rear seat ignites
330 s	Seat and back cushion of the rear seat burn
340 s	Heavy black smoke occupies the upper half of the room
348 s	Fire spreads to the top headrest of the front seat
360 s	Armrest of the rear seat ignites
530 s	Top surface of the front seat cushion cracks with smoke
640 s	Burning materials drip from the rear seat to the floor
835 s	Fire spreads to the back cushion of the front seat
900 s	Burner off, test continues Seats continue to burn
1,130 s	Flames spread (from the end board under the armrest) along the side of the rear seat
1,490 s	Seat cushion of the front seat ignites
1,580 s	Back cushion of the front seat ignites
1,600 s	Upper part of the back cushion of the front seat falls off onto seat and burns
1,645 s	The whole back cushion of the front seat falls off onto seat and burns

Time	Event
1,680 s	Burning materials start dripping from the front of seat onto the floor
1,980 s	No more material dripping
2,100 s	A large part of the front seat cushion burns stably
2,460 s	End test, extinguish

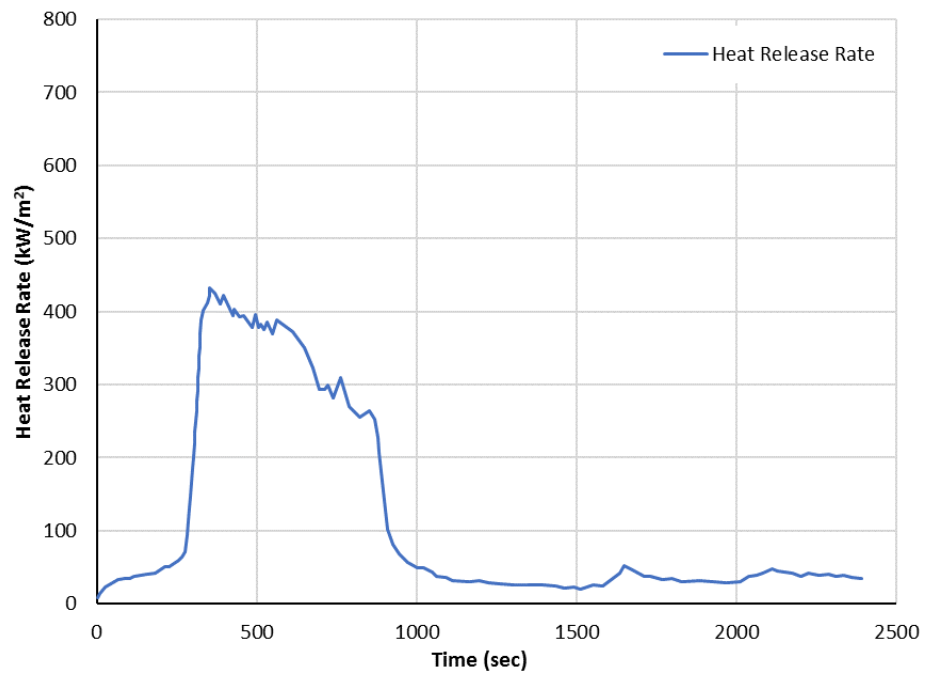


**Figure 10-4. HRR vs. time for seating assembly Sample 2**



**Table 10-5. Test log for seating assembly Sample 3**

Time	Event
0 s	Test starts; burner turned on, 40 kW
25 s	Seat cushion (facing the burner) of the front seat ignites
40 s	Seat cushion (facing the burner) of the rear seat ignites
240 s	Cushion flames extinguish
255 s	Camera moved outside doorway
300 s	Ramp to 160 kW
363 s	Aisle side back cushion (facing the burner) of the rear seat ignites
400 s	All cushions facing the burner burn
630s	Flames on most of the surfaces extinguished except one armrest of the rear seat
900 s	Burner off, test continues Only a small flame on the armrest of the rear seat is burning
1,135 s	Fire on the armrest of the rear seat extinguishes by itself End test

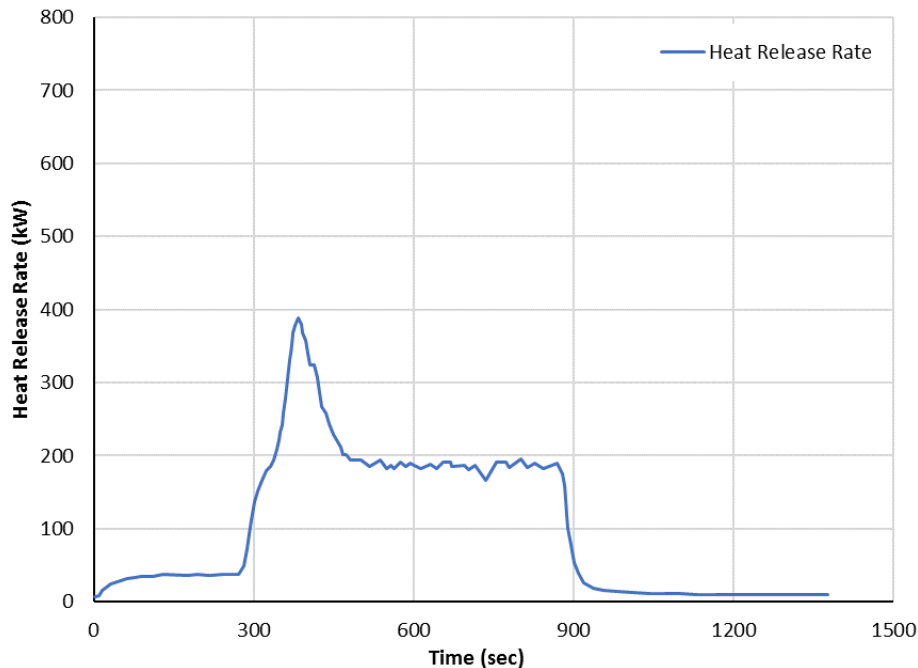


**Figure 10-5. HRR vs. time for seating assembly Sample 3**

#### 10.4 Discussion

All seat assemblies were reported to meet the NFPA 130 seat test requirements, which is testing of a single seat under an open calorimeter with a burner impinging onto the horizontal portion of the seat. In these tests, two seats were tested with a burner between the seats while configured in their end-use configuration inside of a room. This is similar to recommended Fire Scenario #1 in ASTM E2061 [71], which is an exposure fire between or under two interior seating assemblies. Testing inside of a room will also enhance flame spread due to heating from the hot gas layer that develops during the fire. In the tests conducted in this effort, the seats had varying behavior possibly due to the differences in seat end-use configuration as well as the construction materials.

The seat end-use configurations for seat Sample 1 and Sample 2 were similar with the seats facing in the same direction. This resulted in the fire exposing the front portion of one seat and the back portion of the other seat. In addition, the back portion of the front seat was close to the exposure fire. Sample 1 had seat covering on both sides of the seat. As a result, the seat cushion was able to become involved on both seats at a similar time increasing the growth of the fire and HRR. This resulted in flashover being reached inside the room. For seat Sample 2, the back of the seat was constructed of plastic which was sufficiently flame resistant to limit the HRR contribution and involvement of the seat foam. This resulted in slower fire growth and no flashover. Seat Sample 3 had the seats facing each other. This resulted in a larger separation between the vertical parts of the seats which slowed the fire growth.

The other parameter that may have affected the fire growth of the seats was the ignitability and HRR of the individual construction materials. These parameters were not

measured as part of this study, but this testing should be performed to be able to support using these data for modeling the fire growth for these different types and configurations of seating assemblies.

### **10.5 Section Summary**

Large-scale calorimeter tests were performed for three types of seating assemblies inside a NFPA 286 standard room with inert wall and ceiling linings. In each test, two identical full seating assemblies were placed on the floor against the side wall. This testing used the NFPA 286 standard fire exposure of 40 kW for 300 seconds (5 minutes) followed by 160 kW for 600 seconds (10 minutes), for a total test duration of 900 seconds (15 minutes). The location of the fire between two seats used in this testing is consistent with recommended Fire Scenario 1 described in ASTM E2061.

Of the three types of seating assemblies, Sample 1 caused flashover within 480 seconds (8 minutes) during the 160-kW burner regime. Sample 2 did not cause flashover, but after the burner was turned off it continued burning until the test was ended at 2,460 seconds (41 minutes). The best performing seating assembly was Sample 3. It did not cause flashover and the fire extinguished 240 seconds (4 minutes) after the burner was turned off.

The end-use configuration of the seats and their construction materials affected their behavior in these tests. Seats facing the same direction results in the vertical parts of the seats being more exposed to fire conditions in this scenario. In one case (Sample 1), this resulted in sufficient fire growth to cause the fire to reach flashover. The seats facing opposite directions were measured to have the best performance for the seats tested in this study.

The results of these tests including gas temperature rise, combustion product generation, and overall HRR provide validation data and input for the models used to predict fire growth inside of rail cars. These models will be used to demonstrate the fire performance of materials meeting the proposed HRR-based performance requirements. To support this future modeling, it is recommended that cone calorimeter testing be conducted on the seat construction materials to quantify the input parameters for the fire models.

## 11. Conclusion

---

In an effort to improve fire safety of passenger rail cars, this research work focused on establishing heat release rate (HRR) based performance requirements based on small-scale cone calorimeter testing for passenger rail car interior finish materials. The HRR-based performance requirements would allow a better understanding of the fire hazard threat, flashover HRR and contribution of individual materials to a fire inside a rail car. This provides improvements in fire hazard analysis, emergency egress analysis and threats analysis of an enclosed space of a station or tunnel for heat and smoke control, and a better understanding of the performance of various construction materials.

A database of HRR results for passenger rail car components was compiled from the literature and unpublished sources to determine a baseline equivalency for existing standards and provide data for creating HRR criteria for material qualification. Initiating fire exposures within a rail car were quantified and compared with different initiating fires in room-corner fire test standards. The NFPA 286 initiating fire of 40 kW for 5 minutes followed by 160 kW for 10 minutes was determined to be the most suitable standard initiating fire when compared with realistic initiating fires that are plausible inside of a rail car; therefore, it was recommended as a representative exposure fire for the interior of a rail car. An empirical model based on the flammability parameter was developed to predict the occurrence of flashover due to the lining material in NFPA 286 room-corner tests. A fire growth model using FDS was also developed to predict detailed fire growth within a rail car.

Due to the lack of HRR data on rail car materials, both small-scale ASTM E1354 cone calorimeter and ASTM E162 flame spread tests, as well as large-scale NFPA 286 tests were performed on seven rail car interior finish materials. The testing results along with the HRR database provided data to validate the flammability parameter empirical model as well as the fire growth model using FDS. The flammability parameter, which is calculated from the cone calorimeter test data, describes the propensity of a material to cause flashover in a NFPA 286 room-corner test. A flammability parameter threshold of  $F < 0.6$  was determined to be the appropriate value for screening the occurrence of flashover due to a lining material. Materials with a flammability parameter of  $0.6 < F < 0.9$  may be borderline and require additional modeling to determine their behavior in larger spaces, such as a rail car seating area. Failure of materials, such as falling from the surface or delamination, may cause conditions that accelerate or decelerate fire growth. This cannot be predicted using the flammability parameter. FDS predictions of the room-corner tests were in good agreement with the HRRs and gas temperatures measured during the NFPA 286 tests. For the thermoplastic materials, the modeling needed to include the potential for material falling off based on its glass transition temperature. For sandwich composite materials, a delamination failure potential had to be included that allowed the possibility for the facesheet to fall off exposing the core material directly to the fire. With these effects included, the FDS fire growth model could correctly predict if flashover would occur in NFPA 286 tests, validated by the testing results. Both the empirical flammability parameter model and FDS were demonstrated to be capable of generally predicting the performance of materials in large scale. As a

result, both models were validated for use in supporting the development of HRR requirements based on small-scale cone calorimeter testing.

Based on the research efforts above, HRR-based flammability requirements were developed for materials listed in “Other vehicle components” as listed in NFPA 130 and 49 CFR § 238.103.

The evaluation suggests that cone calorimeter tests conducted at 50 kW/m<sup>2</sup> per ASTM E1354 standard should be used for material evaluation. Materials used in seating areas within a rail car can be evaluated using a flammability requirement of maximum average rate of heat emission (MARHE) less than 90 kW/m<sup>2</sup>. No flashover is expected in large rail car spaces (seating area) for these materials. This is also currently used in EN 45545-2 for many materials in HL1 and HL2 applications.

It was also found that small-scale tests may not capture all large-scale behaviors such as melting and facesheet delamination. Layered materials would need to demonstrate that facesheet fall off would not result in poorer performance. One option to do this would be to ensure that each material in the layer meets the flammability performance requirements individually as well as the assembly. Thermoformed materials that melt away resulted in better behavior in the NFPA 286 room corner fire test than expected from the small-scale test. Therefore, an option for large-scale room corner fire testing of a material should be provided to demonstrate material performance.

### **11.1 Recommendations**

The following recommendations are provided based on the findings of this research.

The HRR-based flammability requirements for specific areas developed through the current research should be presented to the NFPA 130 Committee for consideration to be included in the next edition.

A more restrictive requirement for seating areas may be needed for smaller spaces such as bathrooms and sleeping areas, because higher gas temperatures accumulate in smaller spaces resulting in more severe fire conditions. The ASTM E1354 test at 50 kW/m<sup>2</sup> with MARHE less than 60 kW/m<sup>2</sup>, which is used in EN 45545-2 for some HL2 and HL3 applications, was found to be overly restrictive. The range of MARHE between 60 kW/m<sup>2</sup> and 90 kW/m<sup>2</sup> might be appropriate for smaller spaces, but more data and analysis need to be performed to refine the requirement value.

In EN 45545-2, the ISO 5658-2 (ASTM E1321) LIFT is used for evaluating the flaming droplet hazard. Cone calorimeter tests in a horizontal configuration cannot be used to evaluate such hazard. A test is needed to evaluate flaming droplets. Additional research should be conducted to evaluate an appropriate, cost effective test to evaluate flaming droplet hazards.

Further study is recommended to assess whether the smoke measurement from ASTM E1354 can be used instead of ASTM E662. This could potentially save the manufacturer from having to perform this additional test.

Additional research is also required for flammability requirements for materials listed other categories from the NFPA 130 table including “Cushioning,” “Fabrics,” “Other Vehicle Components” that are transparent or adhesive/sealants, and “Elastomers.”

The large-scale calorimeter test results of the seating assemblies including gas temperature rise, combustion product generation, and overall HRR provide validation data and input for the FDS fire growth models used to predict fire growth inside of rail cars. These models will be used to demonstrate the fire performance of materials meeting the proposed HRR-based performance requirements. To support this future modeling, it is recommended that cone calorimeter testing be conducted on the seat construction materials to quantify the input parameters for the fire models.

Testing and modeling are recommended to demonstrate the fire performance of materials meeting the proposed HRR-based flammability requirements developed in the current work. Further research is recommended to continue the HRR modeling and testing effort to refine the FDS model to predict material behaviors and their contributions to fully-developed rail car fires based on HRR-based flammability requirements. In addition, the effects of toxic gases generated by fires due to burning combustible interior finish on people inside of rail cars needs to be further explored.

## 12. References

---

- [1] “ASTM E1354-17 Standard Test Method for Heat and Visible Smoke Release Rates for Materials and Products Using an Oxygen Consumption Calorimeter,” ASTM International, West Conshohocken, PA, 2017.
- [2] DIN EN 45545-2:2016-02, “Railway Applications - Fire Protection on Railway Vehicles - Part 2: Requirements for Fire Behaviour of Materials and Components.” p. 77, 2016.
- [3] “NFPA 130 Standard for Fixed Guideway Transit and Passenger Rail Systems,” National Fire Protection Association, Quincy, MA, 2017.
- [4] “49 CFR 238.103 Fire safety,” *Code of Federal Regulations*, vol. 79, no. 16. pp. 1–28, 2014.
- [5] ASTM E662-15a, “Standard Test Method for Specific Optical Density of Smoke Generated by Solid Materials,” *ASTM International*, p. 26, 2015.
- [6] ASTM E162-15b, “Standard Test Method for Surface Flammability of Materials Using a Radiant Heat,” *ASTM International*, vol. i, p. 12, 2015.
- [7] S. M. and H. B. P. Briggs, S. Metral, Y. Le Tallec, “FIRESTARR Final Report,” 2001.
- [8] V. Babrauskas, “2016 SFPE Handbook 5th Edition HRR-Babrauskas.pdf.”
- [9] Hughes Associates, “PATH PA-5 Train Heat Release Rate History with ASTM E2061 Fire Scenarios,” 2007.
- [10] International Organization for Standardization, “ISO 9705-1:2016 - Reaction to fire tests -- Room corner test for wall and ceiling lining products -- Part 1: Test method for a small room configuration.” International Organization for Standardization, 2016.
- [11] NFPA 286, “Standard Methods of Fire Tests for Evaluating Contribution of Wall and Ceiling Interior Finish to Room Fire Growth,” *National Fire Protection Association*, 2015.
- [12] DIN EN 45545-1:2013-08, “Railway Applications - Fire Protection on Railway Vehicles Part 1: General.” p. 25, 2013.
- [13] K. Mcgrattan, S. Hostikka, R. Mcdermott, J. Floyd, C. Weinschenk, and K. Overholt, “Fire Dynamics Simulator User’s Guide.”
- [14] P. D. Gandhi and J. L. Borgerson, “Investigation of the fire performance of materials and products for use in U.S. railcar and bus applications,” 2008.
- [15] J. A. Capote, J. A. Jimenez, D. Alvear, J. Alvarez, O. Abreu, M. Lazaro, O. A. J. A. Capote, J. A. Jimenez, D. Alvear, J. Alvarez, and M. Lazaro, “Assessment of fire behaviour of high-speed trains’ interior materials: small-scale and full-scale fire tests,” *Fire Materials*, 38(7), pp. 725–743, November 2014.
- [16] C. Baiocchi, S. Messa, Y. LE Tallec, V. LE Sant, A. Sainrat, P. Gil, S. Metral, B.

- Muller, F.-W. Wittbecker, H. Breulet, U. Werther, A. Ebenau, J. Murrell, P. Briggs, A. Morgan, and T. Nisted, "Firestarr WP 4.2 Final report: Small-scale tests on furniture products," *Smt4-Ct97-2164*, p. 49, 2001.
- [17] M. Pezzani et al., "Work package 7.2: Large-scale tests on furniture products."
  - [18] M. Pezzani et al., "Work package 8.2: Real-scale tests on furniture products."
  - [19] M. Hjohlman, M. Försth, and J. Axelsson, *Design Fire for a Train Compartment*. 2009.
  - [20] A. Camillo, "Multi-scale investigation of fire behaviour of a seat and a wall panel from European Railway transport system."
  - [21] E. Guillaume, A. Camillo, and A. Sainrat, "Application of Fire Safety Engineering to Rolling Stock," *Problemy Kolejnictwa*, 160(160), pp. 51–75, 2013.
  - [22] "Hughes 2279 Data."
  - [23] "Hughes 2280 Data."
  - [24] "Hughes 2281 Data."
  - [25] "Hughes 2282 Data."
  - [26] "LTK Engineering Data."
  - [27] National Association of State Fire Marshals, "Recommended Fire Safety Practices for Rail Transit Materials Selection," *Proj. No. DC-26-5243-00*, no. Dc, p. 233, 2008.
  - [28] B. Y. Lattimer, *Heat transfer from fires to surfaces*. 2016.
  - [29] ASTM E2061-15, "Standard Guide for Fire Hazard Assessment of Rail Transportation Vehicles," *ASTM International*, no. C, p. 27, 2015.
  - [30] D. H. Lee, W. H. Park, W. S. Jung, and J. H. Hwang, "Fire Test of Old Type Interiors of Subway Vehicle in ISO 9705 Room," *Journal of the Korean Society of Railway*, 13(5), pp. 481–487, 2010.
  - [31] J. A. Capote, D. Alvear, M. Lázaro, and P. Espina, "Heat release rate and computer fire modelling vs real-scale fire tests in passenger trains," *Fire Materials*, 32(4), pp. 213–229, June 2008.
  - [32] E. House, "EN 13823 : 2002 " Single Burning Item " and EN 11925-2 : 2002 " Ignitability " test report of examination on the reaction to fire performance of wood particle board treated with Envirograf Contents," 2006.
  - [33] D. H. Lee, W. H. Park, and W. S. Jung, "Application Study of Burning Area-Based Summation Method for Fire Curve Estimation," *Structural Longevity*, 7(3), pp. 161–166, 2012.
  - [34] W. H. Park, D. H. Lee, and W. S. Jung, "Large-scale fire test for interior materials of the Korean high speed train," *Structural Longevity*, 7(1), pp. 13–18, 2012.
  - [35] N. White and V. P. Dowling, "Conducting a Full-Scale Experiment on a Passenger Car," *6th Asia-Oceania Symposium on Fire Science and Technology*, pp. 591–



601, 2004.

- [36] R. D. Peacock and E. Braun, "Fire Safety of Passenger Trains, Phase I: Material Evaluation (Cone Calorimeter)," *National Institute of Standards and Technology, NISTIR 6132*, p. 199, 1999.
- [37] R. D. Peacock, J. D. Averill, D. Madrzykowski, D. W. Stroup, P. A. Reneke, and R. W. Bukowski, "Fire Safety of Passenger Trains ; Phase III : Evaluation of Fire Hazard Analysis Using Full-Scale Passenger Rail Car Tests," *National Institute of Standards and Technology, NISTIR 6563*, p. 149, 2004.
- [38] A. Claesson, A. Lönnermark, and H. Ingason, *Laboratory fire experiments with a 1/3 train carriage mockup*, 2012.
- [39] N. White, "Fire Development in Passenger Trains," *M.S. Thesis, Victoria University*, p. 323, 2010.
- [40] B. Y. Lattimer, "2016 SFPE Handbook 5th Edition HF-Lattimer.pdf." .
- [41] J. Quintiere, M. Harkleroad, and Y. Hasemi, "Wall Flames and Implications for Upward Flame Spread," *Combustion Science and Technology*, 48(3–4), pp. 191–222, July 1986.
- [42] F. W. Mowrer and R. B. Williamson, "Flame Spread Evaluation for Thin Interior Finish Materials."
- [43] S. D. and A. G. C. Beyler, S. Hunt, B. Lattimer, N. Iqbal, C. Lautenberger, N. Dembsey, J. Barnett, M. Janssens, "Prediction of ISO 9705 Room/Corner Test Results," 1999.
- [44] B. Lattimer and U. Sorathia, "Composite Fire Hazard Analysis Tool for Predicting ISO 9705 Room-Corner Fire Test," 2004.
- [45] C. Calorimeter, T. Conducted, and I. R. C. Onno, "Results of Cone Calorimeter Tests Conducted at the NFL / IRC," 1992.
- [46] A. Kim and R. Onno, "Inter-Laboratory Study for the Full Scale Room Fire Test: Results of Tests Conducted at the NFL/IRC," *NRC-CNRC International Rep. No. 634*, 1992.
- [47] M. Janssens, "Thermophysical Properties of Wood and Their Role in Enclosure Fire Growth," University of Ghent, Ghent, Belgium, 1991.
- [48] H. C. Tran and M. L. Janssens, "Wall and Corner Fire Tests on selected Wood Products," *Journal of Fire Sciences*, 9(2), pp. 106–124, Mar. 1991.
- [49] M. L. Janssens, S. Dillon, and M. Hirschler, "Using the Cone Calorimeter as a Screening Tool for the NFPA 265 and NFPA 286 Room Test Procedures," *Fire Materials*, 2001.
- [50] V. P. Dowling and N. White, "Fire Sizes in Railway Passenger Saloons," *6th Asia-Oceania Symposium Fire Science Technology*, pp. 3–12, 2004.
- [51] E. Guillaume, A. Camillo, and T. Rogaume, *Application and Limitations of a Method Based on Pyrolysis Models to Simulate Railway Rolling Stock Fire*

*Scenarios*, 50(2), 2014.

- [52] D. Lee, W. Park, W. Jung, N. White, A. Webb, and J. Whang, "Two Cases of Interior Fire Tests within ISO 9705 for Railway Passenger Coach," *11th Fire Materials Conference*, p. 13, 2009.
- [53] G. J. Duggan, "Usage of ISO 5660 data in UK railway standards and fire safety cases," in *Fire Hazards, Testing, Materials and Products*, Rapra Technology Limited, 1997.
- [54] B. Y. Lattimer, S. P. Hunt, M. Wright, and U. Sorathia, "Modeling fire growth in a combustible corner," *Fire Safety Journal*, 38(8), pp. 771–796, December 2003.
- [55] B. Lattimer, "Flame entrainment and its application to compartment fires," *Fire Safety Science*, pp. 883–894, 2008.
- [56] B. Y. Lattimer, S. P. Hunt, M. Wright, and C. Beyler, "Corner fire growth in a room with a combustible lining," *Fire Safety Science*, pp. 419–430, 2003.
- [57] Hughes Associates, "PATH PA-4 Train Heat Release Rate History Design Fire for the World Trade Center Permanent PATH Terminal," 2006.
- [58] Hughes Associates, "PATH PA-5 (partial design) Train Heat Release Rate History Design Fire for the World Trade Center Permanent PATH Terminal," 2007.
- [59] B. H. Chiam, "Numerical Simulation of a Metro Train Fire," *Fire Engineering*, pp. 1–340, 2005.
- [60] ASTM E1354-15a, "Standard Test Method for Heat and Visible Smoke Release Rates for Materials and Products Using an Oxygen Consumption Calorimeter," *ASTM International*, vol. i, pp. 1–20, 2015.
- [61] T. Cleary and J. Quintiere, "A Framework For Utilizing Fire Property Tests," *Fire Safety Science*, vol. 3, pp. 647–656, 1991.
- [62] Hughes Associates, "Analysis of Heat Release Rates of M-3 and M-7 Rail Cars for Use in Determining the Design Fire for the Ventilation Systems for the East Side Access Project," 2001.
- [63] ISO, "ISO 5660-1:1993 Fire tests -- Reaction to fire -- Part 1: Rate of heat release from building products (Cone calorimeter method)," 1993.
- [64] "ISO 5660-1:2015 Reaction-to-fire tests -- Heat release, smoke production and mass loss rate -- Part 1: Heat release rate (cone calorimeter method) and smoke production rate (dynamic measurement)," International Organization for Standardization, Geneva, Switzerland, 2015.
- [65] "ASTM E162-16 Standard Test Method for Surface Flammability of Materials Using a Radiant Heat Energy Source," ASTM International, West Conshohocken, PA, 2016.
- [66] "ISO 5660-3:2012 Reaction-to-fire tests -- Heat release, smoke production and mass loss rate -- Part 3: Guidance on measurement," International Organization for Standardization, Geneva, Switzerland, 2012.

- [67] SFPE, *SFPE Handbook of Fire Protection Engineering*, 5th Ed. New York Heidelberg Dordrecht London, 2016.
- [68] Y. S. and G. L. K. Sumathipala, D. Carpenter, R. Monette, "Small-Scale and Full-Scale Fire Tests of Four Construction Materials," *Institute for Research in Construction*, 2001.
- [69] "[resindesigns](#)," 2016. [Online].
- [70] D. Sculley, "Web-scale K-means Clustering," 2010.
- [71] "ASTM E2061-09a, Standard Guide for Fire Hazard Assessment of Rail Transportation Vehicles." ASTM International, 2009.

## Appendix

---

Federal Railroad Administration. [Heat Release Rate Requirements for Railcar Interior Finish: Appendices A Through E](#), DOT/FRA/ORD-19/39, Department of Transportation, Federal Railroad Administration: Washington, DC, 2019.

## Abbreviations and Acronyms

---

ACRONYMS	EXPLANATION
ASTM	American Society of Testing Materials
EHCav	Average Effective Heat of Combustion
ARHE	Average Rate of Heat Emission
CFR	Code of Federal Regulations
CFD	Computational Fluid Dynamics
CFE	Critical Flux at Extinguishment
CHF	Critical Heat Flux
DOT	Department of Transportation
EHC	Effective Heat of Combustion
EN	European Norms
FRA	Federal Railroad Administration
FRP	Fiber Reinforced Plastic
FDS	Fire Dynamics Simulator
FSF	Flame Spread Factor
HL	Hazard Level
HEF	Heat Evolution Factor
HF	Heat Flux
HRR	Heat Release Rate
HRRPUA	Heat Release Rate Per Unit Floor Area
ISO	International Standards Organization
MARHE	Maximum Average Rate of Heat Emission
MLRPUA	Mass Loss Rate Per Unit Area
NASFM	National Association of State Fire Marshals
NFPA	National Fire Protection Association
NIST	National Institute of Standards and Technology
NRC	National Research Council
PMMA	Polymethyl Methacrylate
PVC	Polyvinyl Chloride
PVDF	Polyvinylidene Fluoride

<b>ACRONYMS</b>	<b>EXPLANATION</b>
RPI	Radiant Panel Index
SBI	Single Burning Item
SEA	Specific Extinction Area
TGA	Thermogravimetric Analysis
THR	Total Heat Release
THRPUA	Total Heat Release Per Unit Area
TRANSFEU	Transport fire safety engineering in the European Union
UL	Underwriters Laboratory
Volpe	Volpe National Transportation Systems Center